
Generation and Characterization of heavy chain antibodies derived from *Camelids*

Katrin Schmidthals



München 2013

Generation and Characterization of
heavy chain antibodies derived from
Camelids

Katrin Schmidthals

Dissertation

zur Erlangung des naturwissenschaftlichen Doktorgrades

an der Fakultät für Biologie

der Ludwig-Maximilians-Universität

München

vorgelegt von

Katrin Schmidthals

aus Penzberg

München, den 18. April 2013

Erstgutachter:	Prof. Dr. Heinrich Leonhardt
Zweitgutachterin:	Prof. Dr. Angelika Böttger
Eingereicht am:	18. April 2013
Tag der mündlichen Prüfung:	13. Juni 2013

Table of Contents

Summary..... 6

Zusammenfassung..... 7

1 Introduction..... 9

 1.1 Antibodies 10

 1.1.1 Structure and Function of Antibodies 11

 1.1.2 Areas of Application 15

 1.2 Display Technologies and Recombinant Antibody Formats 17

 1.2.1 Recombinant Antibody Formats..... 18

 1.2.2 Display Technologies 20

 1.3 Heavy chain antibodies 24

 1.3.1 Structure of Camelidae heavy chain antibodies..... 24

 1.3.2 Genetic background of functional heavy chain antibodies 25

 1.3.3 Unique features of V_HHs 29

 1.3.4 Applications of V_HHs 31

 1.4 Aims and Objectives 34

2 Materials and Methods 35

 2.1 Material 35

Table of Contents

2.1.1	Consumables.....	35
2.1.2	Solutions and Chemicals	37
2.1.3	Instruments.....	40
2.1.4	Cell lines.....	41
2.1.5	Antibodies.....	42
2.1.6	Primer	42
2.1.7	Bacterial strains	43
2.2	Methods	44
2.2.1	Molecular biological Methods.....	44
2.2.2	Cell Culture Methods.....	48
2.2.3	Biochemical Methods	50
2.2.4	Immunological Methods.....	54
2.2.5	Phage Display Technology	59
3	Results.....	67
3.1	Generation and selection of antigen specific V _H Hs.....	69
3.1.1	Antigen selection	69
3.1.2	Amplification of the V _H H repertoire	72
3.1.3	Cloning of V _H H library in pHEN4	75

Table of Contents

3.1.4	Phage Display.....	81
3.1.5	Selection of antigen specific V _H HS by Phage ELISA	100
3.1.6	Selection of antigen specific V _H HS by the F2H-Assay	111
3.2	Characterization of antigen specific V _H HS.....	117
3.2.1	Biochemical characterization	118
3.2.2	Intracellular characterization	134
4	Discussion	139
4.1	V _H H libraries	140
4.1.1	Immunogenicity of Antigens.....	140
4.1.2	V _H H Library Size and Diversity	142
4.2	V _H H Selection.....	144
4.2.1	A new method to select V _H HS for in vivo applications	144
4.3	Compensation of V _H -V _L combination	147
4.4	CDR3, disulfide bonds and functionality	148
4.5	Outlook.....	151
5	Annex.....	153
5.1	References.....	153
5.2	Abbreviations	166

Table of Contents

5.3	Eidesstattliche Erklärung.....	169
5.4	Acknowledgement.....	170
5.5	Publications/Patent applications	172
5.5.1	Publications	172
5.5.2	Patent applications	172

Summary

Antibodies and antibody fragments are essential tools in basic research, diagnostics and therapy. Conventional antibodies consist of two heavy and two light chains with both chains contributing to the antigen-binding site. In addition to these conventional antibodies, camelids (llamas, alpacas, dromedaries and camels) possess so-called heavy chain antibodies (hcAbs) that lack the light chains. The antigen binding site of these unusual antibodies is formed by one single domain only, the so called V_HH domain. The V_HH domain represents the smallest intact antigen binding fragment (~ 15 kDa) and is characterized by very high stability, solubility and specificity. These unique features render V_HHs a promising alternative to conventional antibodies and antibody fragments with a multitude of possible applications.

In the course of this thesis, we aimed to generate and characterize V_HHs suitable for different applications ranging from biochemical studies to immunofluorescence assays and live cell imaging. In order to meet the diverse requirements of the intended downstream applications, a new selection method differing from traditional phage display, called *native panning*, was developed and established. In combination with the protein-protein interaction *fluorescent two-hybrid (F2H) assay*, a new process to identify antigen specific V_HHs functional inside living cells was developed.

We used the immune system of alpacas to generate V_HH libraries against various antigens, ranging from small peptides to large proteins. The libraries were screened by phage display and antigen specific V_HHs were identified by phage ELISA. We were able to identify antigen specific V_HHs against different antigens which were characterized and their functionality was tested in various applications. Furthermore, we could demonstrate that the selection method influences which V_HHs are identified and therefore needs to be chosen very carefully with regard to the intended biochemical and cell biological application. In summary, we developed and established an efficient and versatile process to screen and identify antigen specific V_HHs suitable for different downstream applications.

Zusammenfassung

Antikörper und rekombinante Antikörperfragmente sind unabhömmliche Werkzeuge in der biomedizinischen Forschung, Diagnostik und Therapie. Klassische Antikörper sind durch einen sehr komplexen Aufbau mit zwei schweren und zwei leichten Ketten gekennzeichnet. Neben den klassischen Antikörpern besitzen Cameliden (Lamas, Alpakas, Dromedare und Kamele) zusätzlich so genannte Schwere-Ketten-Antikörper, welchen die leichten Ketten fehlen. Dadurch wird die Antigenbindung lediglich durch eine einzelne Domäne, die V_HH (variable heavy chain of heavy chain antibodies)-Domäne, vermittelt. Die V_HH-Domäne ist das kleinste bisher bekannte, natürlich vorkommende antigenbindende Fragment (~ 15 kDa) und zeichnet sich durch eine hohe Affinität und Spezifität zu ihrem Antigen aus. Aufgrund ihrer geringen Größe und Komplexität können V_HHs schnell und einfach als rekombinantes Protein in bakteriellen Expressionssystemen hergestellt werden. Darüber hinaus besitzen sie eine hohe Stabilität und Löslichkeit. Durch diese Eigenschaften stellen V_HHs eine vielversprechende Alternative zu klassischen Antikörpern und Antikörperfragmenten dar.

Schwerpunkt dieser Arbeit war es neue V_HHs zu identifizieren und zu charakterisieren, die für verschiedenste biochemische und zellbiologische Anwendungen geeignet sind. Um den vielfältigen Anforderungen in Anwendungen gerecht zu werden, wurde ein neues Selektionsverfahren entwickelt und etabliert, das so genannte *native panning*. In Kombination mit dem Protein-Protein-Interaktions *fluorescent two-hybrid (F2H) assay* wurde ein neuer Prozess zur Identifikation von antigenspezifischen V_HHs entwickelt.

Im Rahmen dieser Arbeit wurden antigenspezifische V_HHs gegen verschiedene Antigene identifiziert und charakterisiert. Darüber hinaus wurde deren Eignung und Funktionalität in verschiedenen biochemischen und zellbiologischen Anwendungen getestet. Zusammenfassend wurde ein effizienter und flexibler Prozeß zur Selektion und Identifikation von antigenspezifischen V_HHs für die Verwendung in einer Vielzahl von Anwendungen entwickelt und etabliert.



1 Introduction

The term „Antibody“ was first used in the last decade of the 19th century. In October 1890, Emil von Behring and Shibasaburo Kitasato mentioned the term “Antikörper” in their study “Ueber das Zustandekommen der Diphtherie-Immunität und der Tetanus-Immunität bei Thieren”(Behring and Kitasato, 1890). In their conclusion they suggested that antibodies are able to specifically eliminate diphtheria and tetanus toxins and thus completely prevent the symptoms of the diseases. In 1901 Behring was awarded The Nobel Prize in Physiology or Medicine for his findings.

Today, more than one hundred years after the first mention of antibodies, these molecules are one of the best studied and characterized proteins. This is not only due to their key function in the defense mechanism of higher vertebrates, but also due to their extensive use in biomedical research, diagnostics and therapy with many approaches being unimaginable without employment of antibodies. However, the remarkable success of antibodies has not yet reached its peak and new applications and approaches using antibodies are developed still.

1 Introduction

1.1 Antibodies

Upon an infection of a mammalian organism, two major systems try to counteract the pathogen invasion in the body. Initially, the innate immune system provides an immediate, non-specific response after the invasion of an unknown pathogen (Medzhitov, 2007) (Beutler, 2004). If the infection continues, the response of the adaptive immune system is initiated. The adaptive immune response is antigen-dependent and specific and is developed during the lifetime of an individual. It is based on a highly sophisticated interplay between a variety of different cell types and molecules among which lymphocytes and antibodies are the key elements. There are two types of lymphocytes, T cells and B cells. T cells are responsible for cellular immune response, while B cells are essential for the humoral immune response. In both cases the immune response is stimulated by specific antigens which can range from small chemical structures, through sugars, lipids, peptides and nucleotides to highly complex molecules, such as proteins or protein complexes (Delves and Roitt, 2000) (Collis et al., 2003).

During humoral immune response, B cells are providing both specific and long-lasting protection against a diverse range of pathogens (Harwood and Batista, 2010). Once an antigen is bound to the surface of a B cell via a B cell receptor (BCR), it gets internalized and processed into peptides (Parker, 1993). The processed antigen is returned to the B cell surface and presented via the Major Histocompatibility Complex (MHC) II for antigen specific helper T cell (T_H cell) recognition (Noelle and Snow, 1992). The physical contact between B and T_H cell triggers the production of specific interleukins including IL-4, IL-5 and IL-6 which in turn activate B cells (Parker, 1993). IL-4 activates clonal proliferation, while IL-5 and IL-6 induce the differentiation of the B cell. The activated B cells either differentiate into memory B cells providing long-term protection against secondary infection or into antibody secreting plasma cells (Reth, 1992).

1 Introduction

In the immune system antibodies are responsible for recognition and binding of foreign structures. They protect the host in different ways. First, they neutralize toxic effects of pathogens by binding pathogens and hence preventing infection. Second, they facilitate uptake of the pathogen by phagocytosis and third, they recruit natural killer (NK) cells by binding to the surface of a pathogen enabling NK cells to destroy the antibody-coated cells in a process called antibody-dependent cell-mediated cytotoxicity (ADCC).

1.1.1 Structure and Function of Antibodies

Antibodies are capable of specifically recognizing an enormous variety of different antigens, however, they do not recognize whole antigens, but parts of it referred to as epitopes. The diversity of antibodies is based on their modular architecture making it possible to generate up to 10^{15} different antibodies. The basic antibody molecule (~150 kDa) also referred to as immunoglobulin (Ig), consists of two identical heavy (H) chains and two identical light (L) chains, while two types of light chains (κ and λ) and five types of heavy chains (μ , δ , γ , ϵ and α) can be discriminated. Heavy and light chains are linked covalently by disulfide bonds (Porter, 1963). Both, the heavy (~ 50 kDa) and light chain (~25 kDa) are composed of two regions with distinct variability of their amino acid sequence (Johnson and Wu, 2000) (Hilschmann and Craig, 1965): the variable (V) region at the N-terminus and the constant (C) region at the C-terminus (Cohen and Milstein, 1967). Each light chain consists of one variable domain (V_L) and one constant domain (C_L). Each heavy chain, however, consists of one variable domain (V_H) and up to four constant domains (C_H). The so called hinge region is located between variable and constant regions of the heavy chain forming the typical Y-shaped structure of an antibody.

Antibody molecules can be cleaved in distinct fragments after incubation with the protease papain. It cuts the molecule in the hinge region to yield the Fab (fragment antigen binding; ~45 kDa) and the Fc (fragment crystallizable; ~50 kDa) part of the molecule (see

1 Introduction

Figure 1). The Fab part retains the antigen binding activity while the Fc part contains most of the constant region of the heavy chains (Delves and Roitt, 2000).

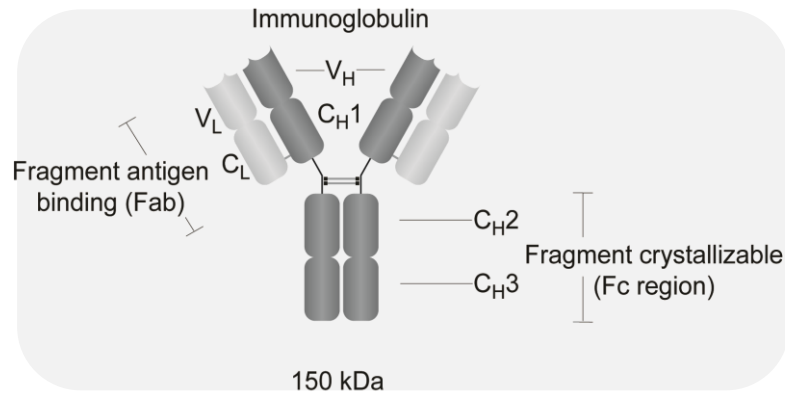


Figure 1: General structure of an immunoglobulin in higher vertebrates. It consists of two identical heavy (each consisting of V_H, C_H1, C_H2, C_H3) and two identical light chains (each consisting of V_L and C_L). Heavy and light chains are covalently linked by disulfide bonds. Figure modified from (Rothbauer et al., 2006).

Five classes of immunoglobulins can be discriminated, IgM, IgD, IgG, IgE and IgA which are defined by their heavy chain (C_H) classes also known as isotypes and designated by the lower Greek letters μ , δ , γ , ϵ and α . After activation of a B cell, IgMs are the first type of immunoglobulins which are secreted (Harriman et al., 1993). IgMs comprise the heavy chain μ and form a soluble pentamer for effective antigen binding. During a somatic recombination process called class switch recombination (CSR) (Li et al., 2004), the gene coding for C_H is changed from C _{μ} to C _{δ} , C _{γ} , C _{ϵ} or C _{α} , allowing for switch of isotype from IgM to either IgD, IgG, IgE or IgA, respectively.

These differences in the heavy chain composition are responsible for distinct characteristics and effector functions of each isotype. As described above, IgMs are the first antibodies to be produced and hence are responsible for activation of phagocytosis. IgA class antibodies are mainly found in mucosal surfaces. IgEs are involved in defense against parasites and play a major role in common allergic diseases whereas IgD isotypes exist only in minor amounts as antibody in serum and its function is still unsolved (Reth, 1992). During

1 Introduction

immune response of higher vertebrates IgGs are with 70-75% of the total immunoglobulins the most abundant antibodies (Cohen and Milstein, 1967).

The five isotypes also show structural differences including the number and location of disulfide bonds, the number of C domains and the length of the hinge region (see Figure 2). The hinge region connects the C_H1 and C_H2 domain and is responsible for the flexibility of an antibody molecule (Padlan, 1994). Since the length of the hinge region varies in the different isotypes, the distance between the antigen binding sites differs. While IgD, IgG and IgA class antibodies have a hinge region, IgM and IgE class antibodies are lacking a hinge region. However, the latter contain an extra C domain thus the C_H2 domain could be viewed as replacement for the hinge region.

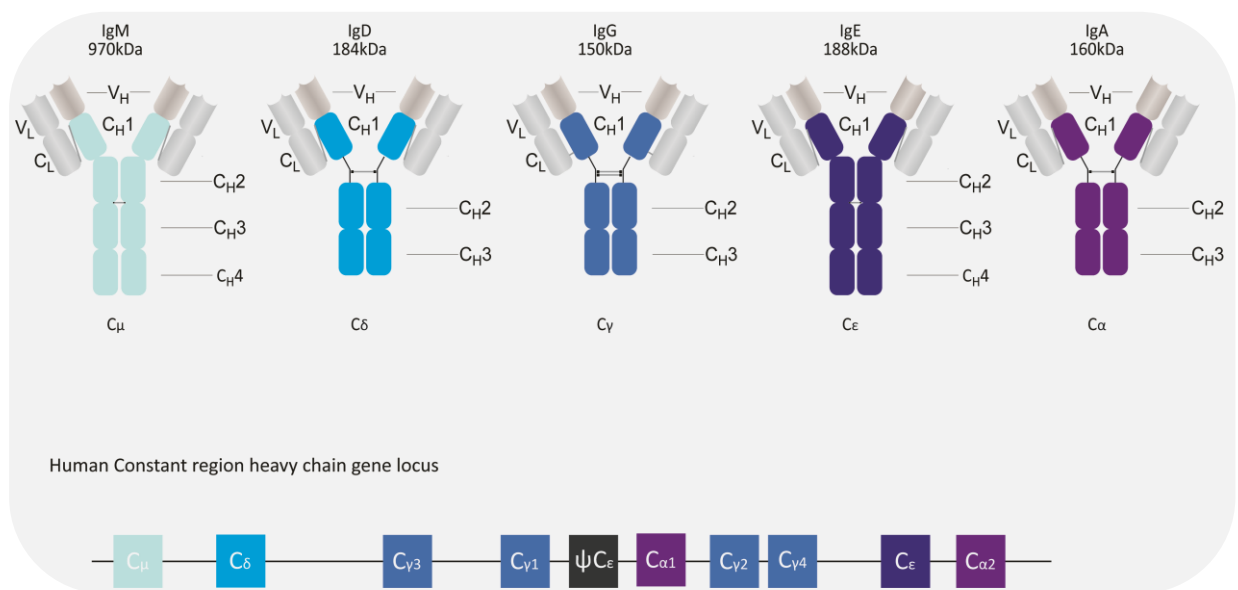


Figure 2: The immunoglobulin isotypes are encoded by a cluster of immunoglobulin heavy chain constant region genes. Each immunoglobulin consists of two identical heavy (V_H and C_H domains) and two identical light chains (V_L and C_L domain). The C region heavy chains are encoded by separate gene segments. The constant region for each isotype is indicated by the same color as the C region gene segment that encodes it. IgM and IgE lack a hinge, but each contains an extra heavy chain domain. Heavy and light chains are covalently linked by disulfide bonds (grey lines) in different number and location. One of the ε genes is a pseudogene (ψ). Figure modified from Murphy, 2012 (Murphy et al., 2012).

1 Introduction

In humans, IgGs can be further divided into four subclasses: IgG1, IgG2, IgG3 and IgG4. The IgG subclasses are named in order of abundance in serum: IgG1 70 %, IgG2 20 %, IgG3 7 % and IgG4 3 % (Ochs and Wedgwood, 1987). The structural differences among IgG subclasses lie in the length of the hinge region and in the distribution of the disulfide bonds (Ochs and Wedgwood, 1987).

IgGs specifically recognize and bind antigens through the variable region located at the N-terminus of the molecule. The variable region differs extensively between antibody molecules, but the sequence variability is not, however, distributed equally throughout the variable regions but concentrated in three so called hypervariable regions. When V_H and V_L domains are paired in the antibody molecule, three hypervariable loops from each domain are brought together creating a single hypervariable site: the antigen-binding site. The hypervariable loops form the complementarity determining regions (CDRs) – CDR1, CDR2 and CDR3. The CDRs are flanked by less variable and highly conserved regions which are called framework regions (FR) (Kabat, 1991). However, mutations in FRs are also known to influence binding since they play an important role in structure preservation, folding yield and stability of the antibody (David et al., 2007) (Padlan, 1994). The CDRs of the light chain are roughly six to ten amino acid residues in length, those of the heavy chain are roughly five to fifteen amino acid residues in length (see Figure 3) (Kabat, 1991) (Johnson and Wu, 2000) (Johnson and Wu, 2000), but they show wide variations in length between species (Collis et al., 2003) (Padlan et al., 1995), especially in the CDR3 of heavy chains (Kabat, 1991) which often plays a central role in antigen binding (Padlan, 1994).

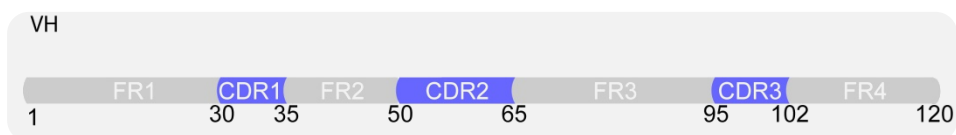


Figure 3: Schematic illustration of a V_H fragment. The three complementarity determining regions (CDRs) are flanked by four framework regions (FR). The numbering refers to the position of the amino acid along the sequence according to the Kabat numbering (Kabat, 1991).

1 Introduction

Since antigen-binding is mediated through CDRs from both V_H and V_L domains, it is the combination of heavy and light chain which determines the antigen specificity. As a result, antibodies naturally are bivalent with two antigen-binding arms of identical specificity (Delves and Roitt, 2000). Antibody-antigen interactions are non-covalent bonds such as hydrogen bonds, salt bridges and van der Waals bonds (van Oss et al., 1986) and the strength of binding is called affinity. The presence of two identical antigen-binding sites allows antibodies to bind simultaneously to two identical antigens and hence increases the total strength of the interaction. This cooperative mode of interaction is termed avidity.

1.1.2 Areas of Application

The extraordinary binding specificities of antibodies make them arguably most valuable tools in biomedical research, diagnostics and therapy. A major breakthrough was the development of the hybridoma technology by Georges Köhler and César Milstein in 1975. Before, polyclonal antibodies were used which recognize many epitopes of the same antigen and which are prone to batch-to-batch variability. By fusion of antibody-producing B cells from an immunized mouse with a myeloma cell line Köhler and Milstein were able to generate an immortal hybridoma cell, capable to generate limitless amounts of antibodies with single antigen specificity, called monoclonal antibodies (mAbs) (Kohler and Milstein, 1975).

In basic research, antibodies are key components in many technologies ranging from proteomics to cell-based assays. The most prominent examples are the Immuno (Western) blot, Immunoprecipitation, Immunofluorescence and Immunohistochemistry. The latter is the “gold standard” in the diagnosis of abnormal cells such as those found in tumors. In many applications in *in vitro* diagnosis antibodies also play a major role with antibody-based immunoassays being the most commonly used type of diagnostic assay (Borrebaeck, 2000). Due to their high specificities antibodies are used in numerous diagnostic tests to detect even very small amounts of drugs or hormones, e.g. monoclonal antibodies to human

1 Introduction

chorionic gonadotropin (HCG) are used in pregnancy test kits (Porter et al., 1988). The unique features of antibodies allow the development of sensitive and accurate assays to quantify and detect markers correlating with specific diseases. Especially the invention of the “sandwich immunoassay” which relies on two antibodies recognizing different epitopes in the same antigen increased the specificity of those assays (Maiolini and Masseyeff, 1975). In addition, antibodies are important clinical reagents used in diagnostic imaging when radiolabelled antibodies are injected into the patient e.g. to bind and to visualize specific antigens located on the surface of certain tumor cells (Holliger and Hudson, 2005).

With more than 20 approved mAbs and more than 200 mAb candidates in the clinical pipeline monoclonal antibodies have become established molecules for therapeutic applications (Nelson and Reichert, 2009). The efficiency of mAbs in cancer therapy lies in their capacity to discriminate tumor-associated antigens at low levels (Holliger and Hudson, 2005). Due to their bimodal mode of action with specific antigen binding on the one hand and effector function activation on the other hand, exogenously administered mAbs function like endogenous antibodies and recruit the body’s intrinsic effector mechanisms to fight cancer cells or inflammatory diseases. In addition, they can also be armed with anticancer drugs, radioisotopes or toxins (Boyiadzis and Foon, 2008).

1 Introduction

1.2 Display Technologies and Recombinant Antibody Formats

Antibodies are an important and growing class of research reagents and biopharmaceutical products. Despite being widely applied, conventional antibodies have several disadvantages. Naturally, immunoglobulins are secreted from plasma cells or are anchored at the cell surface as an essential part of the defense strategy against pathogens; however, their application in cell based assays within the cytoplasm of live cells is limited. The reducing environment of the cytoplasm prevents the oxidative formation of both inter- and intramolecular disulfide bonds which are essential for functional antibody folding (Cattaneo and Biocca, 1999) (Biocca et al., 1990). Thus, the general application of antibodies in cell based assays is restricted to endpoint assays in dead cells or tissues due to necessary fixation and permeabilization techniques.

For diagnostic *in vivo* imaging, the use of antibody molecules can be limited due to their isotype, since the constant Fc parts have the tendency to nonspecifically bind and visualize not only the target of interest but also other structures in the body (Harwood et al., 1985). Due to their complex composition and posttranslational modifications antibodies need to be manufactured in costly eukaryotic expression systems like mouse hybridoma cells (Steinmeyer and McCormick, 2008).

Furthermore, although in basic research monoclonal antibodies are very common and easily handled, the use of antibodies derived from nonhuman sources like mouse in human therapy, however, is hindered by the patients' immune response eliciting human anti-mouse antibodies (HAMA) (Carter, 2001). One approach to avoid this immune response is humanization of antibodies. This can be achieved either by recombinant grafting of the entire variable domains onto human constant regions (Morrison et al., 1988) or through generation of transgenic mice producing human immunoglobulins (Jakobovits, 1995). The most prominent humanized mAbs used in therapeutics are Rituximab (trade name Rituxan®) and Trastuzumab (trade name Herceptin®). Rituximab is used to treat rheumatoid arthritis

1 Introduction

and Non-Hodgkins-Lymphoma (Feldmann, 2002), Trastuzumab is used to treat breast cancer by targeting the human EGFR 2 receptor which is overexpressed on 20-30 % breast cancers (Boyiadzis and Foon, 2008).

Generation of monoclonal antibodies requires immune response following immunization. Thus, antibodies against non-immunogenic substances, such as non-protein components, toxic substances or highly conserved antigens are not easily obtained. In continuous search for improving and extending antibody applications, alternative recombinant antibody formats have been developed.

1.2.1 Recombinant Antibody Formats

Recombinant antibodies are produced by genetic engineering as opposed to naturally occurring in the body. Genetic engineering is used to create antibody libraries based on antibody gene segments that are diversified by mutagenesis. Since recombinant antibodies are generated outside an organism, it is possible to obtain antibodies which usually are not being elicited by the immune system, e.g. due to transient conformational change of an antigen after cofactor binding (Nizak et al., 2003). Among different recombinant antibody fragments scFvs (single-chain variable Fragment) and Fabs (fragment antigen binding) are the most prominent (Knappik and Brundiers) (see Figure 4).

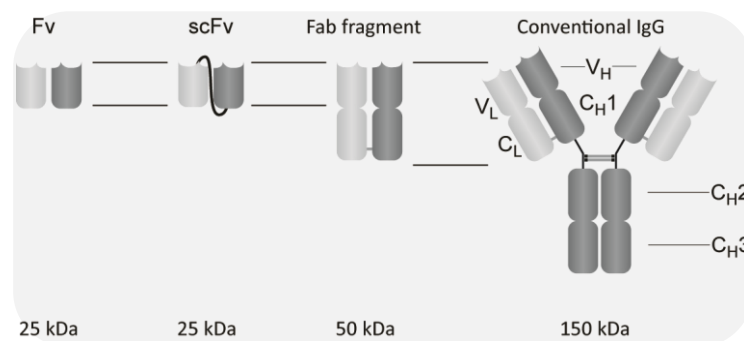


Figure 4: Schematic illustration of different antibody formats derived from conventional antibodies. In dark shading the heavy chain, the light chain in lighter shading. Modified after Zolghadr et al, 2007.

1 Introduction

1.2.1.1 ScFv fragments

The smallest antigen-binding fragment is the single Fv fragment, namely V_H or V_L domain. However, V_Hs have a rather hydrophobic interface which stabilizes the heterodimer with the V_L (Chothia et al., 1985). Thus, single V_H domains tend to aggregate since they have an exposed hydrophobic surface due to the missing V_L interaction (Ward et al., 1989). V_L domains on the other hand may dimerize with themselves and by this block the essential antigen binding site (Pluckthun, 1992).

The next smaller, but much more stable binding unit is the scFv fragment (~25 kDa) hence representing the minimal recombinant antigen-binding fragment of antibodies (Hudson, 1998). It consists of the two variable domains, V_H and V_L. Naturally, V_H and V_L domain are non-covalently associated via a hydrophobic interaction and tend to dissociate (Winter and Milstein, 1991). However, stable Fv fragments can be engineered by linking the two domains with a hydrophilic and flexible linker ((Gly4Ser)₃) to create a single-chain Fv (scFv) fragment (Huston et al., 1988). As scFvs are relatively small, unglycosylated proteins they can be produced in heterologous expression systems like bacteria or lower eukaryotes (Skerra and Pluckthun, 1988). For *in vivo* imaging scFvs provide fast and efficient tissue penetration and show only low non-specific background compared to intact antibodies. In addition, the small size of the fragments has been suggested to permit binding to cryptic epitopes not accessible to full-sized mAbs (Ward et al., 1989). However, scFvs demonstrate short circulating half-lives in the organism due to fast absorbance and excretion by the kidney (Sanz et al., 2005). Furthermore, therapeutic applications or diagnostic applications are still hampered by stability problems since scFvs still have a strong tendency to aggregate due to hydrophobic interactions in a hydrophilic environment (Cattaneo and Biocca, 1999).

1 Introduction

1.2.1.2 Fab fragments

Beside scFvs, Fab (~50 kDa) or F(ab)₂ (~100 kDa) fragments are the second commonly used recombinant antibody fragments. Fabs are generated by proteolytic digestion of full length antibodies and comprise the V_H and C_{H1} domains of the immunoglobulin heavy chain and the V_L and C_L domains of the light chain linked together by a disulfide bond. Fab fragments are used for diagnostic imaging (Behr et al., 1995) and recently were successfully tested for *in vivo* imaging (Elsasser-Beile et al., 2009). Fabs can also be expressed in heterologous systems, but at lower expression levels than scFvs (Hudson, 1998).

1.2.2 Display Technologies

As described above, recombinant antibodies are derived from antibody libraries. The most prominent Fab library is the HuCal library (Knappik et al., 2000) which is a synthetically generated library with randomized CDR-regions. To select desired antibodies from such libraries, display technologies such as bacterial display, ribosome display and phage display have proven to be powerful tools for obtaining antibodies. With these methods, recombinant binding molecules can be selected *in vitro* from comprehensive libraries derived synthetically (Knappik et al., 2000) or from immunized (He et al., 1999) or naïve animals (de Haard et al., 1999).

The basic principle of all display technologies is to physically link the phenotype (binding entity) to the genotype (genetic information) (He and Khan, 2005). While bacterial display enables the display of antibody fragments on surfaces of cells, ribosome display is a cell-free display technique which takes place completely *in vitro*. By generating antibody-ribosome-mRNA complexes individual antibody fragments are linked to their corresponding mRNA and selected through affinity capture via a ligand (Mattheakis et al., 1994; Hanes and Plückthun, 1997).

1 Introduction

1.2.2.1 Phage Display

The most widely used *in vitro* technology is the phage display technology which takes advantage of the coat protein of filamentous bacteriophages (Smith, 1985). The most commonly used bacteriophage in phage display is the filamentous M13 phage (see Figure 5), which can infect *E. coli* without killing or lysing the bacteria. These bacteriophages are characterized by a filamentary structure with a length of $\sim 1\text{-}2\ \mu\text{m}$ and a diameter of $\sim 7\ \text{nm}$. The phage genome of 6400 kb encodes for 11 proteins: five capsid proteins (pIII, pVI, pVII, pVIII, pIX), three assembly proteins (pI, pIV, pXI) and three replication proteins (pII, pV, pX). The capsid comprises five different proteins while pVIII being the most abundant with ~ 2700 copies. The tips of the phages contain five copies of pIII and pVI each on one side and five copies of pVII and pIX each on the other side.

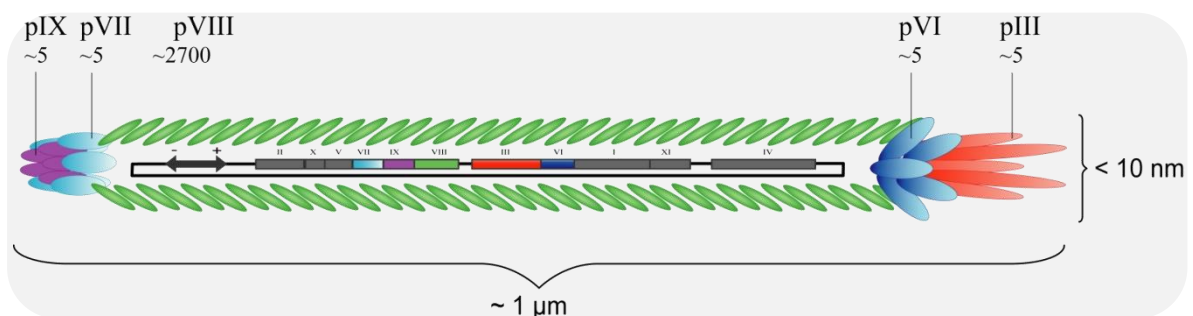


Figure 5: Schematic illustration of M13 phage. Modified from Jegg, 2007.

Phage display enables selection of peptides, proteins or antibodies with desired binding properties from a large collection of variants, a so called phage display library. Such libraries are generated by genetic fusion of genes of interest to those of phage coat proteins (pIII or pVIII) using a special phagemid vector which is then transformed in *E. coli*. Phagemids contain both an *E. coli* and a phage specific replication origin and a selection marker (resistance) (Arbabi Ghahroudi et al., 1997). However, phagemids lack genes responsible for packaging, replication and other coat proteins making them dependent on helper phages which are coinfecting with the phagemids into host bacteria encoding the proteins necessary

1 Introduction

to generate complete phage particles (Sidhu, 2001), hence resulting in release of phage particles expressing the encoded protein on their tip (*display*). In case of antibody phage display, antibodies or antibody fragments are presented.

After infection of phagemid transformed *E. coli* with the bacteriophage, phage particles with the antibody fragment on their tips are released. The appropriate antibody is selected by exposing the phage library to an immobilized antigen, a technique known as panning (McCafferty et al., 1990). During this process, phages that display an antibody fragment which binds to the immobilized antigen will be retained while non-adherent phages will be washed away. Bound phages can be recovered from the surface, reinfected into bacteria and regrown for the next round of enrichment (Willats, 2002) (see Figure 6).

Even being the most widely used selection method for antibody fragments, panning with immobilized antigen may have serious drawbacks regarding the selection of antibody fragments specific for natively folded antigens. Although the immobilization of antigens on plastic surfaces is usually very efficient, it may be problematic since the passive adsorption on plastic is a mechanism of protein denaturation. It has been shown that protein molecules when absorbed on to polystyrene undergo conformational changes (Davies et al., 1994). Hence, antigens may become partially denatured, leading to the selection of antibody fragments which recognize epitopes, only present in denatured molecules (Chames et al., 2001).

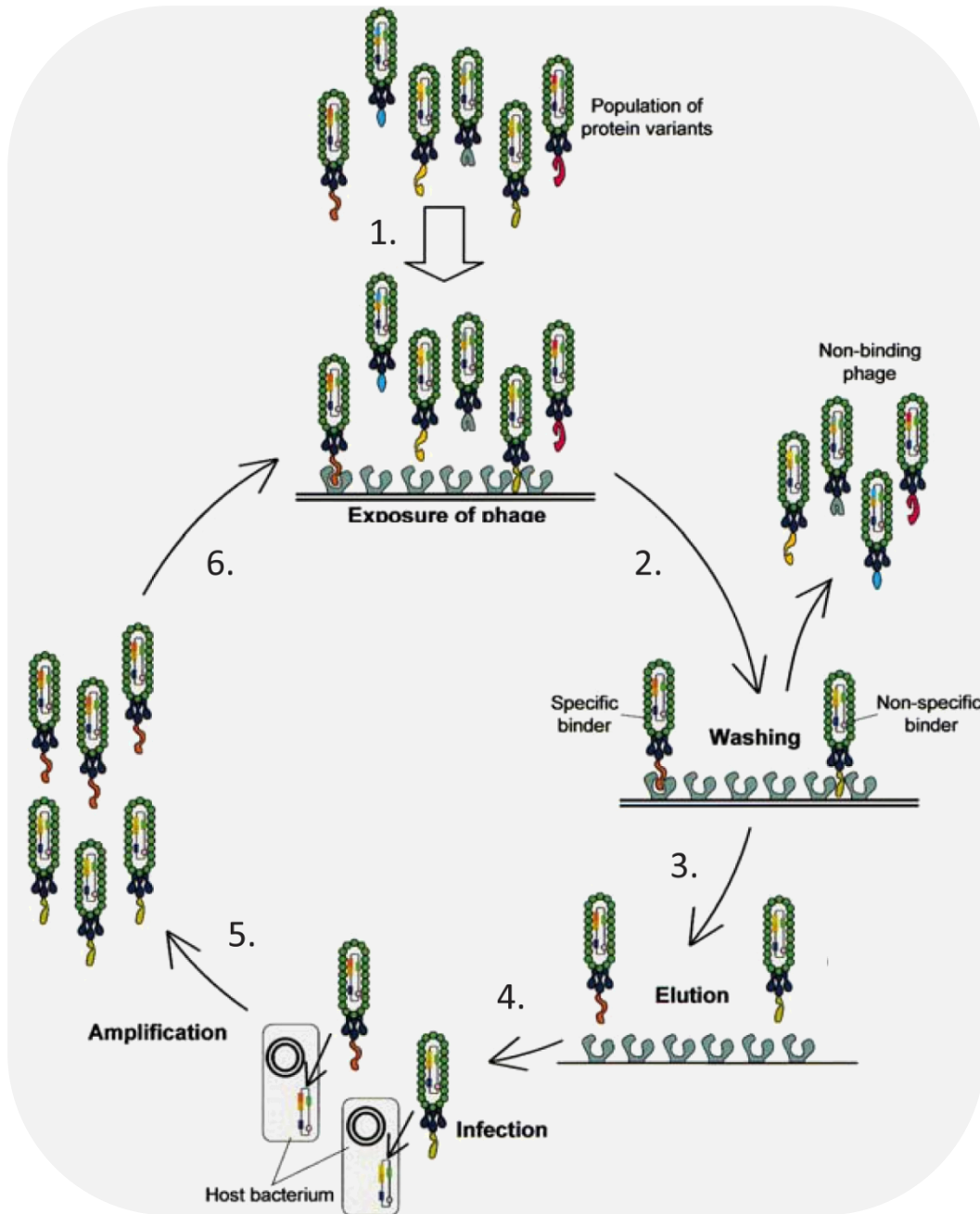


Figure 6: Panning. A phage library with phages presenting antibody variants at their tips is exposed to immobilized antigens (1.). Non-binding phages are washed off, however, some non-specific binding may occur (2.). Bound phages are eluted (3.). Eluted phages are used for infection of *E. coli* (4.). By amplification of the bacteria a further library is generated (5.) and used for the next phage display cycle (6.). Figure modified from Willats et al., 2002.

1.3 Heavy chain antibodies

In search of smaller antigen binding fragments still capable of recognizing antigens with high specificity and affinity, Hamers-Casterman and colleagues made a remarkable discovery in 1993. They found a structurally different kind of antibodies which are part of the humoral immune response in the serum of camelids (camels, dromedaries, llamas, alpacas) (Hamers-Casterman et al., 1993). In addition to conventional IgG antibodies (as described in 1.1), which are well conserved among mammals, camelids contain so called heavy chain antibodies (hcAbs). Accordingly, these antibodies are composed of heavy chains only and are devoid of light chains. HcAbs are absent in other mammals except in pathological cases where parts of the V domain and/or C_H1 exon have been removed (Alexander et al., 1982). Nevertheless, in 1995 Greenberg and colleagues found similar hcAbs in nurse sharks (Greenberg et al., 1995), but evolutionary analysis showed that camelid and shark hcAbs evolved independently (Nguyen et al., 2002). There are many speculations about the driving force for the emergence of heavy chain antibodies in such distantly related species, however, the rationale for the presence of hcAbs is plausible: in addition to the big conventional antibodies, small, single domain antigen binding fragments provide access to inaccessible epitopes like catalytic centers of enzymes (Flajnik et al., 2011).

1.3.1 Structure of Camelidae heavy chain antibodies

HcAbs of camelids derive from classical IgG antibodies and account for 50 % of the circulating immunoglobulins in dromedary (Muyldermans, 2001). The overall structure of the hcAbs resembles that of the classical immunoglobulins with a number of important deviations (see Figure 7). First, the heavy chain of hcAbs is composed of three instead of four domains, the V domain being joined directly to the hinge region and the Fc (Hamers-Casterman et al., 1993). While the two constant domains at the C terminus (C_H2 and C_H3) are highly homologous to the Fc domains of classical antibodies, the C_H1 domain is missing in

1 Introduction

hcAbs. Second, as mentioned above, the light chains are completely absent in hcAbs. Hence, the Fab is reduced to a single variable domain, the so called $V_{\text{H}}\text{H}$ (variable domain of heavy chain antibodies) domain or Nanobody. Antigen binding occurs through this single domain only, representing the smallest intact antigen binding fragment (~ 15 kDa) derived from a functional immunoglobulin.

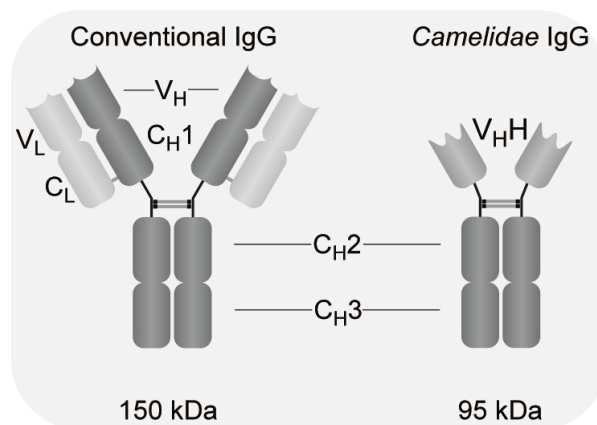


Figure 7: Schematic illustration of a conventional IgG and a Camelidae heavy chain antibody. Antibodies from camelids comprise two heavy chains (each of $V_{\text{H}}\text{H}$, $C_{\text{H}}2$ and $C_{\text{H}}3$) only. These antibodies lack the light chains and the $C_{\text{H}}1$ domain. Antigen binding occurs through one domain only, the $V_{\text{H}}\text{H}$ domain. Figure modified from Rothbauer et al., 2006.

1.3.2 Genetic background of functional heavy chain antibodies

The existence of functional hcAbs required some modifications in the composition of an antibody molecule in order to get along with the loss of the light chain. The first quite obvious modification is the deletion of the $C_{\text{H}}1$ domain which is involved in the assembly process of heavy and light chains of classical antibodies. Heavy chains, after being synthesized, are retained in the endoplasmic reticulum by a chaperon called heavy-chain binding protein (BiP) until they associate with a light chain (Hendershot et al., 1987). The binding of BiP occurs at the $C_{\text{H}}1$ domain. Only after the substitution of the BiP by the light chain, the antibody molecule can proceed towards its secretion. Hence, in hcAbs the absence of the $C_{\text{H}}1$ domain enables the heavy chain to bypass this BiP capturing mechanism

1 Introduction

without the need of being rescued by the light chain. The absence of the C_H1 domain in hcAbs is caused by a mutation in the splice site immediately after the C_H1 exon (Nguyen et al., 1999) (Woolven et al., 1999). These point mutations at the 3' end of the C_H1 are responsible for the removal of the C_H1 encoding sequences by splicing during mRNA maturation (Nguyen et al., 2002).

Compared to human V_H domains, the V_HH FRs show 80 % sequence homology (Muyldermans, 2001). However, in the FR2 region V_HHs show four characteristic amino acid substitutions: Val37Phe or Val37Tyr, Gly44Glu, Leu45Arg or Leu45Cys and Trp47Gly (from V_H to V_HH; numbers refer to the amino acid positions numbered according to Kabat et al. (Kabat, 1991)) (Muyldermans et al., 1994) (see Figure 8). In classical antibody development these V_H residues specifically interact with the V_L domain via hydrophobic interactions. In the absence of a V_L domain, these hydrophobic residues would likely cause unspecific aggregation of hcAbs, when this surface would be exposed to the aqueous environment. Hence, evolutionary conserved substitution of these V_H residues by more hydrophilic residues in V_HHs referred to as hallmark residues (Muyldermans et al., 1994), presumably lowers their tendency to interact with a V_L domain (Muyldermans, 2001) and increase hcAb solubility.

1 Introduction

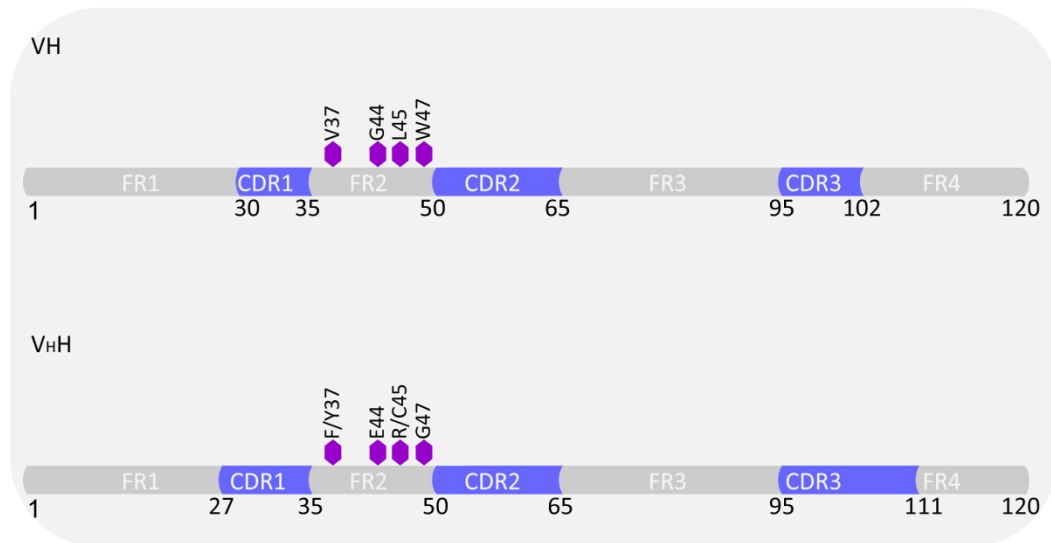


Figure 8: Substitutions in amino acid sequence from V_H s to V_{HH} s. The numbering refers to the position of the amino acid along the sequence according to the Kabat numbering (Kabat, 1991).

As already mentioned, camelids carry both conventional antibodies and hcAbs. Generally, the heavy chain variable domain (both V_H and V_{HH}) is encoded not only by one but multiple gene segments (Hozumi and Tonegawa, 1976) (Tonegawa, 1983) (Delves and Roitt, 2000): the V (*variable*) gene segment, the J (*joining*) gene segment and the D (*diversity*) gene segment (Schilling et al., 1980). During B cell differentiation, the gene segments are specifically ligated in a process called VDJ recombination to form a complete heavy chain variable exon (Tonegawa, 1983) in which the V gene segment encodes the CDR1 and CDR2, while the CDR3 is generated by the joining of the three gene segments. In order to achieve the amino acid substitutions which are specific for V_{HH} s, camelid heavy chains do not arise from the same V genes as classical antibodies (Nguyen et al., 1999). V_{HH} s are encoded by a distinct set of V segments (~40 V segments) resulting in the replacement of specific amino acids in the hydrophobic part which in classical antibodies interacts with the V_L by hydrophilic amino acids (see Figure 9) (Nguyen et al., 2000).

1 Introduction

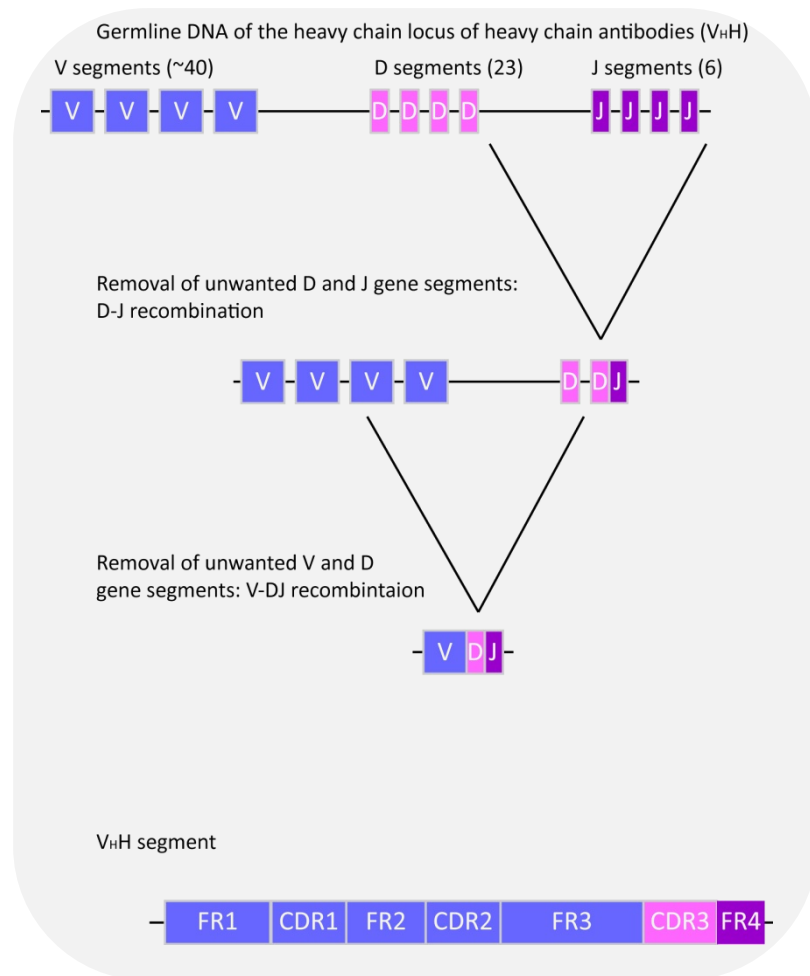


Figure 9: Schematic illustration of VDJ-recombination of the heavy chain locus of heavy chain antibodies (V_H). The heavy chain V regions are assembled from three gene segments. First, the diversity (D) and J segments join which are used for conventional antibody recombination, as well. Then, the V gene segment which is specific for V_H s joins to the DJ segment resulting in a complete V_H exon. The number of gene segments in each region is shown in parentheses.

The existence of only one heavy chain variable fragment may raise the question how the repertoire of V_H s is diversified since the random pairing of V_H and V_L in higher vertebrates further enhances diversification. First, the antibody repertoire in camelids is increased by the expansion of V gene segments having acquired V_H characteristics as described above. Second, hcAbs show more hotspots for somatic hypermutation in the V_H CDR1 region making this region more variable (Nguyen et al., 2000). The process of somatic

1 Introduction

hypermutation (SHM) occurs in activated B cells after finishing gene rearrangements by VDJ recombination (Honjo et al., 2002). SHM alters the DNA sequence of secreted immunoglobulins and further enhances the affinity of the antibody repertoire by introducing point mutations at high rate into the V regions, preferentially into CDRs (Wu et al., 1979). The frequency of mutations in the V region is approximately $10^{-5} - 10^{-3}$ /base pair/generation which is ~ 1 million-fold higher than the spontaneous rate of mutation in most other genes (Rajewsky et al., 1987). However, the extent of SHM in hcAb V domains is much higher than in the classical V_{Hs} (Conrath et al., 2003). Third, CDR3s of V_{Hs} are exceptionally long (up to 17 amino acid residues in dromedary V_{Hs}) compared to the length of CDR3s of conventional V_{Hs} (up to 11 amino acid residues in dromedary V_{Hs}) which might compensate part of the diversity that is provided by the V_L binding site in conventional antibodies (Conrath et al., 2003). This extended CDR3 is often stabilized by an additional disulfide bond cross-linking the CDR3 and CDR1 in camel or CDR3 and CDR2 in llama (Wesolowski et al., 2009).

1.3.3 Unique features of V_{Hs}

V_{Hs} have characteristics that are similar to those - or even exceed those - of classical antibodies. Several advantages result from their single-domain nature and small size of approximately 15 kDa such as rapid blood clearance and fast tissue penetration. In addition, when constructing phage display libraries, the single-domain nature of V_{Hs} offers an advantage over conventional antibody Fab or scFv fragments. Since antigen binding occurs only through one domain which is encoded by one single exon, there is no need for random recombination of the V_H and V_L domains (Verheesen et al., 2006).

Contrary to classical antibodies, V_{Hs} have been found to be outstandingly stable. For instance, they not only show extreme thermal stability at high temperatures of up to 90°C (van der Linden et al., 1999) or after incubation for one week at 37°C (Arbabi Ghahroudi et al., 1997) and maintain their functionality in extremes of pH, in denaturing conditions and

1 Introduction

even in the presence of proteases (van der Linden et al., 1999). Their stability at high temperature indicates that V_HHs have a very good shelf-life and their stability in extremes of pHs enable them to survive under harsh conditions found in the stomach and to remain functional in the gut creating opportunities for oral delivery (Harmsen and De Haard, 2007). Furthermore, V_HHs are naturally soluble in aqueous solutions and show a very low tendency to aggregate, likely due to the increased hydrophilicity of the residues in the FR2 region (Muyldermans, 2001).

V_HHs are suitable for large-scale production in bacterial systems or lower eukaryotes. For example the production process of V_HHs is easily scalable in yeast expression systems with expression levels up to ten times higher than e.g. scFvs (Muyldermans et al., 2009). These production systems enable to produce V_HHs in constant quality which is crucial for their use in diagnostics or therapy.

V_HHs have been shown to have a preference for binding into active sites of enzymes due to their CDR3 regions forming fingerlike extensions (Lauwereys et al., 1998) (De Genst et al., 2006). Hence, V_HHs are able to recognize epitopes which are barely recognized by classical antibodies (Lauwereys et al., 1998). Although they consist of just one single domain it has been shown, that V_HHs bind their antigen specifically with nanomolar affinity (Muyldermans and Lauwereys, 1999).

The single-domain nature of V_HHs could, however, be disadvantageous for binding to small antigens. Peptides or haptens usually bind in a groove or cavity at the V_H-V_L interface (Harmsen and De Haard, 2007). Indeed, Lange et al. immunized llamas with clenbuterol and found conventional but not heavy chain antibodies against this hapten (Lange et al., 2001). Still, V_HHs recognizing peptides or haptens have been successfully isolated (Spinelli et al., 2000) (Ladenson et al., 2006) (Harmsen et al., 2007).

1.3.4 Applications of V_HHs

Owing to their unique biochemical characteristics and robustness, V_HHs are attractive reagents for a variety of diagnostic and therapeutic applications. So far, fast and reliable *in vivo* diagnosis of cancer at an early stage of disease progression remains a major challenge. Ideally, a cancer-imaging agent should visualize the smallest cancer-associated tissues with low levels of unspecific background. Due to fast blood clearance and good tissue penetration V_HHs appear to be promising tools for such *in vivo* imaging approaches. It was shown that a nanobody specifically recognizing lysozyme targeted tumours transgenic for lysozyme (Revets et al., 2005). Furthermore, in cancer diagnostic tests (e.g. prostate cancer) V_HHs are able to differentiate between different isoforms of prostate-specific antigen (PSA) and hence discriminate different stages of prostate cancer (Saerens et al., 2004).

Besides diagnostic applications for *in vivo* imaging, V_HHs have proven useful as specific drug delivery vehicles in tumor targeting (Cortez-Retamozo et al., 2004). Due to their small size they are able to reach hidden antigens delivering the toxic load to the cancerous tissue while healthy cells stay unharmed. Further potential therapeutic areas include inflammation, pulmonary diseases and neurology (Roovers et al., 2007) (Cortez-Retamozo et al., 2004) (Coppieters et al., 2006) (Ablynx, 2012).

1.3.4.1 Chromobodies and Nanotraps

Besides therapeutic and diagnostic approaches, V_HHs are versatile tools for biomedical research. With the rapid expansion of proteomic studies there is a need for the generation of highly specific binding reagents to study the vast number of proteins encoded by the genome (He and Khan, 2005). As recombinant produced and purified protein, V_HHs can be chemically coupled to beads (Rothbauer et al., 2008), matrices (Pichler et al., 2012) and chip surfaces to specifically extract antigens of interest from crude solutions for detection or more complex downstream analysis such as enzymatic activity assays or protein-protein

1 Introduction

interactions. Accordingly, in such *in vitro*-based format, V_HHs are termed Nanotraps (see Figure 10). Nanotraps are widely used in high-throughput proteomics and the manipulation of proteins (Trinkle-Mulcahy et al., 2008) (Webby et al., 2009) (Kirchhofer et al., 2010).

In 2006 it has been shown that V_HHs are not only valuable tools in biochemical assays but may also be used for dynamic antigen detection in living cells and thus enable a novel mode of subcellular analysis (Rothbauer et al., 2006). In modern live cell biology, fluorescent fusion proteins are used to study the spatiotemporal dynamics of a given protein of interest. For this purpose, fluorescent proteins (e.g. green fluorescent protein, GFP (Tsien, 1998)) are fused to the N- or C- terminus of the protein of interest. However, this fusion might result in masking of important domains of the protein. In addition, artificial introduced fluorescent fusion proteins are overexpressed in the cell and may behave differently from their endogenous counterparts who remain invisible (Chalfie et al., 1994) (Leonhardt et al., 1998).

To detect and visualize endogenous proteins, antibodies are used as immunofluorescence reagents. For this purpose, however, the cells to be analyzed have to be fixed and permeabilized so that exogenously added, fluorescently labeled antibodies may enter the cells to bind and visualize their antigens. In contrast to classical antibodies, which are not functional in living cells, V_HHs are small and stable enough to maintain their antigen binding function even in the reducing environment of the cell. Thus, genetic fusion of a V_HH with a fluorescent protein (see Figure 10) enables antibody-mediated detection of endogenous proteins in live cells (Rothbauer et al., 2006). As a consequence, these so-called Chromobodies combine features of recombinant fluorescent fusion proteins and antibody-based detection and may provide data about mobility and dynamics of endogenous proteins localized in different subcellular compartments.

1 Introduction

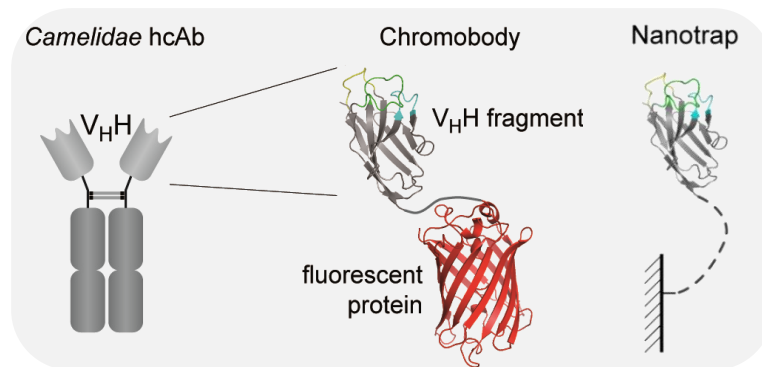


Figure 10: Chromobody and Nanotrap. Chromobodies result from the genetic fusion of the V_HH domain with a fluorescent protein. V_HHs coupled to immobilizing matrices are termed Nanotraps. Modified after Rothbauer et al., 2006.

1 Introduction

1.4 Aims and Objectives

Antibodies are powerful tools in biomedical research, diagnostics and therapy. However, they have many drawbacks due to their size and complex structure. Naturally occurring heavy chain antibodies of camelids recognize and bind their antigens through one domain only, the V_HH domain. The unique features of V_HH domains enable to circumvent the drawbacks of classical antibodies not only through their small size but also through their single-domain nature. The work presented in this thesis focuses on the generation and characterization of antigen specific V_HHs.

The aim of this work is to use the non-conventional immune system of alpacas to generate functional V_HHs against different antigens ranging from fulllength proteins to domains and peptides. These V_HHs are analyzed, characterized and compared in terms of their *in vitro* and *in vivo* functionality. However, specific V_HHs are not easily obtained. In the course of this work optimization in library generation and phage display methods are performed. Adjustments in the generation process of V_HH libraries are necessary since the quality concerning size and diversity is crucial to obtain specific V_HHs. Phage display needs to be adjusted not only with regards to the corresponding antigen, protein or peptide, but also to the application of V_HHs - intracellular or for *in vitro* studies.

The methodology behind this work will be described in chapter 2 and the results will be presented in chapter 3 followed by a discussion in chapter 4.

2 Materials and Methods

2.1 Material

2.1.1 Consumables

Table 1: Applied consumables.

CONSUMABLE	MANUFACTURER
Adhesive Film, aluminium, 96W	VWR International, Ismaning, Germany
Amicon® Ultra Centrifugal Filter Devices	Millipore S.A.S., Molsheim, France
Assay Block, 96 well, 2 ml	Schubert & Weiss, Munich, Germany
Cell Culture Plates, p100	Schubert & Weiss, Munich, Germany
Coverslips 18 x 18 x 0.17 mm	Carl Roth GmbH & Co. KG, Karlsruhe, Germany
Cryotubes, 1,8 ml	Nunc GmbH, Wiesbaden-Biebrich, Germany
Desalting Column PD-10	GE Healthcare, Uppsala, Sweden
ECL (enhanced chemiluminescence)	AG Böttger, LMU Munich, Germany
Electroporation cuvettes	Bio-Rad Laboratories GmbH, Munich, Germany
Falcon Tubes (15 und 50 ml)	Sarstedt AG & Co., Nümbrecht, Germany
Film Super RX 100 NIF 13x18	FUJIFILM PHOTO FILM EUROPE GMBH, Dusseldorf , Germany
Filtropur S 0.45	Sarstedt AG & Co., Nümbrecht, Germany
Filtropur S 0.2	Sarstedt AG & Co., Nümbrecht, Germany
First-Strand cDNA Synthesis Kit	GE Healthcare, Uppsala, Sweden
GFP-multiTrap	ChromoTek GmbH, Martinsried, Germany
Größenstandard DNA (Smart Ladder)	EUROGENTEC s.a., SERAING, Belgium
GST-Trap FF column, 1 ml	GE Healthcare, Uppsala, Sweden
HiTrap™ HP column, 1 ml	GE Healthcare, Uppsala, Sweden
Immuno Plates Maxisorp C 96	Thermo Scientific GmbH, Schwerte, Germany

2 Materials and Methods

Immunotubes Nunc-Immuno, Polystyrene StarTube, MaxiSorp	Thermo Scientific GmbH, Schwerte, Germany
Ligation-Kit 1. T4 DNA Ligase (400,000 units/ml) 2. 10x T4 DNA Ligase Reaction Buffer (500 mM Tris-HCl ; 100 mM MgCl ₂ ; 10 mM ATP ; 100 mM Dithiothreitol ; 250 µg/ml BSA ; pH 7,5)	New England Biolabs, Ipswich, England
Midiprep System PureYield Plasmid	Promega GmbH, Mannheim, Germany
Microscope Slides	VWR International, Ismaning, Germany
µClear 96-well microplate	Greiner Bio-One, Frickenhausen, Germany
µ-slide(I or IV)	Ibidi GmbH, Martinsried, Germany
Multiwell plate, 6 well, steril	Nunc GmbH, Wiesbaden-Biebrich, Germany
Nitrocellulose Membrane	Bio-Rad Laboratories GmbH, Munich, Germany
NucleoSpin Gel and PCR Clean-up Kit	Macherey-Nagel, Düren, Germany
NucleoSpin RNA XS	Macherey-Nagel, Düren, Germany
Parafilm	Brand GmbH & Co. KG, Wertheim, Germany
PCR-Reaction tube, 200 µl/500 µl	Sarstedt AG & Co., Nümbrecht, Germany
PD-10 desalting column	GE Healthcare, Uppsala, Sweden
Petridish, 92 x 16 mm	Sarstedt AG & Co., Nümbrecht, Germany
Petridish, 145 x 20 mm	Greiner Bio-one, Frickenhausen, Germany
pH Indicatorstrips, pH 0-14	Merck KGaA, Darmstadt, Germany
Pipettes (2, 5, 10 und 25 ml)	Sarstedt AG & Co., Nümbrecht, Germany
Pipettetips (10, 20, 200, 1000, 1250 µl)	Sarstedt AG & Co., Nümbrecht, Germany
Reaction tube 1,5 ml / 2 ml (steril)	Sarstedt AG & Co., Nümbrecht, Germany
Superdex 75 10/300 GL	GE Healthcare, Uppsala, Sweden
UltraVette® UV-Küvetten Mikro, 70 – 850 µl	Carl Roth GmbH & Co.KG, Karlsruhe, Germany
UNI-SepMAXI Lymphocyte Separation Tubes	Novamed Ltd., Jerusalem, Israel

2 Materials and Methods

Vaccumbottle without sodium citrate (250 ml) Evozone, Reutlingen, Germany

2.1.2 Solutions and Chemicals

Table 2: Applied solutions and chemicals.

SOLUTIONS AND CHEMICALS	MANUFACTURER
1,4 Dithiothreitol (DTT)	Sigma-Aldrich Chemie GmbH, Munich, Germany
2-Propanol	Carl Roth GmbH & Co. KG, Karlsruhe, Germany
2x YT Medium (2xYT)	Carl Roth GmbH & Co. KG, Karlsruhe, Germany
3,3',5,5'-Tetramethylbenzidin (TMB)	Carl Roth GmbH & Co. KG, Karlsruhe, Germany
Acetic Acid, 99-100%	Carl Roth GmbH & Co. KG, Karlsruhe, Germany
Agarose, molecular biology grade	Serva Electrophoresis GmbH, Heidelberg, Germany
Ammoniumperoxodisulfat (APS)	Carl Roth GmbH + Co KG, Karlsruhe
Ampicillin	AppliChem GmbH, Darmstadt, Germany
ATTO dyes (NHS Ester)	ATTO-TEC GmbH, Siegen, Germany
β -Mercaptoethanol	
BSA	Sigma-Aldrich Chemie GmbH, Munich, Germany
Coomassie Brilliant Blue G250	Serva Electrophoresis GmbH, Heidelberg, Germany
DAPI (4,6-diamidino-2-phenylindole)	Roche Diagnostics GmbH, Mannheim, Germany
DMEM, high Glucose	Sigma-Aldrich Chemie GmbH, Taufkirchen, Germany
di-sodium hydrogen phsophat	Merck KgaA, Darmstadt, Germany
DMSO 100%	Finnzymes Oy, Espoo, Finland
Dnase I	Diagonal GmbH, Münster, Germany
dNTP-Set (dATP, dCTP, dGTP, dTTP, pH 7.5)	PEQLAB Biotechnologie GmbH, Erlangen, Germany

2 Materials and Methods

EDTA	AppliChem GmbH, Darmstadt, Germany
Ethanol, absolut	Sigma-Aldrich Chemie GmbH, Munich, Germany
Ethanol, denatured	Carl Roth GmbH & Co. KG, Karlsruhe, Germany
Ethidiumbromid-Solution (0,025 %)	Carl Roth GmbH & Co. KG, Karlsruhe, Germany
Fluorescein isothiocyanate (FITC)	Thermo Scientific GmbH, Schwerte, Germany
Formaldehyde (37%)	Sigma-Aldrich Chemie GmbH, Munich, Germany
FCS "Gold"	PAA Laboratories GmbH, Cölbe, Germany
Gentamycin (50 mg/ml)	PAA Laboratories GmbH, Pasching, Austria
Gerbu Pharma Adjuvant	Gerbu Biotechnik GmbH, Heidelberg, Germany
Glucose D(+)	Carl Roth GmbH & Co. KG, Karlsruhe, Germany
Glycine	Carl Roth GmbH & Co. KG, Karlsruhe, Germany
Heparin Natrium 25.000	Ratiopharm GmbH, Ulm, Germany
Hydrochloric acid 37%	AppliChem GmbH, Darmstadt, Germany
Hydrogen Peroxide	Fluka Chemie AG, Germany
Hyperphage (M13K07ΔpIII)	Progen Biotechnik GmbH, Heidelberg, Germany
Imidazol	Sigma-Aldrich Chemie GmbH, Munich, Germany
Isopropyl-beta-D-thiogalaktopyranosid (IPTG)	Diagonal GmbH, Münster, Germany
Kanamycin	
Lipofectamin 2000	Life Technologies GmbH, Darmstadt, Germany
LSM 1077 Separation Solution for Lymphocytes	PAA Laboratories GmbH, Pasching, Austria
Luria Broth (LB) Medium	Carl Roth GmbH & Co. KG, Karlsruhe, Germany
Lysozyme	
Magnesium chloride	Sigma-Aldrich Chemie GmbH, Munich, Germany
Methanol, min. 99 %	Carl Roth GmbH & Co. KG, Karlsruhe, Germany
Milkpowder, Blotting Grade	Carl Roth GmbH & Co. KG, Karlsruhe, Germany
NHS-activated Sepharose™ 4 Fast Flow	GE Healthcare, Uppsala, Sweden

2 Materials and Methods

PageRuler™ Prestained Protein Ladder/ PageRuler™ Prestained Protein Ladder Plus	Fermentas GmbH, St.Leon-Rot, Germany
PEI, pH 7/pH10	A. Gahl, LMU Munich, Germany
Phosphate Buffered Saline (PBS), 1x	Sigma-Aldrich Chemie GmbH, Munich, Germany
Phusion™ High-Fidelity DNA Polymerase	New England Biolabs GmbH, Frankfurt, Germany
Pierce protein free blocking buffer	Thermo Scientific GmbH, Schwerte, Germany
Protease Inhibitor Mix M	SERVA Electrophoresis GmbH, Heidelberg, Germany
Polyacrylamide	Carl Roth GmbH & Co. KG, Karlsruhe, Germany
Restrictionenzymes	New England Biolabs GmbH, Frankfurt, Germany
Phenylmethanesulfonylfluoride (PMSF)	SERVA Electrophoresis GmbH, Heidelberg, Germany
Ponceau S	Sigma-Aldrich Chemie GmbH, Munich, Germany
Potassium chloride	Sigma-Aldrich Chemie GmbH, Munich, Germany
RNase A (10 mg/ml)	
Select Agar	Invitrogen GmbH, Karlsruhe, Germany
Smart Ladder / Smart Ladder SF DNA Standard	Eurogentec, Seraing, Belgium
Sodium bicarbonate	Sigma-Aldrich Chemie GmbH, Steinheim, Germany
Sodium carbonate	Sigma-Aldrich Chemie GmbH, Steinheim, Germany
Sodium chloride	Carl Roth GmbH & Co. KG, Karlsruhe, Germany
Sodium dodecyl sulfate pellets (SDS)	Carl Roth GmbH & Co. KG, Karlsruhe, Germany
Sodium hydroxide pellets	
Sulfuric acid, 96 %	Carl Roth GmbH & Co. KG, Karlsruhe, Germany
TEMED	Carl Roth GmbH & Co.KG, Karlsruhe, Germany

2 Materials and Methods

Tris (trisaminomethane)	Carl Roth GmbH & Co. KG, Karlsruhe, Germany
Triton X-100	Carl Roth GmbH & Co.KG, Karlsruhe, Germany
TRIzol Reagent	Life Technologies, Carlsbad, USA
Trypsin/EDTA (1:250)	PAA Laboratories GmbH, Cölbe, Germany
Tween 20	Carl Roth GmbH & Co.KG, Karlsruhe, Germany
Vectashield Mounting Medium	Vector Laboratories Inc., Burlingame, USA

2.1.3 Instruments

Table 3: Applied instruments.

INSTRUMENT	MANUFACTURER
Agarosegelsystem (Mupid)	Bangkok Advanced Technologx Co., Bangkok, Thailand
ÄKTA purifier FPLC-system	GE Healthcare, Uppsala, Sweden
Balance BL 1500S	Sartorius AG, Göttingen, Germany
Digital Sonifer Model 450-D	Branson
DU® 730 Life Science UV/Vis Spectrophotometer	Beckman Coulter
Electroporator	Bio-Rad Laboratories GmbH, Munich, Germany
Epifluorescence microscope Axiovert 135 TV	Zeiss, Jena, Germany
Film developping machine CP1000	AGFA
Geldocumentation system FluorChem 8900	Alpha Innotech Corporation, San Leandro, USA
InCell Analyzer 1000	GE Healthcare, Uppsala, Sweden
Incubator for bacteria	Heraeus
Infinite M1000 Plate reader	Tecan Group Ltd., Männedorf, Switzerland
NanoVue Plus Spectrophotometer	GE Healthcare Biosciences AB, Uppsala, Sweden
Proteingel apparatus Mini-Protean II	Bio-Rad Laboratories GmbH, Munich, Germany

2 Materials and Methods

Shaker for bacteria cultures, Certmonat H+R	B. Braun
Speedvac RVC 2-18	Martin Christ Gefriertrocknungsanlagen GmbH, Osterode, Germany
Tabletop centrifuge Mikro 22 R	Hettich Zentrifugen,
Tabletop centrifuge CR 4.12	Jouan GmbH, Fernwald, Germany
Thermocycler Mastercycler gradient	Eppendorf AG, Hamburg, Germany
Thermoshaker Thermomixer comfort	Eppendorf AG, Hamburg, Germany
Trans-Blot SD Blotting aparatus	Bio-Rad Laboratories GmbH, Munich, Germany
Ultracentrifuge Centrikon H-401	Kontron Hermle

2.1.4 Cell lines

Table 4: Applied cell lines.

CELL LINE	TYPE
HeLa Kyoto	Human cervical carcinoma cell line
HEK293T	Human embryonic kidney cell line
BHK clone #2	Transgenic baby hamster kidney cell line containing a <i>lac</i> operator array (Tsukamoto et al., 2000)

2 Materials and Methods

2.1.5 Antibodies

Table 5: Applied primary antibodies.

ANTIBODY (SPECIES)	MANUFACTURER
Anti-His ₆ (C-term) (mouse)	GE Healthcare, Uppsala, Sweden
Anti-His ₆ (C-term)-HRP (mouse)	Invitrogen GmbH, Karlsruhe, Germany
Anti-Dnmt1 (rat)	Dr. Elizabeth Kremmer, Munich, Germany
Anti-GFP (mouse)	Roche Diagnostics GmbH, Mannheim, Germany
Anti-GST (rat)	Dr. Elizabeth Kremmer, Munich, Germany
Anti-PCNA (rat)	Dr. Elizabeth Kremmer, Munich, Germany

Table 6: Applied secondary antibodies.

ANTIBODY (SPECIES)	MANUFACTURER
HRP/Anti-M13 Monoclonal Conjugate (mouse)	GE Healthcare, Uppsala, Sweden
Anti-mouse-HRP (sheep)	GE Healthcare, Uppsala, Sweden
Anti-goat-HRP (rabbit)	Zymed GmbH, Vienna, Austria
Anti-rat-HRP (goat)	Dianova
Anti-rat-Alexa Fluor 647 Conjugate	Cell Signaling Technology,
Llama IgG-heavy and light chain antibody HRP conjugated	Bethyl Laboratories Inc, Montgomery, USA

2.1.6 Primer

Primer used for polymerase chain reactions were synthesized by Metabion AG (Martinsried, Germany). To amplify the V_HH-repertoire of an alpaca from the cDNA derived from peripheral B cells the following primer were used.

2 Materials and Methods

Table 7: Primer used for amplification of V_HHs.

PRIMER	SEQUENCE
Call 001	5'- GTC CTG GCT GCT CTT CTA CAA GG-3'
Call 002	5'- GGT ACG TGC TGT TGA ACT GTT CC-3'
SM017	5'- CCA GCC GGC CAT GGC TCA GGT GCA GCT GGT GGA GTC TGG-3'
SM018	5'- CCA GCC GGC CAT GGC TGA TGT GCA GCT GGT GGA GTC TGG-3'
A4-short	5'- CAT GCC ATG ACT CGC GGC CCA GCC GGC CAT GGC-3'
38 reverse	5'- GGA CTA GTG CGG CCG CTG GAG ACG GTG ACC TGG GT-3'

2.1.7 Bacterial strains

Different bacterial strains (Table 8) were used according to the intended application. For the production of phage particles and the generation of phage-libraries, the *E. coli* strain TG1 was used. This strain is a so called “suppressor strain” and encodes for an additional transfer-RNA which recognizes the Amber stop codon (TAG). Hence, instead of the termination of the protein synthesis glutamate is incorporated in the polypeptide chain.

JM109 and BL21 cells were used for protein expression. XL-1 Blue cells were used for cloning work.

Table 8: Bacterial strains

STRAIN	MANUFACTURER
Chemical-Competent <i>E. coli</i> JM109	
Chemical-Competent <i>E. coli</i> XL-1 Blue	Agilent Technologies GmbH & Co.KG, Waldbronn, Germany
Chemical-Competent <i>E. coli</i> BL21	Life Technologies
Electroporation-Competent <i>E. coli</i> TG1	Agilent Technologies GmbH & Co.KG, Waldbronn, Germany

2 Materials and Methods

2.2 Methods

2.2.1 Molecular biological Methods

2.2.1.1 Culturing of bacteria

Culturing of bacteria was conducted in LB-Medium or 2xYT-Medium at 37°C in an incubator shaker. The appropriate antibiotic was added according to the antibiotic resistance gene encoded by the respective plasmid.

The optical density of the culture was measured at 598 nm (OD₅₉₈) with an UV/Vis spectrophotometer (DU® 730 Life Science UV/Vis, Beckman Coulter).

2.2.1.2 Cryoconservation of bacterial cultures

For long-term storage (-80°C) of bacterial cultures glycerol stocks were made with 15% (w/v) final concentration glycerol.

2.2.1.3 Transformation of competent *E. coli* cells

Chemical-competent JM109 and XL-1 Blue cells were transformed by heat-shock transformation: ~ 50 ng plasmid DNA or 5 µl ligation was added to the bacteria and incubated 30 min on ice following a heat shock at 42°C for 30 s. After 2 min incubation on ice 100 µl SOC-Medium (20 g bacto tryptone, 5 g yeast extract, 0,5 g NaCl, ad 1 l ddH₂O, 10 mM MgCl₂, 10 mM MgSO₄, 397 µl 50 % Glucose) was added and incubated at 37°C/200 rpm for 1 h. The whole bacteria suspension was applied on to an agar plate containing the appropriate antibiotic and was incubated at 37°C over night.

2 Materials and Methods

2.2.1.4 Preparation of Plasmid-DNA

Depending on the intended application and necessary amount of plasmid DNA two different methods were applied to prepare plasmid DNA.

For sequence analysis and cloning procedures plasmid DNA was prepared by alkaline lysis. After genomic DNA, cell debris and proteins are separated plasmid DNA was precipitated with ethanol. The DNA pellet was dried and resuspended in 40 μ l H₂O.

For the preparation of plasmid DNA for transfections, the Midiprep System PureYield Plasmid (Promega) was used according to the manufacturer's protocol.

2.2.1.5 Quantification of DNA

The concentration of DNA was measured spectrophotometric (NanoVue Plus, GE Healthcare; absorbance 260 nm).

2.2.1.6 Polymerase chain reaction

Polymerase chain reaction (PCR) was used to amplify DNA fragments and to introduce restriction sites via primers for a subsequent cloning step if required. A typical amplification reaction includes the sample of template DNA, two oligonucleotide primers, deoxynucleotide triphosphates (dNTPs), reaction buffer and the thermostable DNA Phusion-polymerase (Table 9). PCR results in the exponential synthesis of a distinct DNA sequence by repeated denaturing, hybridization and extension cycles with 25-30 cycles usually carried out (Table 10).

2 Materials and Methods

Table 9: Exemplary PCR-preparation scheme.

COMPONENT	AMOUNT/VOLUME	FINAL CONCENTRATION
Template DNA	50 ng	50 ng
Forward primer (c= 10 pmol/ μ l)	1 μ l	0,2 μ M
Reverse primer (c= 10 pmol/ μ l)	1 μ l	0,2 μ M
5x Phusion buffer	10 μ l	1x
dNTP mix (c= 10mM/nucleotide)	1 μ l	200 μ M/nucleotide
Phusion Polymerase	1 μ l	0,08 U/ μ l
ddH ₂ O	ad 50 μ l	

Table 10: Exemplary PCR program

STEP	TEMPERATURE	TIME	NUMBER OF CYLCES
Initial denaturing	94°C	30 s	1
Denaturing	94°C	15 s	
Annealing	58°C	15 s	25-30
Extension	72°C	20 s	
Final extension	72°C	7 min	1
	4°C	∞	

2.2.1.7 DNA restriction digestion

For restriction digestion of DNA fragments or plasmid DNA endonucleases from New England Biolabs were used and restriction digestion was performed following the manufacturer's protocol.

2 Materials and Methods

2.2.1.8 Agarose gel electrophoresis with DNA

Agarose gel electrophoresis enables the user to monitor the PCR procedures or restriction digestions, but also to size fractionate DNA molecules in order to purify these from the gel. Agarose gel electrophoresis was performed in 0,5x Tris-Acetate-EDTA-buffer (TAE-buffer) with agarose concentrations of 0,8% (w/v), 1,0% (w/v) or 1,5% (w/v). DNA was detected by ethidium bromide (EtBr) (final concentration: 0,025 µg/ml). As standard, the markers SmartLadder or SmartLadder SF (Eurogentec) were used. After electrophoresis the gel was placed on an UV light box and the fluorescent ethidium bromide-stained DNA pictured using the imaging system FluorChem 8900 (Alpha Innotech Corporation).

2.2.1.9 DNA purification from agarose gels

DNA fragments visualized on an UV light box were removed from the gel by the use of scalpels. Once captured, the DNA was eluted from the jellified agarose following the instructions of the NucleoSpin® Extract II-Kit (Macherey-Nagel). Elution volume was 30 µl.

2.2.1.10 DNA Ligation

Purified and restriction enzyme-treated DNA fragments were ligated into the desired plasmid vectors, which also have been treated with the respective endonucleases producing compatible overhangs. After the vector and insert DNA have been prepared and their concentration determined via agarose gel electrophoresis a 1:3 molar ratio of vector and insert was used for the reaction (Table 11). All ligations were performed with ATP-dependent T4 DNA ligase and the provided buffer (New England Biolabs) either 4 hours at room temperature or overnight at 16°C. Following the reaction, the ligated DNA was transformed into an appropriate host strain, *E. coli* JM109 or XL-1 Blue as described in 2.2.1.3.

2 Materials and Methods

Table 11: Exemplary ligation preparation.

COMPONENT	AMOUNT/VOLUME	FINAL CONCENTRATION
10x T4 Ligase Buffer	1 μ l	1x
T4 DNA ligase	1 μ l	1 U
DNA Vector	1 μ l	0,025 pmol
DNA Insert	1 μ l	0,076 pmol
ddH ₂ O	ad 10 μ l	

2.2.1.11 DNA sequencing

The sequencing of DNA was performed by MWG, Ebersberg.

2.2.2 Cell Culture Methods

2.2.2.1 Cultivation of mammalian cells

Cell culture was carried out in a sterile bench applying sterile working techniques. If not indicated else, cells were cultivated in DMEM supplemented with 10% fetal calf serum at 37°C, 5% CO₂ and 95% humidity. Subconfluent grown cells were passaged every 2-3 days with trypsin/EDTA.

2.2.2.2 Seeding of cells

For microscopic experiments cells were seeded at appropriate density (40-60% confluence) either on 18 x 18 glass cover slips in a 6-well plate (Nunc) or for high-throughput screens in μ Clear 96-multiwell plates (Greiner).

For the production of cell extracts from HEK293T cells, they were seeded 1:3 in p100 cell culture dishes.

2 Materials and Methods

2.2.2.3 Transfection of plasmids

In general, cells were transfected 4-6 h after seeding. For imaging of fixed samples on cover slips, 4 µg plasmid DNA, 16 µl PEI pH 10 (polyethylenimin) and 150 µl pure DMEM (without serum) was incubated 10-15 min at room temperature and added to the cells. After 4 – 6 h the medium was replaced by fresh medium and the cells were incubated over night.

For high-content imaging in 96-well plates, the reverse Lipofectamine 2000 transfection protocol as provided by the manufacturer (Life Technologies) was applied. In brief, the transfection mix containing 0.1 µg DNA and 0.2 µl Lipofectamine 2000 was prepared in 50 µl pure DMEM (without serum) per well. Cells were seeded on top (after 20 minutes incubation) and transfection takes place over night.

For the transfection of HEK293T cells in p100 cell culture dishes 72 µl transfection reagent PEI pH 7, 24 µg plasmid DNA and 600 µl pure DMEM (without serum) was incubated 10-15 min at room temperature and added to the cells. The cells were incubated over night.

2.2.2.4 Fixation of cells

For fixation cells were washed twice with 1x PBS and fixed with 3,7% formaldehyde in PBS for 15 min at room temperature. The fixation solution was discarded and exchanged with PBS followed by two washing steps with 0,02% Tween20 in PBS (PBST). Cells were permeabilized and counterstained for 5-10 min with 0,2% Triton X-100 in PBST and 0,02 µg/ml 4,6-diamidino-2-phenylindole (DAPI). After another washing step (3x with PBST), cover slips were mounted in Vectashield (Vector Laboratories). Multiwell plates are stored in PBST at 4°C.

2.2.2.5 Microscopy

Fixed cells expressing fluorescent fusion proteins were analyzed by wide-field epifluorescence microscopy (Axiovert 135 TV, Zeiss). F2H images were acquired on the InCell

2 Materials and Methods

analyzer 1000 (GE Healthcare). An automated segmentation analysis protocol was previously established. Interactions were verified through manual inspection.

2.2.3 Biochemical Methods

2.2.3.1 Expression and purification of recombinant proteins from *E. coli*

2.2.3.1.1 Induction of protein expression in *E. coli*

All proteins (V_{H} domains, antigens for immunization/screening) were expressed in *E. coli*. under the control of the *lac*-promotor. The *lac*-operon is induced by lactose only temporary since lactose is metabolized by the bacteria. In order to achieve a constant activity of the *lac*-operon, the structural analog Isopropyl β -D-1-thiogalactopyranoside (IPTG) is used. IPTG binds, the same way as lactose, to the *lacI* repressor, inactivates it and in that way hinders its binding to the *lac*-operator. However, the bacteria cannot metabolize it resulting in a constant induction of the *lac*-promotor and hence in the expression of the fusionprotein.

In brief, bacteria cultures were grown at 37°C until OD_{598} 0,7-0,9 was reached. Protein expression was induced by adding 0,5 mM IPTG. Proteins were expressed overnight at room temperature. Bacteria were harvested by centrifugation at 5000 rpm for 10 min at 4°C. Afterwards pellets were stored at -20°C or resuspended in binding buffer (his-tagged proteins: 1x PBS, 0,5 M NaCl, 20 mM imidazol, pH 8; GST-tagged proteins: 1x PBS, 1 mM DTT) and further processed.

2.2.3.1.2 Lysis of bacteria

Bacteria were lysed in binding buffer plus protease inhibitor phenylmethanesulfonylfluoride (PMSF) (0,5 mM) by adding lysozyme (0,1 mg) with subsequent sonification (20 sec maximum amplitude, 20 sec break, repeat 6x). Insoluble

2 Materials and Methods

components and non-lysed cells were separated by centrifugation. Supernatant was filtrate through a 0,45 µm filter.

2.2.3.1.3 Purification of proteins using affinity chromatography

Proteins were purified using affinity chromatography via the hexahistidine-peptide his-tag and Ni²⁺ sepharose or the glutathione S-transferase. All purifications were performed using the ÄKTA purifier FPLC-system (GE Healthcare) and 1 ml HisTrap HP columns (GE Healthcare) with flow rate of 1 ml/min or 1 ml GST-Trap FF columns (GE Healthcare) with flow rate of 0,5 ml/min. The HisTrap columns were equilibrated with 5 column volumes in binding buffer (1x PBS, 0,5 M NaCl, 20 mM imidazol, pH 8). Bound proteins were eluted in 1 ml fractions by adding elution buffer with higher imidazol concentrations (1x PBS, 0,5 M NaCl, 500 mM imidazol, pH 6,8). The GST-Trap FF columns were equilibrated with 5 column volumes in binding buffer (1x PBS, 1 mM DTT). Bound proteins were eluted in 1 ml fractions by adding elution buffer (200 mM NaCl, 15 mM glutathione, 50 mM Tris pH 9, 2 mM DTT).

2.2.3.1.4 Gel filtration chromatography

Gel filtration chromatography was performed using the ÄKTA purifier FPLC-system and a Superdex 75 gelfiltration column. The flow rate of all steps was 0,5 ml/min. The column was equilibrated with two column volumes with 1x PBS. Peak fractions of the affinity chromatography eluate were pooled and maximal 2 ml of the eluate was applied to the column. Proteins were collected in 0,5 ml fractions.

2 Materials and Methods

2.2.3.2 SDS-PAGE

Proteins were separated by SDS-PAGE according to Table 12.

Table 12: Composition of separation gel and stacking gel for SDS-PAGE.

GEL	COMPONENTS
Separation gel	8-12% (w/v) Acrylamide; 0,08-0,3% (w/v) Bisacrylamide; 375 mM Tris/HCl pH 8,8; 0,1% SDS, 0,05% (w/v) APS, 0,05% (v/v) TEMED
Stacking gel	5% (w/v) Acrylamide; 0,033% (w/v) Bisacrylamide; 60 mM Tris/HCl pH 6,8; 0,1% SDS, 0,05% (w/v) APS, 0,1% (v/v) TEMED

2.2.3.3 Coomassie staining

SDS gels were Coomassie stained according to the manufacturer's protocol.

2.2.3.4 Western Blot

Proteins were transferred from SDS-gels to nitrocellulose membranes (Bio-Rad) by semi-dry blotting. Transfer was carried out at 240 mA. The membrane was incubated for 1h in 3% milk powder in Tris buffered saline with 0,075% Tween-20 (TBST) at room temperature and, subsequently incubated with the primary antibody diluted in 3% milk-TBST at 4°C over night. The membrane was washed 3 times in TBST for 5 min to remove unbound antibodies. Binding of the secondary antibody was performed diluted in 3% milk-TBST for 1 h at room temperature. The membrane was washed 3 times with TBST for 5 min. The membrane was then either treated with ECL-solution (if HRP-conjugated secondary antibody was used) and bound proteins were detected on a film or were detected with the Image Quant software on a Typhoon Scanner.

2 Materials and Methods

2.2.3.5 Chemical labeling

In order to use recombinant V_HHs in immunofluorescence they were labeled with Fluorescein isothiocyanate (FITC) (Thermo Scientific) or ATTO-fluorescent dyes (ATTO-TEC) via N-Hydroxysuccinimide (NHS) according to the manufacturer's protocols. Labeled proteins and free fluorescent dyes were separated using PD-10 desalting columns (GE Healthcare).

2.2.3.6 Dot blot

Dot blot analysis was performed to map the epitope of an antigen specific V_HH. 2 µg of peptide or recombinant protein were spotted on nitrocellulose and incubated with FITC labeled V_HHs. The binding signals were obtained by scanning on a Typhoon Scanner and normalized against the background. Quantification of the signals was performed with the Image Quant software on a Typhoon Scanner. Peptides were solved either in 1x PBS or DMSO.

2.2.3.7 Coupling of V_HHs to NHS-Sepharose

Purified V_HHs were covalently coupled to Sepharose beads (GE Healthcare) via NHS according to the manufacturer's protocol.

2.2.3.8 Immunoprecipitation using mammalian cells

For one immunoprecipitation reaction ~10⁷ HEK293T cells were resuspended in lysis buffer (20 mM Tris/Cl pH7,5, 150 mM NaCl, 0,5 mM EDTA, 0,5% NP-40) plus 1 mM PMSF, 1x protease inhibitor mix (Serva), 0,5 µg/µl DNase and 2,5 mM MgCl₂. The soluble fraction was separated by centrifugation and the supernatant was diluted with dilution buffer (20 mM Tris/Cl pH 7,5, 150 mM NaCl, 0,5 mM EDTA). 50 µl slurry of NHS-activated Sepharose beads covalently coupled with a V_HH as described in 2.2.3.7 were equilibrated by washing 3 times with dilution buffer. HEK293T cell lysate was added to the equilibrated beads and incubated for 4 h at 4°C and subsequent SDS-PAGE analysis followed.

2 Materials and Methods

2.2.3.9 Immunoprecipitation using *E. coli*

Bacteria expressing the appropriate protein were induced as described in 2.2.3.1.1. For one immunoprecipitation culture volume corresponding to an OD_{600nm} of 0,5 was centrifuged and the pellet was resuspended in lysis buffer (20 mM Tris/Cl pH 7,5, 150 mM NaCl, 0,1% Triton X-100, 0,5 mM EDTA) plus 200 mM PMSF, 0,5 µg/µl DNase, 2,5 mM MgCl₂ and 0,1 mg/ml lysozyme and incubated 30 min on ice. The soluble fraction was separated by centrifugation and diluted with dilution buffer (20 mM Tris/Cl pH 7,5, 150 mM NaCl, 0,5% NP-40, 0,5 mM EDTA). 50 µl slurry of NHS-activated Sepharose beads covalently coupled with a V_HH as described in 2.2.3.7 were equilibrated with dilution buffer as described in 2.2.3.8. The lysate was added to the equilibrated beads and incubated over night at 4°C. The beads were washed twice with dilution buffer and subsequent SDS-PAGE analysis followed.

2.2.3.10 Immunoprecipitation using recombinant protein

Immunoprecipitation was performed as described in 2.2.3.9, but 20 µg of the appropriate recombinant protein was added instead of *E. coli* lysate.

2.2.4 Immunological Methods

In the course of this work libraries generated from immunized alpacas were used to select antigen specific V_HHs. The alpacas were immunized with different antigens ranging from protein to peptide either produced recombinantly in *E. coli* or insect cells or synthesized (see Table 13).

2 Materials and Methods

Table 13: Applied antigens.

APPLIED ANTIGEN	SOURCE
γ H2AX-KLH	Synthesized by PSL GmbH
HIV-1 CA	<i>E. coli</i> (provided by Hans-Georg Kräußlich)
PCNA	<i>E. coli</i> (provided by M. Cristina Cardoso)
β -Catenin-GST	<i>E. coli</i> (provided by Oliver Pötz)
hDnmt1	Insect cells (provided by Carina Frauer)

2.2.4.1 Immunization

To generate immune V_HH libraries, four alpacas Anna, Ferdl, Annabel and Sina were injected with antigen six to seven times. The immune response of the alpacas was enhanced by using Gerbu Pharma Adjuvant #3003 to guarantee a gentler immune reaction in comparison to Freud's Adjuvants. The alpacas are kept at the "Lehr- und Versuchsgut der Tierärztlichen Fakultät" of the University Munich in a herd of ten animals. The immunizations were performed subcutaneous in the clean-shaven neck of the alpaca by Dr. Stefan Nüske.

Alpaca Anna was immunized with γ H2AX-KLH for 49 days following the immunization scheme depicted in Table 14. The same immunization scheme was used for the immunization of alpaca Ferdl immunized with non-infective HIV-capsid protein.

2 Materials and Methods

Table 14: Immunization scheme for alpaca Anna and Ferdl. Anna was immunized with γ H2AX-KLH for 49 days. Ferdl was immunized with non-infective HIV-capsid protein.

DAY	AMOUNT ANTIGEN (μ G)
0	500
7	125
14	125
21	125
35	125
49	125

Alpaca Annabel was immunized with PCNA for 103 days with immunization scheme depicted in Table 15. After 3 month rest period, Annabel was immunized with β -Catenin-GST for 103 days with the same immunization scheme.

Table 15: Immunization scheme for alpaca Annabel. Annabel was immunized with PCNA for 103 days. 3 months later Annabel was immunized with β -Catenin-GST for 103 days.

DAY	AMOUNT ANTIGEN (μ G)
0	500
7	125
14	125
21	125
35	125
49	125
103	125

Alpaca Sina was immunized with hDnmt1 for 87 days with the immunization scheme depicted in Table 16.

2 Materials and Methods

Table 16: Immunization scheme for alpaca Sina. Sina was immunized with hDnmt1 for 87 days.

DAY	AMOUNT ANTIGEN (μG)
0	600
7	120
14	120
21	250
35	250
49	250
87	250

2.2.4.2 ELISA of preimmune and immune sera

Before the first immunization and after a certain time period blood samples (100 ml) were taken from each alpaca. The blood was drawn by Dr. Stefan Nüske from the external jugular vein (*Vena jugularis externa*) of the alpaca in vacuum bottles (Evozone) pretreated with Heparin (Ratiopharm). Sera were generated by centrifugation of blood (2000 rpm, 10 min and 4°C). The supernatant was filled in 5 ml aliquots. For short-term storage, the aliquots were kept at 4°C, for long-term storage, aliquots were kept at -20°C. Preimmune sera (PS) were generated from blood samples before an immunization while immune sera (IS) were generated after a specific time depicted in Table 17. The period between the first immunization and the taking of blood is 60, 91, 107 or 115 days in order to allow the animal for an appropriate immune response.

2 Materials and Methods

Table 17: Overview of preimmune and immune sera.

ANTIGEN/ANIMAL	DAY	PS/IS
Anna	19.01.2007	PS
yH2AX-KLH (Anna)	27.03.2007	IS
Annabel	12.05.2009	PS
β-Catenin-GST	21.07.2009	IS
Sina	03.11.2009	PS
hDnmt1	02.02.2010	IS

For the serum ELISA, 1 µg of the appropriate antigen was coated in a 96 well plate (Maxisorp, Thermo Scientific) and the serum (PS or IS) was added in serial dilutions. Bound alpaca antibodies were detected with an HRP-conjugated anti-Llama IgG antibody (Bethyl Laboratories). By adding substrate solution containing the chromogenic substrate 3,3',5,5'-Tetramethylbenzidin (TMB) a conversion reaction catalyzed by the HRP takes place resulting in a blue coloring of the solution. The reaction was stopped by adding sulfuric acid resulting in a yellow coloring which was measured in a microplate reader (Infinite M1000, Tecan; absorbance 450 nm).

2.2.4.3 Isolation of B cells

The isolation of B cells was performed by Ficoll-gradient. During the first experiments, UNI-SEP_{MAXI} (NOVAmed) was used yielding ~ 5 x 10⁶ B cells. To further enhance the B cell yield, Lymphocyte Separation Medium LSM 1077 (PAA) was tested resulting in ~ 1 x 10⁸ B cells. Even though both separation methods are based on Ficoll, higher numbers of B cells were obtained by applying the LSM 1077. The isolation was carried out according to the respective manufacturer's instructions. The cell number was determined by counting in a Neubauer counting chamber.

2 Materials and Methods

2.2.5 Phage Display Technology

2.2.5.1 Construction of a V_HH library

2.2.5.1.1 RNA extraction from B cells

To prepare total RNA from B cells during the first experiments, 1×10^6 B cells were used and RNA was extracted with TRIzol reagent (Life Technologies) according to the manufacturer's protocol resulting in RNA yields between 0,6 – 0,9 μg . To maximize the RNA yield and hence enabling the generation of a maximum sized library, Nucleospin RNA XS Kit (Macherey-Nagel) was used according to the manufacturer's protocol during later experiments resulting in higher RNA yields between 0,75 – 4,2 μg . To further enlarge the RNA yield, during the latest experiments also the number of B cells was increased: 2×10^7 B cells were used for RNA preparation resulting in equal RNA yields of up to 11,2 – 17,6 μg . The concentration of the RNA was measured spectrophotometric (NanoVue Plus, GE Healthcare; absorbance 260 nm).

2.2.5.1.2 RNA-agarose gel electrophoresis

Gelectrophoretical analysis of RNA were performed with agarose gels used for DNA-agarose gel electrophoresis (1% (w/v), 0,025 $\mu\text{g}/\text{ml}$ ethidium bromide, 1x Tris-Acetate-EDTA (TAE) buffer).

2.2.5.1.3 cDNA synthesis

Complementary DNA (cDNA) was amplified using the First-Strand cDNA Synthesis Kit from GE Healthcare according to the manufacturer's protocol.

2 Materials and Methods

2.2.5.1.4 Amplification of V_HH repertoire

Polymerase chain reaction (PCR) was used to amplify the V_HH repertoire and to introduce restriction sites via primers for a subsequent cloning step. The amplification of V_HHs is performed by 3 subsequent nested PCR reactions using 6 different V_HH-specific primers. As DNA template for the first PCR (PCR1, see Table 18) cDNA from isolated B cells was used. The amplification product of the first PCR was loaded on an agarose gel (as described in 2.2.1.8), purified and eluted (as described in 2.2.1.9) and was used as template for the second PCR (PCR2, see Table 19). The amplification product of the second PCR was prepared accordingly and was used as template for the third PCR (PCR3, see Table 20). For all three PCRs one PCR program was used (see Table 21).

Table 18: Preparation scheme PCR1.

COMPONENT	AMOUNT	FINAL CONCENTRATION
Template DNA (cDNA)	3 µl	
Call001 (c= 10 pmol/µl)	0,5 µl	0,2 µM
Call002 (c= 10 pmol/µl)	0,5 µl	0,2 µM
5x Phusion buffer	5 µl	1x
dNTP Mix (c= 10mM/nucleotide)	0,5 µl	200 µM/nucleotide
Phusion Polymerase	0,5 µl	0,08 U/µl
ddH ₂ O	15 µl	

2 Materials and Methods

Table 19: Preparation scheme PCR2.

COMPONENT	AMOUNT	FINAL CONCENTRATION
Template DNA (PCR1)	1 μ l	
Call002 (c= 10 pmol/ μ l)	0,5 μ l	0,2 μ M
SM017 (c= 10 pmol/ μ l)	0,25 μ l	0,1 μ M
SM018 (c= 10 pmol/ μ l)	0,25 μ l	0,1 μ M
5x Phusion buffer	5 μ l	1x
dNTP Mix (c= 10mM/nucleotide)	0,5 μ l	200 μ M/nucleotide
Phusion Polymerase	0,5 μ l	0,08 U/ μ l
ddH ₂ O	17 μ l	

Table 20: Preparation scheme PCR3.

COMPONENT	AMOUNT	FINAL CONCENTRATION
Template DNA (PCR2)	1 μ l	
A4 short (c= 10 pmol/ μ l)	1 μ l	0,2 μ M
38 reverse (c= 10 pmol/ μ l)	1 μ l	0,2 μ M
5x Phusion buffer	10 μ l	1x
dNTP Mix (c= 10mM/nucleotide)	1 μ l	200 μ M/nucleotide
Phusion Polymerase	1 μ l	0,08 U/ μ l
ddH ₂ O	35 μ l	

2 Materials and Methods

Table 21: PCR program used for the amplification of the VHH repertoire.

STEP	TEMPERATURE	TIME	NUMBER OF CYLCES
Initial denaturing	94°C	3 min	1
Denaturing	94°C	15 s	
Annealing	55°C	15 s	35
Extension	72°C	30 s	
Final extension	72°C	8 min	1
	4°C	∞	

The amplification product of PCR3 was prepared accordingly followed by a restriction digestion with the endonucleases *NcoI* and *NotI* (see Table 22). In parallel the plasmid vector pHEN4 was also treated with the endonucleases (see Table 23) producing compatible overhangs in order to ligate them according to 2.2.1.10 in up to 30 ligation preparations. The ligations were dialyzed against ddH₂O.

Table 22: Restriction digest of PCR3.

COMPONENT	AMOUNT
DNA PCR3	30 µl
<i>NotI</i>	1 µl
<i>NcoI</i>	1 µl
Buffer	5 µl
ddH ₂ O	13 µl

2 Materials and Methods

Table 23: Restriction digest of pHEN4.

COMPONENT	AMOUNT
pHEN4	10 µg
<i>NotI</i>	0,5 µl
<i>NcoI</i>	0,5 µl
Buffer	1 µl
ddH ₂ O	ad 10 µl

2.2.5.1.5 Transformation of TG1 cells and library generation

Electro-competent TG1 cells (Agilent) were used to generate V_HH-libraries. They were transformed by electroporation with the ligation preparations according to the manufacturer's protocol. For each library up to 30 transformations were performed. The transformed bacteria were plated on 2xYT plates containing 100 µg/ml ampicillin and 2% (w/v) glucose (2xYTamp/glu plates) and incubated overnight. From these plates single clones were picked randomly in order to determine the diversity of the library by sequencing analysis (2.2.1.11). In addition the library size was determined by counting the single clones on each plate.

The plates were floated off with 10 ml 2xYT medium containing 100 µg/ml ampicillin and 2% (w/v) glucose (2xYTamp/glu medium) and glycerol stocks were prepared of each library according to 2.2.1.2 resulting in the primary phage display libraries.

2.2.5.2 Cultivation and preparation of phage particles

To produce phage particles presenting the V_HH library on their tips, TG1 cells containing the V_HH library were inoculated in 2xYTamp/glu medium and infected with the hyperphage (Progen) within their logarithmic growth phase. After an incubation time of 30 min the culture was harvested by centrifugation and the pellet was resuspended in 2xYT medium containing 100 µg/ml ampicillin and 25 µg/ml kanamycin (2xYTamp/kana medium) and

2 Materials and Methods

incubated shaking over night at 37°C. The next day the recombinant V_HH-containing phages are found in the supernatant which was purified by centrifugation. After an incubation with 20% polyethylene glycol 6000 (PEG 6000) for 1 h on ice, the phage particles were precipitated by centrifugation (30 min, 4000 rpm, 4°C). The pellet was resuspended in 1x PBS and represents the V_HH-library which can be used for panning.

2.2.5.3 Determination of library sizes

To assess library sizes, the phage titer was determined by counting colony forming units (cfu) of TG1 cells which were infected with phage particles and plated on selection agar. It is assumed that each phage particle infects one bacterial cell which thereby acquires an ampicillin resistance resulting in one bacterial colony once this bacterial cell is plated on agar including ampicillin.

2.2.5.4 Solid phase panning

Solid phase panning is a conventional, widely used method to select antibodies or antibody fragments. To perform the panning, 10 µg antigen were coated in immunotubes (Thermo Scientific) overnight at 4°C. In order to block the free binding capacity of the polystyrol wall, 4% skimmed milk powder in PBS (MPBS) or (in later experiments) Pierce protein free blocking buffer (PFBB) (Thermo Scientific) was added.

Before the first panning round a so called absorption panning was performed. The phage particles (generated as described in 2.2.5.2) were added to an immunotube which was not coated with antigen but blocked with MPBS or protein free blocking buffer (PFBB) in order to eliminate V_HH-phage particles unspecifically binding to components of milk/ the blocking solution. The phages in the supernatant were then used for solid phase panning and added to the immunotube coated with the appropriate antigen and incubated 90 min at room temperature. In parallel a negative control was performed with no antigen coated in the immunotube. After 10 to 30 washing steps (number of washings steps increases with each

2 Materials and Methods

panning round) with PBS/Tween20 0,05% the phages were eluted with 0,1 M HCl and neutralized with bicarbonate buffer (1M Tris/Cl, pH 9,0) or 100 mM triethylamine (TEA) solution, pH 12 and neutralized with 1M Tris, pH 7,4-8. The eluted phage particles were used for reinfection of TG1 cells which were then used for the subsequent panning round.

2.2.5.5 Native panning

Native panning varies from solid phase panning in terms of the presentation of the antigen. In solid phase panning recombinant antigen is directly coated to the surface of immunotubes. In native panning cell lysate from HEK293T cells expressing the antigen in fusion with GFP (prepared as described in 2.2.3.8) was prepared, immunoprecipitated using the GFP-multiTrap (ChromoTek GmbH) (Pichler et al., 2012) and used as antigen for phage display.

Phage particles presenting V_H Hs on their tips were prepared as described in 2.2.5.2. In order to decrease V_H Hs unspecifically binding to GFP, lysate of HEK293T cells expressing GFP only was immunoprecipitated in the GFP-multiTrap and used as antigen. Phages were added and incubated. The unbound phages were added to the immunoprecipitated antigen-GFP-fusion protein. After an incubation time of 2 h at room temperature 10-20 washing steps were performed with PBST and 1 washing step with PBS. Bound phages were eluted as described in 2.2.5.4 and used for reinfection.

2.2.5.6 Phage ELISA

Phage ELISA was used to select phage clones presenting antigen specific V_H Hs on their tips. To this end phage particles were cultivated and prepared as described in 2.2.5.2 in 96-well assay blocks (Schubert & Weiss). Antigens were coated (1 μ g/well) in 96-well MaxiSorp microtiter plates (Thermo Scientific) and blocked with MPBS or PFBB as described in 2.2.5.4. Phage particles were added and incubated for 2 h at room temperature. After 3 washing

2 Materials and Methods

steps with PBST (0,05% Tween20) and 3 washings steps with PBS bound phages were detected with an anti M13-HRP antibody (GE Healthcare) as described in 2.2.4.2.

3 Results

The multitude of established as well as unique applications of V_{HH} s, ranging from classical biochemical methods (as Nanotraps) over cell biological techniques (in immunofluorescence) to live cell detection of endogenous proteins (as Chromobodies) elucidates the complexity of their functional requirements. In order to meet the necessary specifications the whole upstream screening and identification process has to be adjusted.

The main objective of this thesis was to develop a robust and reliable process essential in the course of the generation of antigen specific V_{HH} s for intended downstream applications. This comprises the selection of the antigen, design of the corresponding phage display library and an efficient selection process (see Figure 11). Furthermore, during this thesis antigen specific V_{HH} s were functionally characterized in different approaches for their applicability as Nanotraps and Chromobodies.

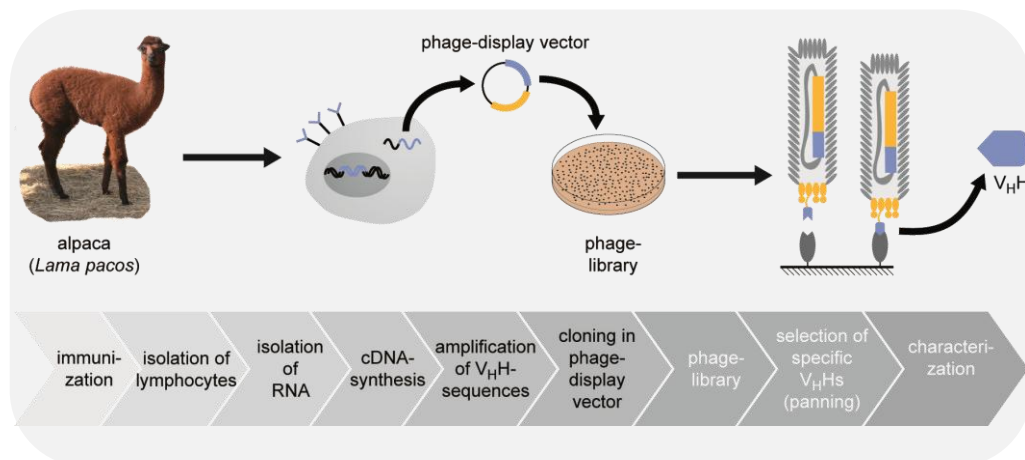


Figure 11: Schematic overview of the generation process of antigen specific V_{HH} s (Zolghadr, 2007).

The results are divided in two sections. The first section depicts strategies to generate and identify antigen specific V_{HH} s. As the very first step to generate antigen specific binding molecules, alpacas were immunized with a set of different antigens.

3 Results

Subsequently, the V_HH repertoire was cloned into a phagemid vector resulting in a comprehensive phage display library. To screen for antigen specific V_HHs phage display with several rounds of panning was performed, resulting in the selection of antigen specific V_HHs. According to the downstream application the method phage display was modified. First, solid phase panning with recombinant proteins was used to select for antigen specific V_HHs. Next, a *native panning* strategy was developed. For this purpose, antigen was expressed in mammalian cells to promote the selection of V_HHs recognizing the native confirmation of the antigen. Antigen specific clones were identified either by phage ELISA or by combining the phage display with the cell based fluorescent-2 hybrid (F2H) screening assay.

In the second section, antigen specific V_HHs were characterized according to the intended application by two different approaches: biochemical functionality and intracellular, *in vivo* functionality. To further understand the mode of binding, the epitopes of the V_HHs were mapped by phage ELISA and Dot Blot analysis. In order to test the functionality of the antigen specific V_HHs and their suitability as Nanotraps biochemical assays like immunoprecipitations and pulldown assays were performed. In addition, to test their capacity to recognize (partially) denatured antigens, they were analyzed in immunofluorescence experiments. An important aspect is the intracellular functionality of the V_HHs fused to fluorescent fusion proteins – so called Chromobodies, hence they were analyzed regarding their functionality in live cell imaging in mammalian cells.

3 Results

3.1 Generation and selection of antigen specific V_HHs

3.1.1 Antigen selection

One of the most crucial steps in generating antigen specific V_HHs is the immune response following immunization. Hence, one goal of this thesis was to analyze immune response in regard to antigen characteristics. Therefore, five different kinds of antigens ranging from peptides to complex proteins were immunized (see Table 24).

Table 24: Overview of applied antigens.

APPLIED ANTIGEN	CHARACTERISTICS
γH2AX-KLH	Peptide coupled to KLH
HIV-1 CA	Middle-sized, viral protein (24 kDa)
PCNA	Middle-sized protein (28 kDa)
β-Catenin-GST	Fusion-protein (118 kDa)
hDnmt1	Large protein (150 kDa)

- 1) Histone H2AX is a protein associated with the DNA and involved in DNA-repair. After a DNA-doublestrand break occurs, H2AX gets phosphorylated at serine 139. The phosphorylated version is referred to as γH2AX (Rogakou et al., 1998). During this thesis the peptide KATQAS (amino acid residues 134-139) was immunized coupled to the carrier KLH (Keyhole Limpet Hemocyanin found in arthropods and mollusca) in order to enhance the immune response to the non-immunogenic peptide.
- 2) The HIV-1 capsid protein (HIV-1 CA) is an internal capsid domain of the HIV-1 GAG polyprotein which orchestrates viron assembly of HIV-1 (Helma et al., 2012). For immunization recombinant HIV-1 CA was produced in *E. coli* and purified via a C-terminal his₆-tag (kindly provided by H. G. Kräußlich, Universitätsklinikum Heidelberg, Germany).

3 Results

- 3) The proliferation cell nuclear antigen (PCNA) is involved in DNA-replication and forms a homotrimer. It comprises the central loading platform for enzymes involved in DNA replication (Moldovan et al., 2007). Like HIV-1 CA, for immunization recombinant PCNA was produced in *E. coli* and purified via a C-terminal his₆-tag (kindly provided by M. C. Cardoso, MDC Berlin, Germany).
- 4) β -Catenin is the key mediator of the wnt-pathway. Within cells, β -Catenin is localized at the plasma membrane where it is involved in the formation of cell-cell contacts. Beside the membrane bound fraction a soluble pool fraction of β -Catenin exists in the cytoplasm and the nucleus. After induction of the wnt-pathway β -Catenin is translocated into the nucleus and acts as transcriptional coactivator (Valenta et al., 2012). Immunization was performed using a N-terminally Glutathione S transferase (GST) version of human β - Catenin (kindly provided by O. Poetz, NMI Reutlingen, Germany). Glutathione S-transferase (GST) is a 26 kDa protein used to purify proteins (Terpe, 2003).
- 5) The large human protein DNA (cytosine-5)-methyltransferase 1 (hDnmt1) is an epigenetic marker and maintains DNA methylation patterns during DNA-replication (Goll and Bestor, 2005). As the recombinant production of Dnmt1 in *E. coli* was only minor efficient, Dnmt1 was produced using a baculovirus system and purified via a C-terminal his₆-tag (kindly provided by C. Frauer, LMU Munich, Germany).

During the immunization period each alpaca received intramuscular injections at weekly intervals (kindly conducted by S. Nüsske, LMU Munich, Germany). On bleeding day, 100 – 150 ml blood was collected from each alpaca. To monitor the humoral immune response of the alpacas a solid-phase ELISA on immobilized antigen using serum samples from day 0 (pre immunization) and post immunization was performed exemplary for γ H2AX, hDnmt1 and β -Catenin-GST. Bound alpaca antibodies were detected by an anti-lama IgG antibody which specifically recognizes the Fc part of the alpaca antibodies. The results of these experiments

3 Results

show strong reactivity of the serum post immunization, but not pre immunization. Figure 12 shows the serum test for alpaca *Sina* before (Figure 12 A) and after the immunization (Figure 12 B) with hDnmt1 and for alpaca *Annabel* after the immunization with GST- β -Catenin (Figure 12 C). The post immunization test for γ H2AX did not show increased reactivity (data not shown).

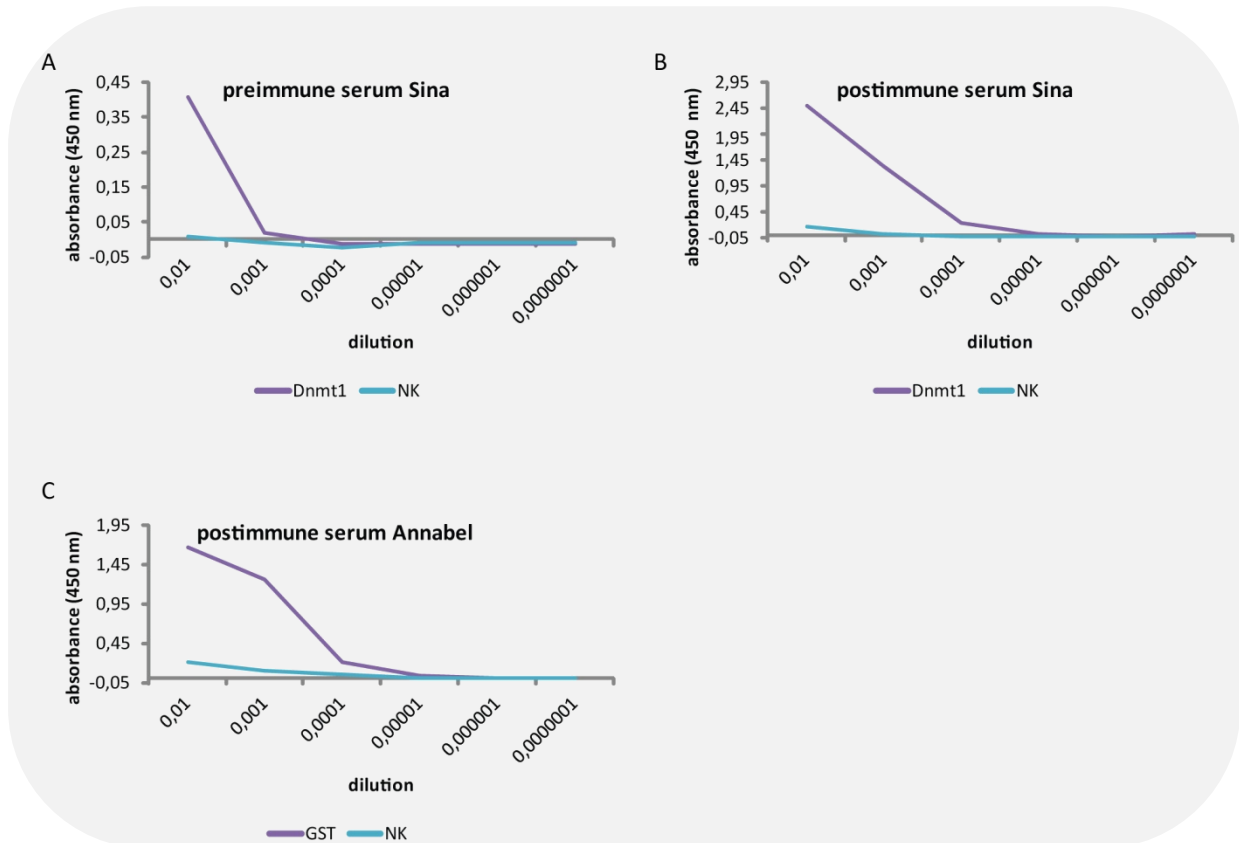


Figure 12: Immune response in alpaca. Alpaca *Sina* was immunized with recombinant hDnmt1, alpaca *Annabel* was immunized with GST- β -Catenin. Blood samples from *Sina* were taken at day 0 and 91 post immunization and the serum anti-hDnmt1 response was evaluated in solid phase ELISA. Blood samples from *Annabel* were taken at day 103 post immunization and the serum anti-GST response was evaluated in solid phase ELISA. (A) Preimmune serum anti-hDnmt1 response on recombinant hDnmt1 (NK: Ubiquitin). (B) Postimmune serum anti-hDnmt1 response on hDnmt1 (NK: VSVG). (C) Postimmune serum anti-GST response on GST (NK: GFP).

3 Results

3.1.2 Amplification of the V_HH repertoire

Following the test, that the alpaca generated antibodies against the specific antigen in general, the V_HH repertoire of the immunized animal was amplified to create a comprehensive V_HH phage display library.

3.1.2.1 RNA extraction and cDNA synthesis

To select antigen specific V_HHs from a V_HH library via phage display, the library size and diversity is of vital importance. B cells from immunized alpacas were used as basis to generate a comprehensive V_HH library since they should preferentially contain mRNA encoding for antigen specific V_HHs. One important step to ensure a large and diverse library is to maximize the mRNA yield.

First, the preparation of a maximum number of intact B cells from peripheral blood is required. In brief, 100 – 150 ml heparinized blood from immunized alpacas was added to Ficoll density gradient media filled tubes and the separation process of B cells from other blood components was performed by centrifugation. As described in the materials and methods section, different strategies were tested in order to enhance the yield of B cells, finally resulting in $\sim 1 \times 10^8$ B cells. Subsequently, total RNA was extracted from the prepared B cells. Again, different methods as described in the material and methods section were tested and optimized in order to enhance the RNA yield, finally resulting in 11,2 – 17,6 μg RNA per 1×10^8 B cells. The extracted RNA was used as template for cDNA synthesis using oligo dT primers.

3.1.2.2 PCR amplification

The next crucial steps in library generation are the polymerase chain reactions (PCR reactions) performed to amplify the V_HH repertoire. Several different variations regarding the number of PCR cycles, the primer composition and the number of PCRs were performed.

3 Results

The highest diversity was achieved by 3 subsequent nested PCR reactions employing 6 different primers as depicted in Figure 13.

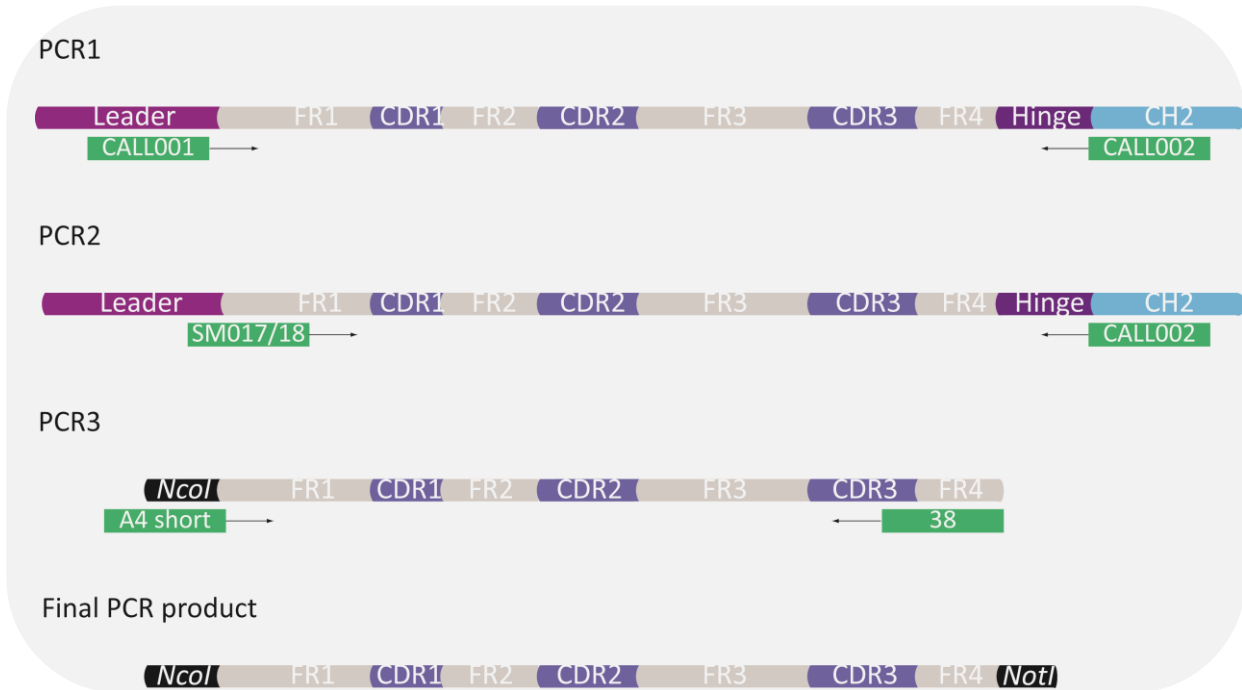


Figure 13: Schematic overview of the three subsequent polymerase chain reactions (PCRs) with the most important restriction sites plotted.

CDNA from total RNA was used as template to amplify genes encoding the variable domains of the heavy chain antibodies. After the first PCR two specific products are obtained (see Figure 14 A) allowing for the discrimination between V_H and V_{HH} repertoire. The first product with a size of ~ 1 kb encoding the variable regions V_H , the C_{H1} , the hinge and parts of the C_{H2} exons of the heavy chain of conventional antibodies. The second PCR product runs at $\sim 0,7$ kb and encodes the variable regions V_{HH} , hinge and part of the C_{H2} exons of the heavy chain antibodies (see Figure 14 A). The PCR product at $\sim 0,7$ kb was used as template in the next PCR step. In a second, nested PCR the restriction site *NcoI* is introduced. The PCR product ranging from FR1 to C_{H2} is $\sim 0,7$ kb in size (see Figure 14 B) was used as template in the last PCR step. Within the third PCR three more restriction sites (*SfiI*, *NotI*) necessary for

3 Results

subsequent cloning steps are introduced. The primer anneal in FR1 and FR4 resulting in amplification of V_HHs with ~ 0,4 kb in size (see Figure 14 C).

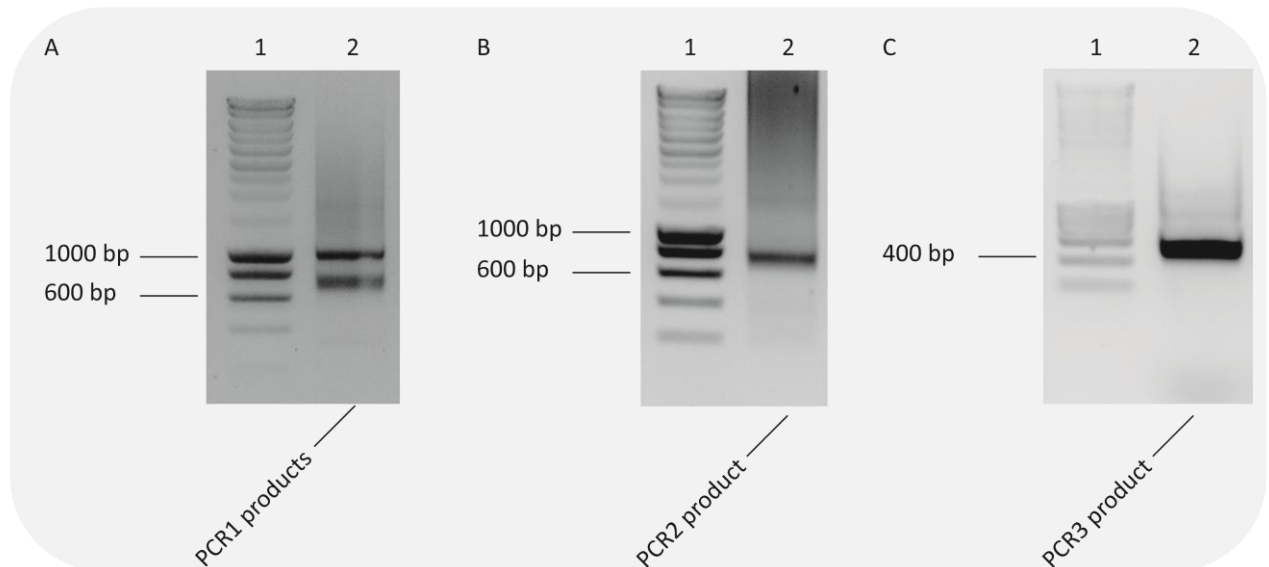


Figure 14: Exemplary overview of PCRs. (A) In a first PCR reaction the specific primers CALL001 and CALL002 amplify the repertoire of V_HHs (~ 0,7 kb) and V_HS (~ 1 kb). Lane 1: MW marker, Lane 2: PCR. The whole PCR reaction sample was separated on a 1 % agarose gel for 40 min at 100 V. (B) In a second PCR reaction the specific primers SM017/018 and CALL002 specifically amplify the repertoire of V_HHs and the restriction site *NcoI* is introduced. Lane 1: MW marker, Lane 2: PCR. The whole PCR sample was separated on a 1 % agarose gel for 40 min at 100 V. (C) In a third nested PCR reaction the specific primers A4 short and 38 introduce the restriction sites *SfiI*, *NotI*. Lane 1: MW marker, Lane 2: PCR. 10% PCR sample was separated on a 1 % agarose gel for 40 min at 100 V. Shown are representative results of the amplification of V_HHs from alpaca Sina.

3.1.3 Cloning of V_HH library in pHEN4

In order to obtain a highly diverse and large V_HH phage display library the ligation step of the V_HH repertoire and the corresponding phagemid vector pHEN4 and the subsequent transformation are the next important steps. In order to do so, the V_HH repertoire was ligated after amplification into the phagemid vector pHEN4 upstream and in frame with the capsid protein gene gIII using the restriction sites *NcoI* and *NotI* and transformed by electroporation into *E. coli* TG1 cells resulting in a phage display library, called primary library (see Figure 15).

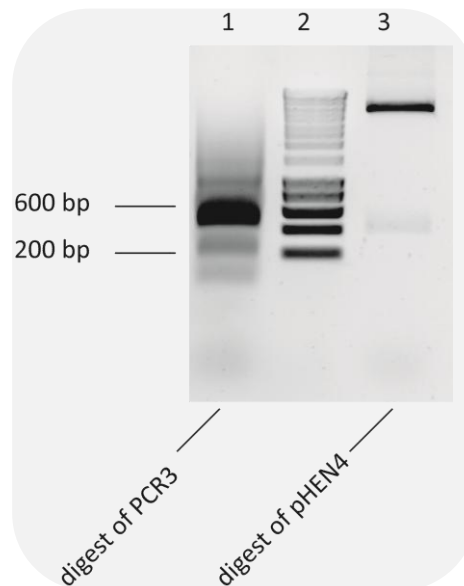


Figure 15: Digest of PCR3 and pHEN4 with *NcoI* and *NotI*. Lane 1: digested PCR3, Lane 2: MW marker, Lane 3: digested pHEN4. Samples were separated on a 1 % agarose gel for 40 min at 100 V. Shown are representative results of the amplification of V_HHs from alpaca Sina.

To maximize the V_HH library sizes, not only the absolute amount of DNA ligated but also the number of successful transformations is crucial. Initially, 4 - 6 ligation preparations were done; later up to 30 ligations were prepared. The number of transformations was increased from 3 x 40 µl during the first experiments to 30 x 40 µl during the latest experiments.

3 Results

Another important factor influencing library size is transformation efficiency displayed by the discharge time constant during electroporation which should be close to 5 ms and is decreased in the presence of salt. In addition, the presence of salt may cause short-circuits during electroporation which destroy the transformation preparation. Hence, to prepare salt free DNA the ligations were purified by phenol/chloroform extraction and ethanol precipitation during the first experiments. The electroporations showed time constants of 3,7 - 4,1 ms. Later, the protocol was further modified and ligations were dialyzed achieving higher time constants of up to 4,9 ms resulting in increased transformation efficiency.

To determine the size of the primary libraries, TG1 cells when transformed with the primary phage library were plated in serial dilutions and colony forming units (cfu) were counted. The library sizes for the different antigens are depicted in Table 25.

Table 25: Sizes of primary libraries.

APPLIED ANTIGEN	LIBRARY SIZE
γ H2AX-KLH	6×10^3 clones
HIV-1 CA	$1,1 \times 10^4$ clones
PCNA	$8,1 \times 10^3$ clones
GST- β -Catenin	$6,2 \times 10^5$ clones
hDnmt1	$1,5 \times 10^5$ clones

To verify the quality of the library regarding the insertion of the V_HH in the pHEN4, DNA of randomly picked colonies was digested with restrictions enzymes *NcoI* and *BstEII*. The results show that 70 % to 80 % of the transformants had an insert of proper size with ~ 0,4 kb. The slightly different sizes of the V_HH fragments indicate the diversity of the V_HH primary library (see Figure 16).

3 Results

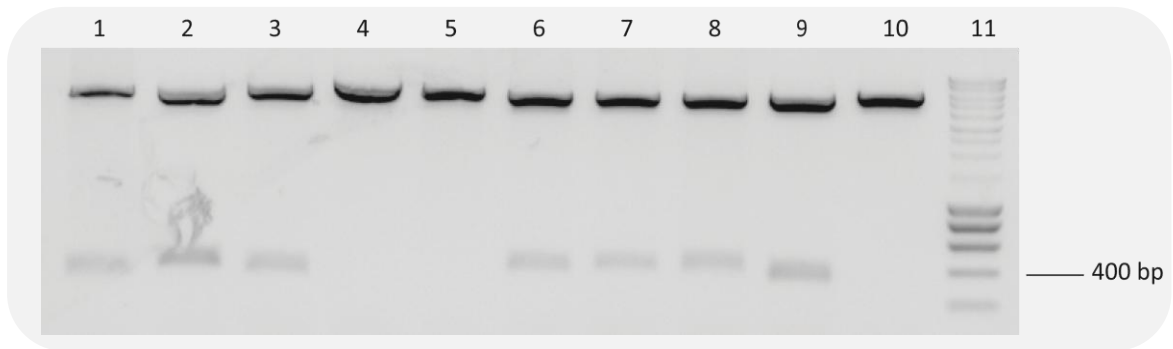


Figure 16: Restriction analysis of V_HH primary library. Lane 1 – 10 : Exemplary the digest of DNA of randomly picked clones from the *Sina-V_HH* primary library with *NcoI* and *BstEII* is shown. Lane 11: MW marker. Samples were separated on a 1 % agarose gel for 40 min at 100 V.

The cloning of the PCR product with the corresponding restriction enzymes results in an open reading frame of the pHEN4 phagemid adding an N-terminal *pelB* leader sequence to the putative V_HH domain which facilitates the transport of the expressed protein to the bacterial periplasm to ensure the correct formation of the essential disulfide bonds. In parallel a C-terminal gIII fusion is generated. Between V_HH and gIII an amber stop codon is located (see Figure 17). Stop codons generally signal the termination of translation. However, depending on the bacterial strain, the amber stop codon is read by a corresponding tRNA allowing the translation of the stop codon in the amino acid glutamine and hence the production of a full-length fusion protein. For this to occur, the primary library is transformed into the suppressor strain TG1 and the amber stop codon gets translated, resulting in the expression of the surface fusion protein V_HH-pIII for further analysis in phage display.



Figure 17: Schematic of V_HH gene locus in pHEN4.

To further analyze the diversity of the libraries, at least ten randomly picked single clones from each library were sequenced. Four out of five libraries were found to be highly diverse (see Figure 18 and Figure 19). Within these four primary libraries (HIV-1_primary, β -Catenin-

3 Results

GST_primary, PCNA_primary and Dnmt1_primary) all sequences were unique. Within the primary library of γ H2AX one of the sequences appears three times, another sequence appears twice. The CDR3s show differences in length between four (Dnmt1_primary#1) and 26 (γ H2AX _primary#1) amino acid residues. In the FR2 region, the characteristic hydrophilic amino acid substitutions at positions 37, 44, 45, 47 can be found, except for some sequences showing the hydrophobic residues of classical V_HS, e.g β -Catenin-GST_primary#5.

3 Results



Figure 18: Sequence alignment of V_HH amino acid sequences of primary libraries: (A) HIV-1, (B) γ H2AX, (C) β -Catenin-GST. Color code (used throughout): CDR1: red, CDR2: blue, CDR3: green, hallmark residues: violet. Numbering after Kabat et al. (Kabat, 1991).

3 Results

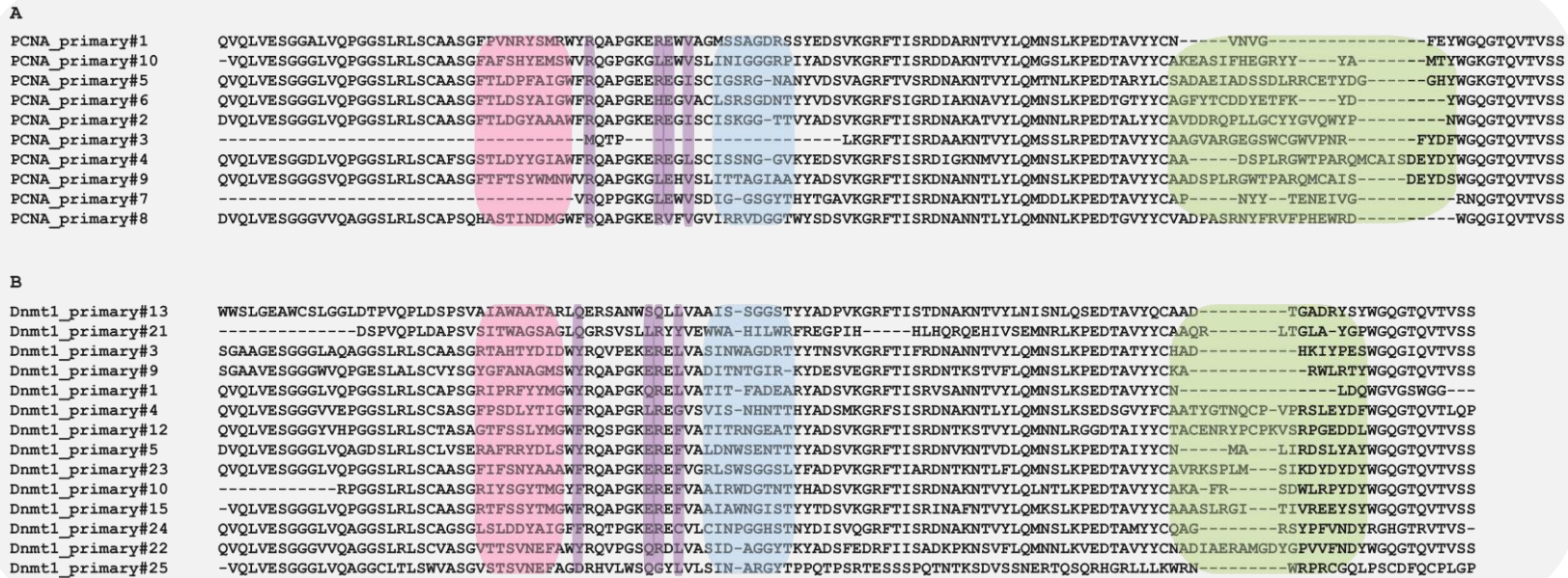


Figure 19: Sequence alignment of V_H amino acid sequences of primary libraries: (A) PCNA, (B) hDnmt1. Color code: CDR1: red, CDR2: blue, CDR3: green, hallmark residues: violet. Numbering after Kabat et al. (Kabat, 1991).

3 Results

3.1.4 Phage Display

To select antigen specific V_HHs the phage display method was applied. Even though this method is widely used to select antibody fragments, it requires experience, effort and optimization to robustly select functional antigen specific molecules. Initially, classical solid phase panning with immobilized antigens was performed (Bradbury and Marks, 2004). For solid phase panning recombinant antigen was produced in *E. coli*, insect cells or synthetically manufactured. In the progress of this work, this protocol was adapted and optimized according to the proposed downstream application of the selected V_HHs and a unique panning strategy was developed, the so called *native panning*. Here, antigen expressed in mammalian cells is used for panning selecting for V_HHs which recognize the native folded antigen.

3.1.4.1 Solid Phase Panning

To isolate antigen specific V_HHs the primary libraries were used in recursive rounds of selection on the appropriate antigen (see Table 26).

Table 26: Antigens used in phage display.

SCREENED ANTIGEN	CHARACTERISTICS
yH2AX-BSA	Peptide coupled to BSA (synthetically manufactured)
HIV-1 CA	Fulllength viral protein (24 kDa; produced in <i>E. coli</i>)
HIV-1 CA N-terminal domain	Domain of viral protein (15 kDa; produced in <i>E. coli</i>)
PCNA	Middle-sized protein (28 kDa; produced in <i>E. coli</i>)
GST	Protein tag (26 kDa; produced in <i>E. coli</i>)
hDnmt1	Large protein (150 kDa; produced in insect cells)

The antigens were immobilized in plastic immunotubes and phages presenting V_HHs on their tips were added. After a defined number of washing steps with increased stringency

3 Results

the phages were eluted and used for re-infection of TG1 cells in preparation for the next round of panning.

Even though there are many protocols available to select antibody fragments using solid phase panning, during the work for this thesis a number of optimizations were necessary to secure the selection of antigen specific V_HHs. In order to obtain antigen specific V_HHs only, the selection and enrichment of nonspecific phages needs to be avoided. Since filamentous phages, like M13, have been shown to bind nonspecifically to support surfaces like immunotubes (Bradbury and Marks, 2004) blocking is vital. Therefore, different blocking methods were tested. Traditionally, 4 % skimmed milk powder in PBS is used for blocking. However, we found out that phages strongly bind components of milk (data not shown). Consequently, to reduce unspecific binding of the phages to components of milk, protein free blocking solution (Pierce Biotechnology Inc.) was used, resulting in decreased unspecific binding (data not shown). To further eliminate phages which still bind to the immunotube surface, the eluted phages were added to blocked immunotubes without coated antigen after the first panning round. The unbound phages were used for re-infection of TG1 cells representing antigen specific phages.

The next critical step is the elution of bound V_HHs from the antigen. On the one hand, it is crucial to elute all bound phages to obtain the full repertoire of antigen specific V_HHs. On the other hand, the elution method needs to be as gentle as possible to make sure the V_HHs are not damaged resulting in non-functional V_HHs. In general, phages presenting antibody fragments on their tips can be eluted from the antigen in a number of different ways ranging from acidic (Roberts et al., 1992) to basic solutions (Marks et al., 1991) or proteolytic cleavage (Ward et al., 1996). Here, two different approaches were tested: acidic elution with 0,1 M HCl and basic elution with 0,1 M triethylamine showing the latter being the more suitable elution method resulting in more functional phages (data not shown).

3 Results

In general, at least three panning rounds were performed, except for GST and HIV-1 CA N-terminus, where fewer rounds were sufficient to generate potent antigen specific V_HHs (one panning round and two panning rounds, respectively). For each panning round the respective antigen is coated in an immunotube. In addition, a negative control without coated antigen is performed in parallel in order to evaluate the number of phages binding unspecifically to the surface of the immunotubes or components of the blocking solution. In each subsequent panning round, the number of washing steps was increased to enhance stringency. Before and after each round of panning the library size was evaluated by counting the colony forming units (phage titer) of TG1 cells infected with phage particles (as described in 2.2.5.3). Figure 20 and Figure 21 show the library sizes before and after each performed panning. The phage titer usually increases between panning rounds indicating that selection is occurring, as shown in Figure 20 B, Figure 20 B and Figure 21 C.

3 Results

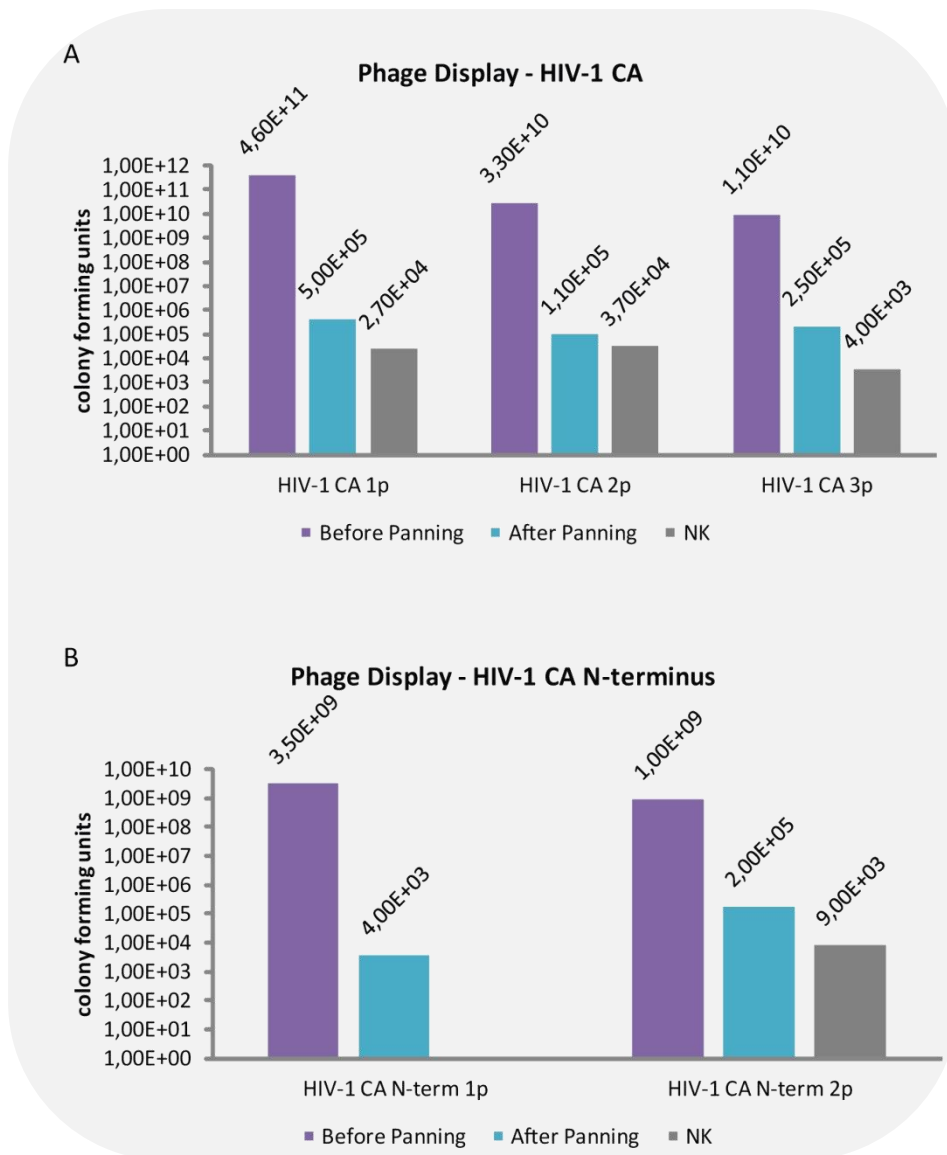


Figure 20: Overview of library sizes of HIV-1 capsid pannings. (A) The number of colony forming units for 3 panning rounds against the fulllength HIV-1 CA, HIV-1 CA 1p, HIV-1 CA 2p and HIV-1 CA 3p, is depicted. The numbers show, that there is no significant change of phage titer over the three panning rounds. (B) The number of colony forming units for 2 panning rounds against the N-terminus of the HIV-1 CA, HIV-1 CA N-term 1p and HIV-1 CA N-term 2p, is depicted. The results show, that the number of colony forming units increases from panning to panning.

3 Results

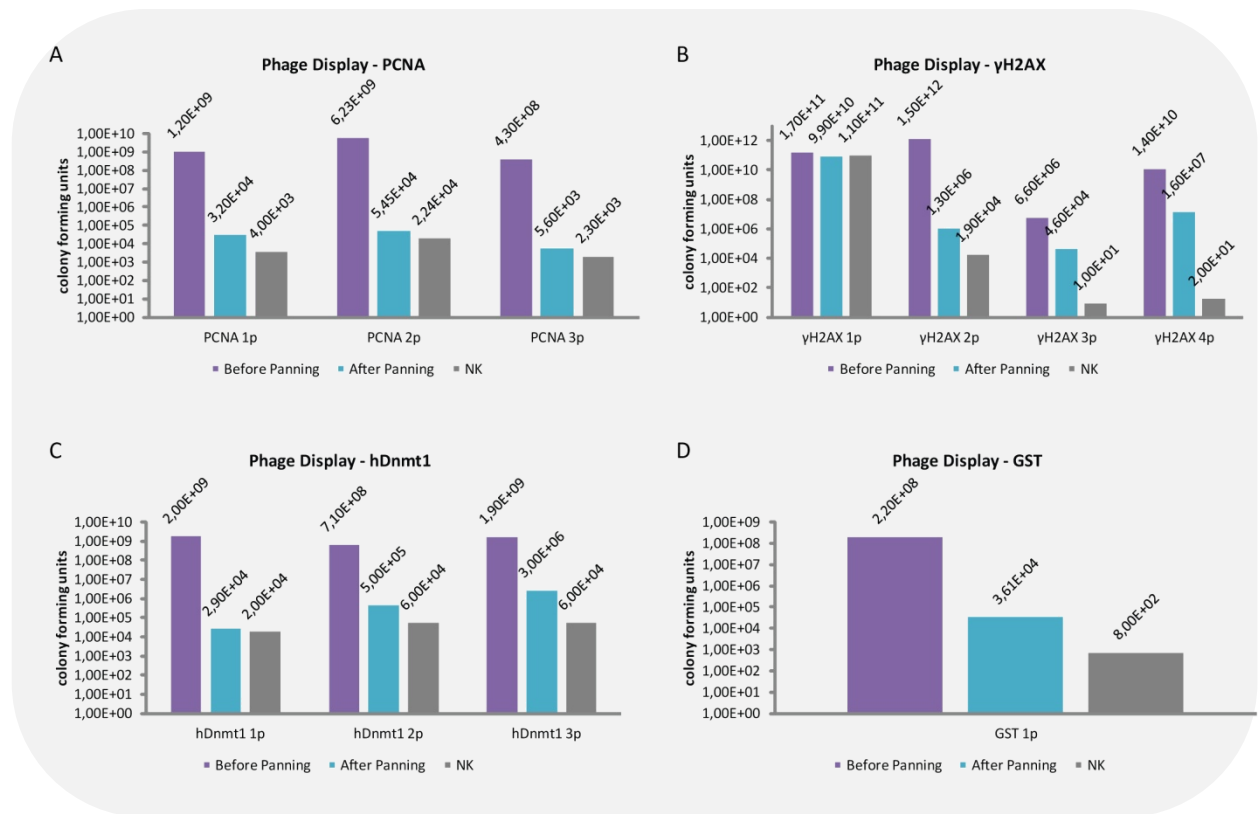


Figure 21: Overview of library sizes panning against PCNA, γH2AX, hDnmt1, GST. (A) The number of colony forming units for 3 panning rounds against PCNA, PCNA 1p, PCNA 2p and PCNA 3p, is depicted. The numbers show, that there is no significant change of phage titer over the three panning rounds. (B) The number of colony forming units for 4 panning rounds against γH2AX, γH2AX 1p, γH2AX 2p, γH2AX 3p and γH2AX 4p, is depicted. The numbers of colony forming units after the first panning round and the corresponding negative control are almost identical hinting that no selection occurs. In subsequent panning rounds the phage titer increases panning by panning. (C) The number of colony forming units for 3 panning rounds against hDnmt1, hDnmt1 1p, hDnmt1 2p and hDnmt1 3p, is depicted. The numbers of colony forming units after the first panning round and the corresponding negative control are almost identical hinting that no selection occurs. In the 2 subsequent panning rounds the numbers show, that there is significant change of phage titer from panning to panning. (D) The number of colony forming units for 1 panning round against GST, GST 1p, is depicted.

3 Results

3.1.4.2 Native Panning

As described in 1.2.2.1, solid phase panning may have several drawbacks regarding the presentation of the antigen. In order to select antigen specific V_HHs recognizing epitopes of native proteins for *in vivo* applications the presentation of the antigen is crucial. Several methods are known employing antigen specific antibodies or biotinylated antigen captured by streptavidin beads (Hawkins et al., 1992). As described in 3.1.4.1 filamentous phages have strong tendency to bind unspecifically to a variety of structures. Therefore, the application of biotinylated antigen has high potential to raise biotin but not antigen specific V_HHs. To circumvent these problems, the *native panning* method was developed during this thesis with hDnmt1 as proof of principle (Figure 22).

In brief, in a first step hDnmt1 was genetically fused to the green fluorescent protein (GFP). GFP alone and the fusion protein GFP-hDnmt1 were expressed in mammalian cells and cell lysate was produced. For the panning GFP and the GFP-hDnmt1 was purified using a 96-well microplate comprising an immobilized GFP-binding protein (GFP-Trap) (Figure 22 (1)) (Pichler et al., 2012). Phage particles derived from the hDnmt1 primary library presenting V_HHs on their tips were produced. To avoid the enrichment of GFP specific V_HHs the phages were added to the immobilized GFP, followed by a defined number of washing steps (Figure 22 (2)). Half of the unbound phages were added to the immobilized GFP-hDnmt1 to select for hDnmt1 specific V_HHs (Figure 22 (3) and (4)). In parallel, the other half of the unbound phages were added to a well with no antigen immobilizes in order to assess the number of phage unspecifically binding to the surface of the microplate. After a defined number of washing steps, the phages were eluted and used for re-infection of TG1 in preparation of a subsequent panning round. Figure 23 shows the results of solid phase and native panning against hDnmt1. After the first panning round, there is no unspecific background using native panning and the library size is 10 times bigger than after solid phase panning. After the second panning, however, there is unspecific background with both panning methods and the library after solid phase panning is 10 times bigger than after native panning.

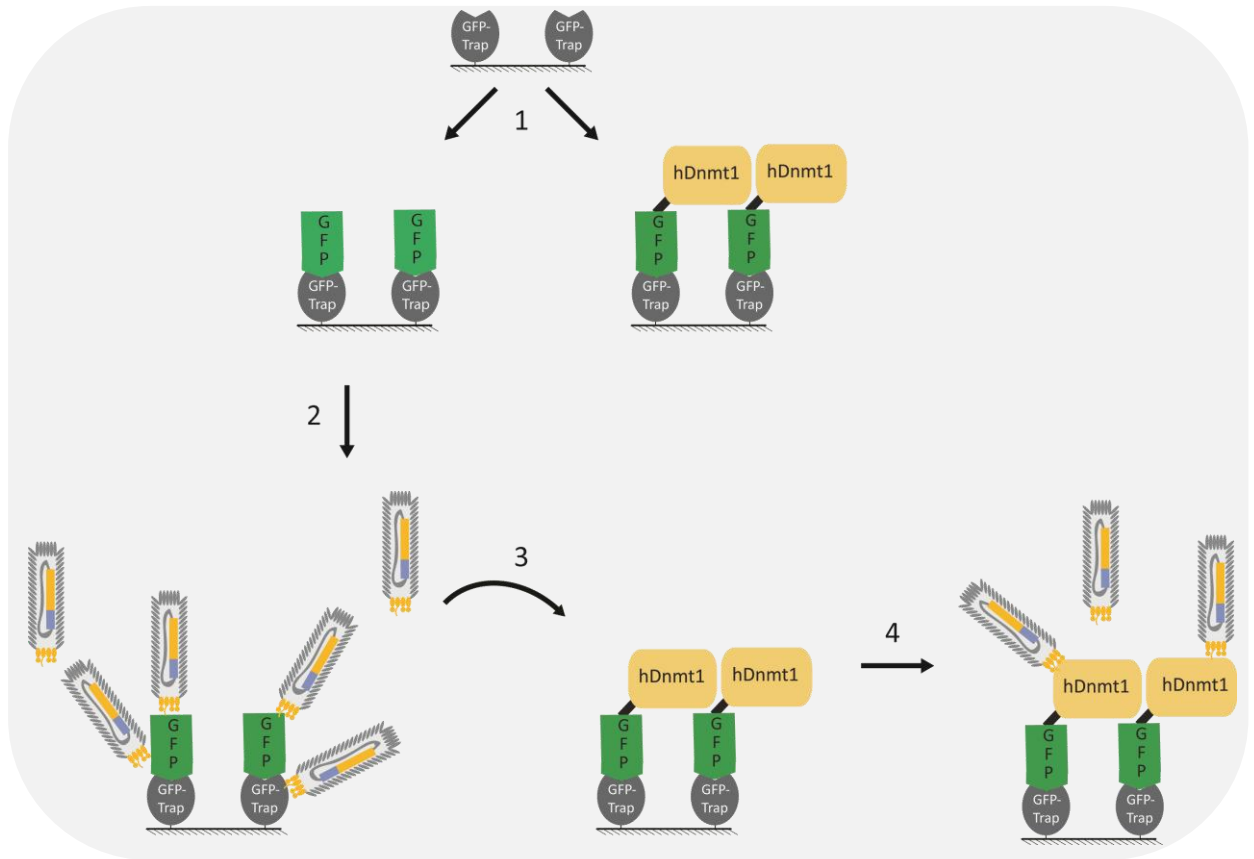


Figure 22: Schematic outline of the *native panning* strategy to enrich phages displaying V_HHs specific for hDnmt1. (1) Cell lysate expressing GFP and GFP-hDnmt1 was added to a 96-well microplate with immobilized GFP-Trap resulting in the immobilization of GFP and GFP-hDnmt1, respectively. (2) Phage particles presenting V_HHs from the primary hDnmt1-library on their tips were added to the immobilized GFP in order to eliminate V_HHs unspecifically binding to the surface of the microplate, the GFP-Trap or GFP. (3) Unbound phages were added to the immobilized GFP-hDnmt1. (4) Unbound phages were washed away and bound phages were eluted.

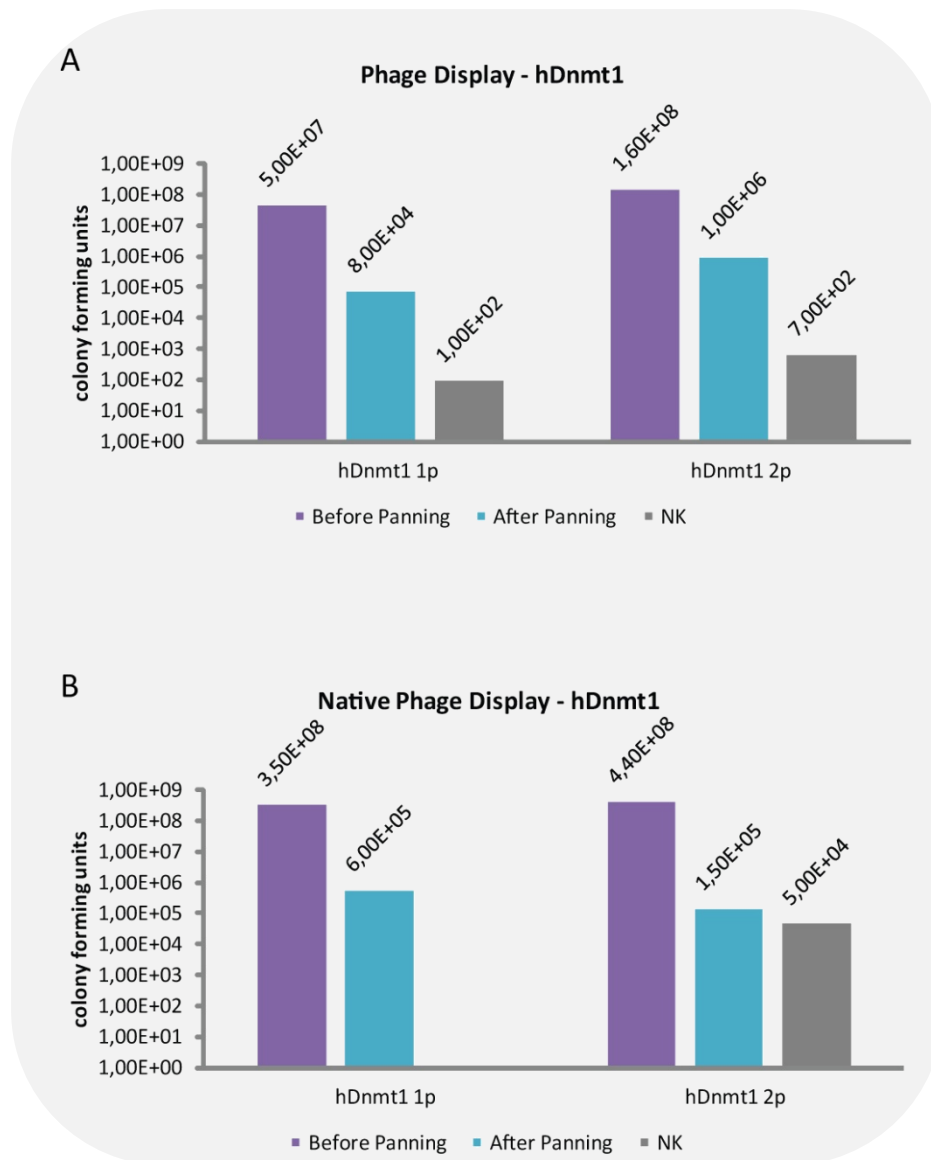


Figure 23: Overview of library sizes of solid phase panning and native panning against hDnmt1. (A) The number of colony forming units for 2 panning rounds against hDnmt1, hDnmt1 1p and hDnmt1 2p, is depicted. The numbers show, that there is significant change of phage titer from panning to panning. A negative control (NK) was performed in parallel with blocked immunotubes. (B) The number of colony forming units for 2 native panning rounds against hDnmt1, hDnmt1 1p and hDnmt1 2p, is depicted. The numbers show, that there is no significant change of phage titer. A negative control (NK) was performed in parallel using immobilized GFP-Trap without precipitated antigen.

3.1.4.3 Sequence analysis after Phage Display

Several rounds of panning against an antigen lead to enrichment of specific V_HHs. To analyze the enrichment of antigen specific V_HHs on DNA level after each panning round, 4 - 15 randomly picked single clones were sequenced after the panning rounds (see Figure 24 to Figure 28), except for the panning of the β -Catenin-GST library against GST – here, a phage ELISA was performed directly after panning.

3 Results



Figure 24: Sequence alignment of V_H amino acid sequences of single clones from γ H2AX libraries after solid phase panning against γ H2AX-BSA. (A) 1. panning round, (B) 2. panning round, (C) 3. panning round. Color code: CDR1: magenta, CDR2: blue, CDR3: green, hallmark residues: violet, identical sequences are marked with a red bar. Numbering after Kabat, 1991.

3 Results



Figure 25: Sequence alignment of V_HH amino acid sequences of single clones from HIV-1 libraries after solid phase panning against fulllength HIV-1 capsid protein.

(A) 1. panning round, (B) 3. panning round. Color code: CDR1: magenta, CDR2: blue, CDR3: green, hallmark residues: violet, identical sequences are marked with a red bar. Numbering after Kabat, 1991.

3 Results

A

```
HIV-1-Nterm_2p#1  QVQLVESGGGLVQAGGSLRSLCAASGYFSSYAMGWERQAPGKERE FVAAI SWIESTTDYADSVKGRFTI SRDNAKKT LHLQMNSLKPEDTAVYYCAACDI PFGQAFCALYDYWGQGTQVTVSS
HIV-1-Nterm_2p#4  -----MGWFRQAPGKERE FVAAI SWIESTTDYADSVKGRFTI SRDNAKKT LHLQMNSLKPEDTAVYYCAACDI PFGQAFCALYDYWGQGTQVTVSS
HIV-1-Nterm_2p#5  QVQLVESGGGLVQAGGSLRSLCAASGYFSSYAMGWERQAPGKERE FVAAI SWIESTTDYADSVKGRFTI SRDNAKKT LHLQMNSLKPEDTAVYYCAACDI PFGQAFCALYDYWGQGTQVTVSS
HIV-1-Nterm_2p#6  QVQLVESGGGLVQAGGSLRSLCAASGYFSSYAMGWERQAPGKERE FVAAI SWIESTTDYADSVKGRFTI SRDNAKKT LHLQMNSLKPEDTAVYYCAACDI PFGQAFCALYDYWGQGTQVTVSS
HIV-1-Nterm_2p#8  QVQLVESGGGLVQAGGSLRSLCAASGYFSSYAMGWERQAPGKERE FVAAI SWIESTTDYADSVKGRFTI SRDNAKKT LHLQMNSLKPEDTAVYYCAACDI PFGQAFCALYDYWGQGTQVTVSS
HIV-1-Nterm_2p#7  QVQLVESGGGLVQAGGSLRSLCAASGYFSSYAMGWERQAPGKERE FVAAI SWIESTTDYADSVKGRFTI SRDNAKKT LHLQMNSLKPEDTAVYYCAACDI PFGQAFCALYDYWGQGTQVTVSS
```

Figure 26: Sequence alignment of V_H H amino acid sequences of single clones from HIV-1 library after solid phase panning against HIV-1 capsid protein N-terminus.

(A) 2. panning round. Color code: CDR1: magenta, CDR2: blue, CDR3: green, hallmark residues: violet, identical sequences are marked with a red bar. Numbering after Kabat, 1991.

3 Results



Figure 27: Sequence alignment of V_H amino acid sequences of single clones from PCNA libraries after solid phase panning against PCNA. (A) 1. panning round, (B) 2. panning round, (C) 3. panning round. Color code: CDR1: magenta, CDR2: blue, CDR3: green, hallmark residues: violet, identical sequences are marked with a red bar. Numbering after Kabat, 1991.

3 Results

A

```

Dnmt1_SP_1p#2  -VQLVESGGGSVHAGDSLRLSCAAEGRTVSSYALGWFRQAPGREFEFVATI SWGGATTNYADSVRGRFTISRDNKNTVYLQMNLSLKPEDTAVYYCAVGEN----TAQIRRINIKSWGQGTQVTVSS
Dnmt1_SP_1p#3  QVQLVESGGGLVQAGDSLRLSCAAEGRTVSSYALGWFRQAPGKEREFEVATI SWGGATTDYADSVRGRFTVSRDNKNILYLQMNLSLKPEDTAVYYCAVGEN----TAQIRRLNIRSWGQGTQVTVSS
Dnmt1_SP_1p#8  QVQLVESGGGLVQAGDSLRLSCAAEGRTVSSYALGWFRQAPGKEREFEVAAISRAGGSIIYADSVKGRFTISRDNKNTMYLQMNLSLKPEDTAVYYCAADSSGA--YLSRAWRVDSWGQGTQVTVSS
Dnmt1_SP_1p#6  QVQLVESGGGLVQAGGSLKLACAASGLTFSNYAMAWFRQGSQKQRELVAAINWRSG-TYYADSVLGRFTISRDNKNTVYLQMNLSLKPEDTAVYYCASAVSPL--KMSTEIHEYNSWGQGTQVTVSS
Dnmt1_SP_1p#4  DVQLVESGGGLVQTGGSLRLSCTASERTFSGHLMGWFRQAPGKREFFLSAISWWSGKTYAEVVKGRFTISRDNKNTLYLQMNLSLKPEDTALYRCATAGRE---RYYTDPAGYVYWGQGTQVTVSS
Dnmt1_SP_1p#7  QVQLVESGGGLVQAGDSLRLSCTVSEAFGYVLMGWFRQAPGKEREFEVATISWGGATTDYADSVRGRFTVSRDNKNTVYLQMNLSLKPEDTAVYYCAVGEN----TAQIRRLNIRSWGQGTQVTVSS
Dnmt1_SP_1p#1  QVQLVESGGGLVQAGGSLRLSCAAEGRTVSSYALGWFRQAPGKEREFEVAAITWGSSTNYADSVKGRFTISRDNKNTVYLQMNLSLKPEDTAVYYCAADSSGA--YLSRAWRVDSWGQGTQVTVSS
Dnmt1_SP_1p#5  QVQLVESGGGLVQAGGSLRLSCAAEGRTVSSYALGWFRQAPGKEREFEVATISGSGGTYADSVKGRFTISRDNKNTVYLQMNLSLKPEDTAVYYCAAGLT----TSSLVANTPPTWGQGTQVTVSS
Dnmt1_SP_1p#9  ----VESGGGLVQAGGSLRLSCTVSEAFGYVLMGWFRQAPGKEREFEVATISGSGGTYADSVKGRFTISRDNKNTVYLQMNLSLKPEDTAVYYCAAGLT----TSSLVANTPPTWGQGTQVTVSS
  
```

B

```

Dnmt1_N_1p#6  QVQLVESGGGYVHPGGSRLRLSCTASAGTFSFLYMGWFRQSPGKEREFEVATITRNGEATYADSVKGRFTISRDNKNTVYLQMNLSLKPEDTAVYYCAVGEN----TAQIRRLNIRSWGQGTQVTVSS
Dnmt1_N_1p#7  -VQLVESGGGYVHPGGSRLRLSCTASAGTFSFLYMGWFRQSPGKEREFEVATITRNGEATYADSVKGRFTISRDNKNTVYLQMNLSLKPEDTAVYYCAVGEN----TAQIRRLNIRSWGQGTQVTVSS
Dnmt1_N_1p#4  QVQLVESGGGFVQAGGSLRLSCAAEGRTIY-YAMGWFRQAPGKEREFEVAAIGWGLNSTAYSDSVKGRFTISRDNKNTVYLQMNLSLKPEDTAVYYCAVGEN----TAQIRRLNIRSWGQGTQVTVSS
Dnmt1_N_1p#5  QVQLVESGGGLVQAGGSLRLSCAAEGRTIY-YAMGWFRQAPGKEREFEVAAIGWGLNSTAYSDSVKGRFTISRDNKNTVYLQMNLSLKPEDTAVYYCAVGEN----TAQIRRLNIRSWGQGTQVTVSS
Dnmt1_N_1p#8  QVQLVESGGGLVQAGGSLRLSCAAEGRTIY-YAMGWFRQAPGKEREFEVAAIGWGLNSTAYSDSVKGRFTISRDNKNTVYLQMNLSLKPEDTAVYYCAVGEN----TAQIRRLNIRSWGQGTQVTVSS
Dnmt1_N_1p#9  QVQLVETGGGLVQAGGSLRLSCTASAGTFSFLYMGWFRQSPGKEREFEVATITRNGEATYADSVKGRFTISRDNKNTVYLQMNLSLKPEDTAVYYCAVGEN----TAQIRRLNIRSWGQGTQVTVSS
Dnmt1_N_1p#3  QVQLVESGGGLVQAGGSLRLSCTASAGTFSFLYMGWFRQSPGKEREFEVATITRNGEATYADSVKGRFTISRDNKNTVYLQMNLSLKPEDTAVYYCAVGEN----TAQIRRLNIRSWGQGTQVTVSS
Dnmt1_N_1p#1  DVQLVESGGGWVQAGSSRVLSCAAEGRTIY-YAMGWFRQAPGKEREFEVAAITWGSSTNYADSVKGRFTISRDNKNTVYLQMNLSLKPEDTAVYYCAVGEN----TAQIRRLNIRSWGQGTQVTVSS
Dnmt1_N_1p#2  QVQLVESGGGLVQAGSSRVLSCAAEGRTIY-YAMGWFRQAPGKEREFEVAAITWGSSTNYADSVKGRFTISRDNKNTVYLQMNLSLKPEDTAVYYCAVGEN----TAQIRRLNIRSWGQGTQVTVSS
  
```

Figure 28: Sequence alignment of V_HH amino acid sequences of single clones from hDnmt1 libraries after (A) solid phase panning against hDnmt1 and (B) native panning round against hDnmt1-GFP. Color code: CDR1: magenta, CDR2: blue, CDR3: green, hallmark residues: violet, identical sequences are marked with a red bar. Numbering after Kabat, 1991.

3 Results

The V_HH sequence alignments of single clones after the pannings depicted in Figure 24 to Figure 28 show the characteristic hydrophilic amino acid substitutions (the so called hallmark residues) in the FR2 region at positions 37, 44, 45, 47. However, in addition to antigen specific V_HHs also conventional V_H domains comprising hydrophobic residues at the hallmark positions in FR2 were found among the enriched sequences (e.g. γ H2AX_1p#4, PCNA_2p#3 or Dnmt1_N_1p#8). One reason for an enrichment of V_H domains could be slight contamination with V_H encoding DNA during the PCR amplification steps which were amplified due to the high sequence homologies between V_HHs and V_HS and then were selected as single domains during phage display.

To compensate the loss of the variable light chain and to increase the antigen binding sites V_HHs often have extended CDR3s (Muyldermans et al., 1994). This general rule can be confirmed by the sequenced clones (see Figure 29). These extended CDR3s are often found in V_HH domains which also possess an additional cysteine residue, beside the conserved cysteine residues at position 22 and 98 which are responsible for the formation of a disulfide bond between FR1 and FR3. Here, 78 % of the V_HH sequences comprising a long CDR3 (more than 15 amino acid residues) possess at least one additional cysteine residue.

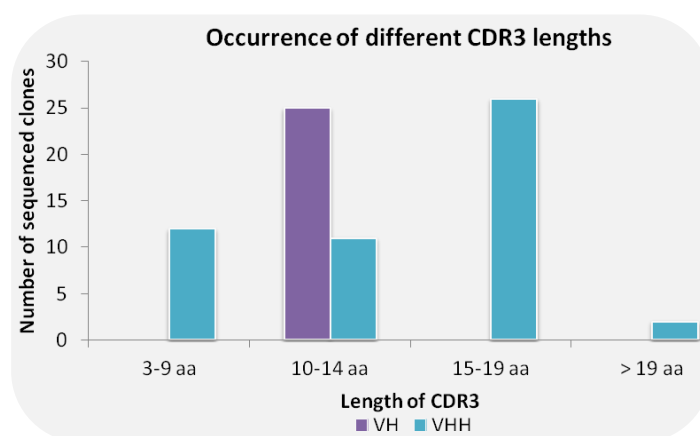


Figure 29: Occurrence of CDR3 lengths of V_HH selected after phage display. V_HH and V_H sequences from clones sequenced after the panning rounds (see Figure 24 - Figure 28). Numbering after Kabat, 1991.

3 Results

Independent of the antigen or panning round, a significant number of V_HHs comprise up to three additional cysteine residues in their CDRs. It has been shown that additional cysteines in V_HHs can either form a CDR3 intraloop disulfide bond or an interloop cysteine bridge connecting CDR3 with CDR1 which stabilizes the V_HH (Davies and Riechmann, 1996) or enables the formation of alternative antigen binding scaffolds (Conrath et al., 2003). The results show, that the V_HHs sequenced preferentially possess no or two additional cysteines while V_Hs preferentially possess no additional cysteine in their CDRs (see Table 27).

Table 27: Frequency of occurrence of clones with or without additional cysteines in their CDRs. The dataset contained 27 V_H and 53 V_HH clones.

	V _H (%)	V _H H (%)
No cysteine	96	58
1 cysteine	4	2
2 cysteines	0	38
3 cysteines	0	2

The sequence analysis of clones panned against γ H2AX-BSA (see Figure 24) reveal that none of the binding molecules contain an additional cysteine after the first panning round, however, the sequence analysis after the third panning shows only one V_HH sequence comprising two additional cysteine residues located in CDR2 and CDR3. This additional disulfide bridge could be important to stabilize the antigen recognition interface consisting of the hypervariable region CDR2 and CDR3 of the V_HH. Interestingly, all V_HH domains selected against fulllength HIV-1 capsid protein (see Figure 25) do not have additional cysteine residues, while the selected V_HH sequences against the N-terminal domain of HIV-1 capsid protein comprise two additional cysteine residues in their CDR3 which is much longer, too (see Figure 26). The sequences of clones after pannings against PCNA show a decreasing number of cysteine residues after each subsequent panning round (see Figure 27). This could be due to the fact that an additional cysteine bridge is not needed to generate a stable

3 Results

folded hypervariable region. None of the V_HH sequences of clones panned against hDnmt1 in solid phase panning possess an additional cysteine residue, while two clones with two additional cysteine residues can be found after native panning (see Figure 28).

The V_HH sequence alignments of single clones after the solid phase panning against γ H2AX-BSA in Figure 24 reveal an enrichment of one sequence after the first (e.g. γ H2AX_1p#5), second (e.g. γ H2AX_2p#2) and after the third panning round (e.g. γ H2AX_3p#2) as well. However, the enriched sequences differ after each panning round. Considering the high phage titer for the negative control after the first panning round against γ H2AX-BSA (Figure 21) this result indicates an enrichment of unspecific V_HHs, e.g. binding to the carrier BSA or a component of the blocking solution.

The V_HH sequence alignments of single clones after solid phase panning against fulllength HIV-1 capsid protein (Figure 25) show an enrichment of one sequence after the first panning (e.g. HIV-1_1p#2). Even though the sequences HIV-1_1p#1 and HIV-1_1p#4 are similar in CDR2 and CDR3, they differ in CDR1 in two amino acid residues. This occurrence may be explained by the CDR1 of V_HHs being a hotspot for somatic hypermutation (Nguyen et al., 2000). The sequenced clones after the first panning round can be found after the third panning round, as well. In addition, a third enriched sequence can be found after the third panning round (e.g. HIV-1_3p#3). It is remarkable that all identified V_HHs directed against the fulllength HIV-1 capsid protein have extremely short CDR3s, comprising just four amino acid residues. In contrast, the V_HH sequences of single clones after the second solid phase panning round against the N-terminus of HIV-1 capsid protein (Figure 26) possess long CDR3s of 15 amino acid residues including one additional cysteine residue in the CDR3 and in the CDR2. Since both panning rounds were performed using the same phage display library, these results can be traced back to the different V_HHs being derived from different B-cell pools. After the solid phase panning against the N-terminus of HIV-1 capsid protein only one sequence was enriched after the second panning round which implies an enrichment of an antigen specific V_HH.

3 Results

In Figure 27 the V_HH sequence alignments of single clones after solid phase panning against PCNA are depicted. After the second panning round two sequences are enriched with one being a V_H (e.g. PCNA_2p#2) and the other one being a V_HH (e.g. PCNA_2p#5). The CDR2 and CDR3 of the V_H PCNA_2p#1, #2, #3 and #12 show a significant homology, but #1 and #3 differ in the CDR1 in three and one amino acid residues, respectively. This may be explained by somatic hypermutation, however, V_HS generally have more conserved amino acid residues in their CDR1s than V_HHs (Muyldermans et al., 2009). After the third panning round (see Figure 27 C) only one CDR3 sequence (e.g. as shown in PCNA_3p#15) is strongly enriched. However, the clones comprising this particular CDR3 differ in the CDR1 by two (e.g. PCNA_3p#2) to four (e.g. PCNA_3p#20) amino acid residues, demonstrating that at least two different V gene fragments were fused to the same D-J gene fragment. The clones sequenced after the panning against PCNA show strong enrichment of V_HS after the subsequent panning rounds.

Figure 28 shows the V_HH sequence alignments of single clones after the panning against hDnmt1 with two different panning approaches being employed: solid phase panning and native panning. Figure 28 A shows the alignment of V_HH sequences after solid phase panning using recombinant hDnmt1 purified from insect cells. Two sequences derived from solid phase panning show a high similarity: Dnmt1_SP_1p#2 and Dnmt1_SP_1p#3. However, these sequences differ in the CDR3 by two and in CDR2 by one amino acid residue. Figure 28 B shows the alignment of V_HH sequences of single clones after the native panning using hDnmt1-GFP from cell lysate. Here, one sequence is enriched (e.g. Dnmt1_N_1p#6). In addition, two clones, Dnmt1_N_1p#1 and #2 are similar in CDR2 and CDR3, but they differ in CDR1 by two amino acid residues. These minor differences can be explained by the high somatic hypermutation rate in V_HHs (Nguyen et al., 2000). In contrast to all clones sequenced after the solid phase panning this enriched sequence has two additional cysteine residues in CDR3. Interestingly, sequences derived from single clones after solid phase

3 Results

panning cannot be found after native panning, indicating that different epitopes are recognized with regard to the mode of antigen presentation.

3.1.5 Selection of antigen specific V_HHS by Phage ELISA

After several rounds of panning the resulting libraries contain a variety of antigen specific V_HHS. In order to evaluate the success of the enrichment process and to identify antigen specific V_HHS for further applications such as Nanotrap or Chromobody, phage ELISA (enzyme-linked immunosorbent assay) was performed. The method phage ELISA measures the binding of solution-phase phages and is particularly advantageous since it is a simple and robust method to confirm the binding specificity of single phage clones. Especially in case of poor bacterial expression of the V_HH domain, analysis of phages is superior to analysis of V_HH domains prepared from induced bacterial cultures. Additionally, phage ELISA is advantageous because of the signal amplification due to the detection of the coat protein pVIII which occurs in multiple copies within the phage surface. In brief, recombinant antigen was coated in a microtiter plate. 19 to 48 single phage clones from panned phage libraries were added, presenting individual V_HHS on their tips. The clones were tested for their antigen specificity on the appropriate antigen. In order to verify this result and exclude unspecific V_HHS, the single clones were tested on a negative control in parallel.

Although being a very sensitive method, phage ELISA is prone to give false positive results and required several optimization steps. First, the unspecific binding of phages to the surface of microtiter plates needs to be avoided by using the appropriate blocking solution. In the beginning of this thesis 4 % skimmed milk powder in PBS was used. As described in 3.1.4.1, phages show high unspecific binding to components of milk, hence, protein free blocking solution was used later. Second, to ensure a successful selection of antigen specific V_HHS, efficient coating of the antigen needs to be controlled. Hence, appropriate immobilization of an antigen was monitored by using an antigen specific antibody in a classical ELISA approach. Last, when working with peptides coupled to carriers like KLH or BSA unspecific binding of phages to the carrier protein can occur. To avoid the selection of phages binding unspecifically to carriers, the carrier protein was exchanged for the panning

3 Results

and phage ELISA. At the beginning of this work, γ H2AX peptide coupled to the carrier KLH was used for immunization, phage display and phage ELISA making it impossible to distinguish between V_H Hs specific for the peptide or the carrier protein. Therefore, in later experiments, the carrier was changed to BSA in the panning and the subsequent phage ELISAs.

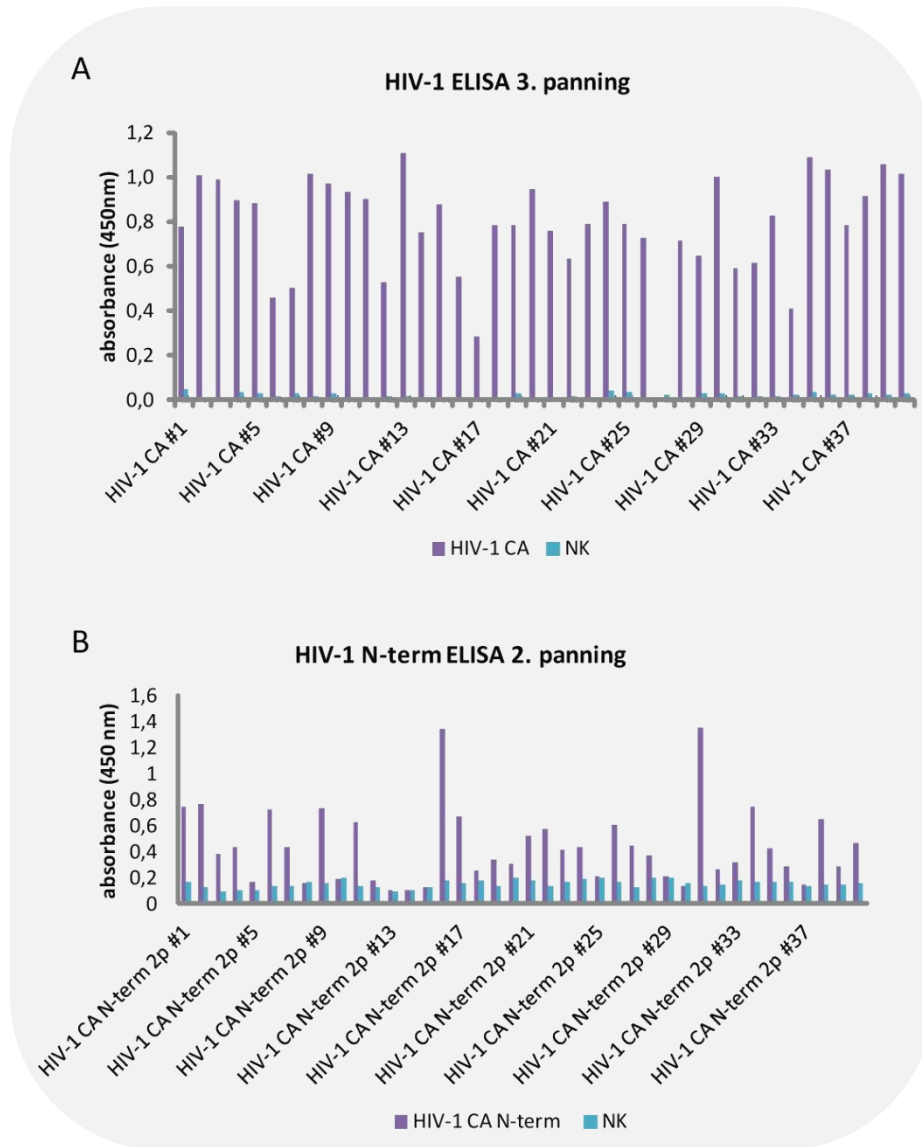


Figure 30: Analysis of HIV-1 capsid specific V_H Hs by phage ELISAs. The binding of phages presenting individual V_H Hs on their tips was measured at 450 nm. (A) HIV-1 ELISA after third panning round with immobilized HIV-1 capsid protein. (B) HIV-1 ELISA after second panning round with immobilized N-terminus of HIV-1 capsid protein. NK: negative control.

3 Results

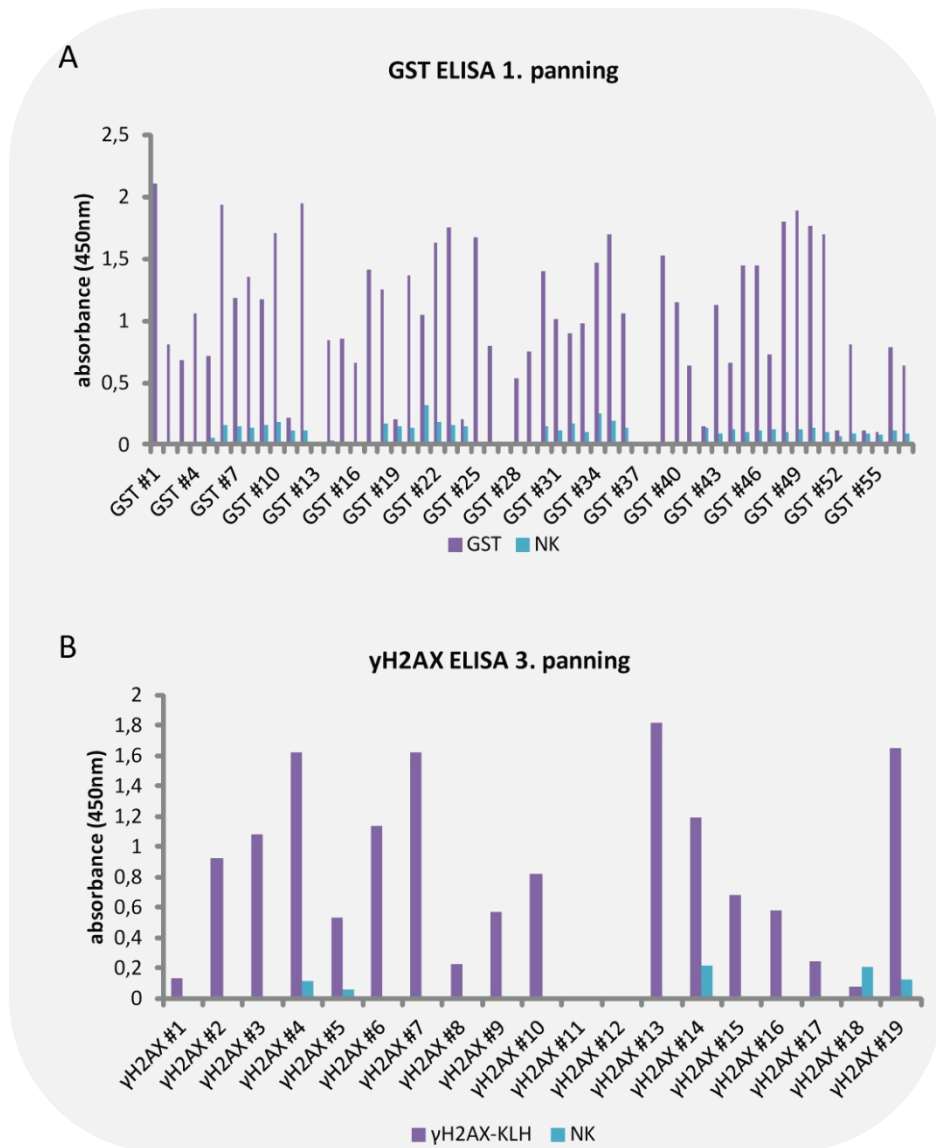


Figure 31: Analysis of GST and yH2AX specific V_HHs by phage ELISAs. The binding of phages presenting individual V_HHs on their tips was measured at 450 nm. (A) GST ELISA after first panning round with immobilized GST (B) yH2AX ELISA after third panning round with immobilized yH2AX-BSA. NK: negative control.

3 Results

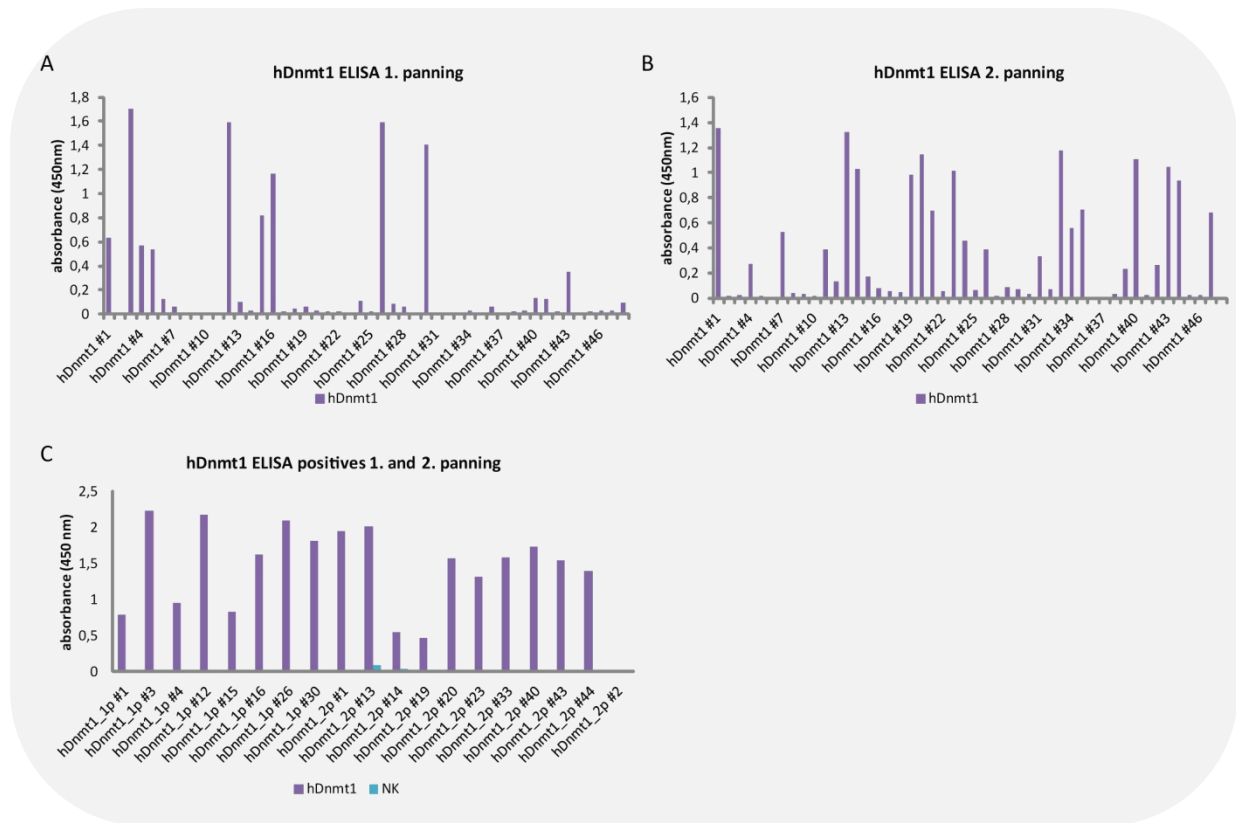


Figure 32: Analysis of hDnmt1 specific V_HHs by phage ELISAs. The binding of phages presenting individual V_HHs on their tips was measured at 450 nm. (A) Dnmt1 ELISA after first panning round with immobilized hDnmt1. (B) Dnmt1 ELISA after second panning round with immobilized hDnmt1. (C) Dnmt1 ELISA of ELISA positives from (A) and (B) with immobilized hDnmt1. NK: negative control.

In order to identify single V_HHs specific for the appropriate antigen, 19 (γH2AX ELISA 3. panning) to 48 (Dnmt1 ELISA 1. panning) single phage clones were tested in phage ELISA. The results in Figure 30 to Figure 32 show, that all libraries contain antigen specific V_HHs. The percentage of antigen specific clones (signal intensity defined empirically as > 1) varies between 5 % and 51 % (see Table 28).

3 Results

Table 28: Overview of antigen specific clones identified in phage ELISA.

	ANTIGEN SPECIFIC CLONES IDENTIFIED IN PHAGE ELISA (%)
HIV-1 3. panning	20
γ H2AX 3. panning	37
HIV-1 Nterm 2. panning	5
GST 1. panning	51
Dnmt1 1. panning	10
Dnmt1 2. panning	21

In order to identify HIV-1 capsid protein specific V_HHs 40 single phage clones were tested after the third panning round for their specificity to HIV-1 capsid protein (see Figure 30 A). The results show that 20 % of the clones recognize HIV-1 capsid protein while none of the tested clones recognizes the negative control (GFP). Apparently, the desired enrichment of HIV-1 capsid specific V_HHs during the panning occurred.

In Figure 30 B the result of the phage ELISA of selected phage clones after the second panning round against the N-terminal domain of HIV-1 capsid protein is depicted. In order to select for specific V_HHs 40 clones were tested. Although the sequencing results after the second panning round (Figure 26 A) imply the selection of just one specific V_HH, the phage ELISA, however, results in only 5 % positive clones.

In order to identify GST-specific V_HHs, a phage ELISA was performed testing 57 clones after the first panning against GST with 51 % of the clones being specific for GST (see Figure 31 A). This result is in accordance with the panning results with the phage titer for the negative control being 50 % of the phage titer for the antigen specific phages (see Figure 20 D).

3 Results

Figure 31 B shows the result for the identification of γ H2AX specific V_H Hs with 19 single phage clones being tested against γ H2AX-BSA and GFP as negative control after the third panning round. The result shows that 37 % of the tested clones specifically recognize γ H2AX-BSA. This is contrary to the phage display results shown in Figure 21 B with the phage titer being almost zero for the negative control.

Figure 32 shows the phage ELISA results of selected phage clones after the solid phase panning against hDnmt1. Clearly, more antigen specific clones can be identified after the second panning round (21 %) than after the first panning round (10 %). Within these two phage ELISA experiments no negative controls were performed, however, to verify the specificity for hDnmt1 all positive phages from the first and second panning were repeatedly tested including GFP as a negative control (Figure 32 C). The result shows that all V_H Hs identified in the first phage ELISA are specific for hDnmt1 and do not recognize GFP.

3.1.5.1 Sequence analysis after Phage ELISA

Phage ELISA enables the identification of antigen specific V_H Hs. To analyze the protein sequences of antigen specific V_H Hs, the DNA of 5 - 31 single clones obtained in phage ELISA was subjected to sequence analysis. The first phage ELISA performed during this thesis was the phage ELISA to identify HIV-1 specific V_H Hs (see Figure 30 A). It was not clear which threshold level regarding the signal intensity needs to be defined in order to select positive clones, hence, the DNA of all clones tested in ELISA was sequenced and analyzed resulting in a threshold of $OD_{450nm} = 1$ for subsequent phage ELISA experiments.

Interestingly, all sequences of positive clones derived from phage ELISA shown in Figure 35 to Figure 38 are V_H Hs and show the characteristic hydrophilic amino acid substitutions (the so called hallmark residues) in the FR2 region at positions 37, 44, 45, 47. In summary, the results show, that only 43 % of the antigen specific V_H Hs identified in phage ELISA possess an

3 Results

extended CDR3. 62 % of the V_H Hs with extended CDR3s possess at least one additional cysteine residue independently of the antigen or panning round.

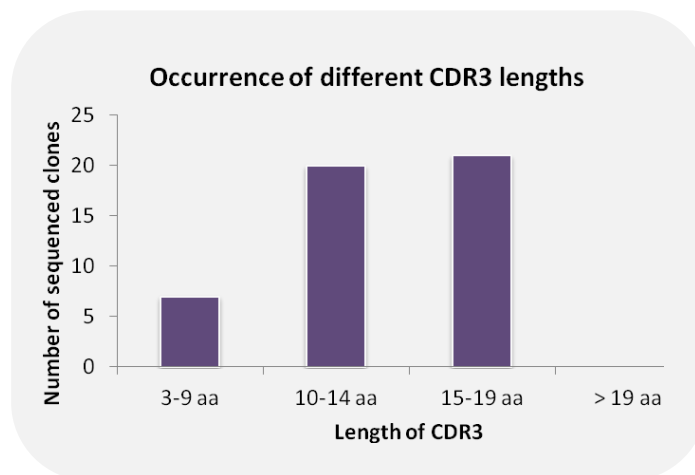


Figure 33: Occurrence of CDR3 lengths of antigen specific V_H Hs selected via phage ELISA. V_H H and V_H sequences from clones sequenced after the panning rounds (see Figure 24 - Figure 28). Numbering after Kabat, 1991.

The V_H H sequence analysis of positive clones selected in phage ELISA against HIV-1 capsid protein (Figure 34) shows an enrichment of six different sequences: e.g. HIV-1_3p_ELISA#2 (HIV#2), HIV-1_3p_ELISA#1 (HIV#1), HIV-1_3p_ELISA#9 (HIV#9), HIV-1_3p_ELISA#10 (HIV#10), HIV-1_3p_ELISA#12 (HIV#12) HIV-1_3p_ELISA#13 (HIV#13) and HIV-1_3p_ELISA #19 (HIV#19). The sequences of HIV#1 and HIV#9 are highly similar; however, they vary by one amino acid residue in the CDR3, by three amino acid residues in the CDR2 and by one amino acid residue in the CDR1. The differences in the CDR3 is due to the use of different D segments during VDJ recombination, the differences in CDR1 and CDR2 could be the result of somatic hypermutation during affinity maturation. In addition, HIV-1_3p_ELISA#26 has the same CDR3 as HIV#9, but differs in CDR2 by one amino acid residue which may be explained by somatic hypermutation, as well. All identified sequences can also be found within the sequences after the 1. and the 3. panning round against HIV-1 capsid protein (see Figure 25). Again, as shown in the sequence analysis after the panning rounds, all HIV-1 capsid protein specific V_H Hs comprise very short CDR3s with no additional cysteine residues. In contrast,

3 Results

87,5 % of the V_HH domains selected against the N-terminal domain of HIV-1 capsid protein comprise an extended CDR3 and two additional cysteine residues in their CDR3, e.g. HIV-1-N-term_2p_ELISA#1 (HIV-Nterm#1) (see Figure 36).

The V_HH sequence analysis of positive clones derived after phage ELISA against γ H2AX-BSA in Figure 35 shows an enrichment of one sequence e.g. γ H2AX_3p_ELISA#3. This sequence contains two additional cysteines located in the CDR2 and CDR3. Interestingly, this sequence can be found after the 3. panning round already (see Figure 24 C), verifying positive selection of antigen specific V_HHs during phage display. Another CDR3 is enriched (e.g. γ H2AX_3p_ELISA#4), however, these sequences do not have additional cysteine residues and differ in CDR1 and CDR2 which can be explained by the use of the same D segment but different V segments during VDJ-recombination.

In Figure 37 the V_HH sequence alignments of single positive clones for GST are depicted with two enriched sequences: e.g. GST_1p_ELISA#35 and e.g. GST_1p_ELISA#25. Both enriched sequences neither possess an extended CDR3 nor additional cysteine residues. In addition, several sequence pairs seem very similar, e.g. GST_1p_ELISA#1 and GST_1p_ELISA#39 or GST_1p_ELISA#23 and GST_1p_ELISA#50. However, they have slight sequence difference in CDR3 (one amino acid residue) and CDR2. The differences in the CDR3s may be explained by the use of different D segments during VDJ recombination while the differences in the CDR2s may be explained by somatic hypermutation since there is no sequence difference within the CDR1s implying the use of different V segments.

Figure 38 shows the V_HH sequence alignments of single positive clones for hDnmt1 resulting in two enriched sequences: e.g. Dnmt1_1p_ELISA#26 and e.g. Dnmt1_1p_ELISA#30. Both enriched sequences possess an extended CDR3, but only one of the sequences has two additional cysteine residues.

3 Results

```

HIV-1_3p_ELISA#2  QVQLVESGGGLVQAGGSLRSLCAASGSTFFSVNAMAWYRQAPGKQREWVAGINVDGDSSTVYADSVKGRFTISRDNAKNTMWLQMNLLKPEDTAVYYCKISTIPWGQGTQVTVSS
HIV-1_3p_ELISA#6  QVQLVESGGGLVQAGGSLRSLCAASGSTFFSVNAMAWYRQAPGKQREWVAGINVDGDSSTVYADSVKGRFTISRDNAKNTMWLQMNLLKPEDTAVYYCKISTIPWGQGTQVTVSS
HIV-1_3p_ELISA#7  QVQLVESGGGLVQAGGSLRSLCAASGSTFFSVNAMAWYRQAPGKQREWVAGINVDGDSSTVYADSVKGRFTISRDNAKNTMWLQMNLLKPEDTAVYYCKISTIPWGQGTQVTVSS
HIV-1_3p_ELISA#8  QVQLVESGGGLVQAGGSLRSLCAASGSTFFSVNAMAWYRQAPGKQREWVAGINVDGDSSTVYADSVKGRFTISRDNAKNTMWLQMNLLKPEDTAVYYCKISTIPWGQGTQVTVSS
HIV-1_3p_ELISA#11 QVQLVESGGGLVQAGGSLRSLCAASGSTFFSVNAMAWYRQAPGKQREWVAGINVDGDSSTVYADSVKGRFTISRDNAKNTMWLQMNLLKPEDTAVYYCKISTIPWGQGTQVTVSS
HIV-1_3p_ELISA#14 QVQLVESGGGLVQAGGSLRSLCAASGSTFFSVNAMAWYRQAPGKQREWVAGINVDGDSSTVYADSVKGRFTISRDNAKNTMWLQMNLLKPEDTAVYYCKISTIPWGQGTQVTVSS
HIV-1_3p_ELISA#16 QVQLVESGGGLVQAGGSLRSLCAASGSTFFSVNAMAWYRQAPGKQREWVAGINVDGDSSTVYADSVKGRFTISRDNAKNTMWLQMNLLKPEDTAVYYCKISTIPWGQGTQVTVSS
HIV-1_3p_ELISA#25 QVQLVESGGGLVQAGGSLRSLCAASGSTFFSVNAMAWYRQAPGKQREWVAGINVDGDSSTVYADSVKGRFTISRDNAKNTMWLQMNLLKPEDTAVYYCKISTIPWGQGTQVTVSS
HIV-1_3p_ELISA#33 QVQLVESGGGLVQAGGSLRSLCAASGSTFFSVNAMAWYRQAPGKQREWVAGINVDGDSSTVYADSVKGRFTISRDNAKNTMWLQMNLLKPEDTAVYYCKISTIPWGQGTQVTVSS
HIV-1_3p_ELISA#32 QVQLVESGGGLVQAGGSLRSLCAASGSTFFMSHVMAWYRQAPGKERELVAAIRSGDSSTVYTDVSKDRFTISRDDDKNTMYLQMNLLKPEDTAMYYCKATGSSWGQGTQVTVSS
HIV-1_3p_ELISA#35 QVQLVESGGGLVQAGGSLRSLCAASGSTFFMSHVMAWYRQAPGKERELVAAIRSGDSSTVYTDVSKDRFTISRDDDKNTMYLQMNLLKPEDTAMYYCKATGSSWGQGTQVTVSS
HIV-1_3p_ELISA#30 QVQLVESGGGLVQAGGSLRSLCAASGSTFFMSHVMAWYRQAPGKERELVAAIRSGDSSTVYTDVSKDRFTISRDDDKNTMYLQMNLLKPEDTAMYYCKATGSSWGQGTQVTVSS
HIV-1_3p_ELISA#24 QVQLVESGGGLVQAGGSLRSLCAASGSTFFMSHVMAWYRQAPGKERELVAAIRSGDSSTVYTDVSKDRFTISRDDDKNTMYLQMNLLKPEDTAMYYCKATGSSWGQGTQVTVSS
HIV-1_3p_ELISA#23 QVQLVESGGGLVQAGGSLRSLCAASGSTFFMSHVMAWYRQAPGKERELVAAIRSGDSSTVYTDVSKDRFTISRDDDKNTMYLQMNLLKPEDTAMYYCKATGSSWGQGTQVTVSS
HIV-1_3p_ELISA#21 QVQLVESGGGLVQAGGSLRSLCAASGSTFFMSHVMAWYRQAPGKERELVAAIRSGDSSTVYTDVSKDRFTISRDDDKNTMYLQMNLLKPEDTAMYYCKATGSSWGQGTQVTVSS
HIV-1_3p_ELISA#1  QVQLVESGGGLVQAGGSLRSLCAASGSTFFMSHVMAWYRQAPGKERELVAAIRSGDSSTVYTDVSKDRFTISRDDDKNTMYLQMNLLKPEDTAMYYCKATGSSWGQGTQVTVSS
HIV-1_3p_ELISA#3  QVQLVESGGGLVQAGGSLRSLCAASGSTFFMSHVMAWYRQAPGKERELVAAIRSGDSSTVYTDVSKGRFTISRDDDKNTMYLQMNLLKPEDTAMYYCKATGSSWGQGTQVTVSS
HIV-1_3p_ELISA#9  QVQLVESGGGLVQAGGSLRSLCAASGSTFFMSNVMAWYRQAPGKARELIAAIRGGDMSTVYDDSVKGRFTITRDDDKNILEYLMNLLKPEDTAMYYCKASGSSWGQGTQVTVSS
HIV-1_3p_ELISA#20 QVQLVESGGGLVQAGGSLRSLCAASGSTFFMSNVMAWYRQAPGKARELIAAIRGGDMSTVYDDSVKGRFTITRDDDKNILEYLMNLLKPEDTAMYYCKASGSSWGQGTQVTVSS
HIV-1_3p_ELISA#26 -VQLVESGGGLVQAGGSLRSLCAASGSTFFMSNVMAWYRQAPGKARELVAAIRSGDFSTVYDGSVKGRFTISRDDDKNTMYLQMNLLKPEDTAMYYCKASGSSWGQGTQVTVSS
HIV-1_3p_ELISA#5  QVQLVESGGGLVQAGGSLRSLCLAS-SFYDSLVIAWYRQAPGKQRELVAIDSSGTSSTVYTDVSKGRFTISRDNAKHTVYLMQDSLNPDDTAVYFCKSTGTSWGPGTQVTVSS
HIV-1_3p_ELISA#10 -VQLVESGGGLVQAGGSLRSLCLAS-SFYDSLVIAWYRQAPGKQRELVAIDSSGTSSTVYTDVSKGRFTISRDNAKHTVYLMQDSLNPDDTAVYFCKSTGTSWGQGTQVTVSS
HIV-1_3p_ELISA#12 -VQLVESGGGLVQAGGSLRSLCLAS-SFFDSNVIAWYRQAPGKQRELVAIDSSGTSATVYTDVSKGRFTISRDNAEHTVYLMQDSLNPDDTAVYFCKPGTTSWGQGTQVTVSS
HIV-1_3p_ELISA#15 -VQLVESGGGLVQAGGSLRSLCLAS-SFFDSNVIAWYRQAPGKQRELVAIDSSGTSATVYTDVSKGRFTISRDNAEHTVYLMQDSLNPDDTAVYFCKPGTTSWGQGTQVTVSS
HIV-1_3p_ELISA#28 -VQLVESGGGLVQAGGSLRSLCLAS-SFFDSNVIAWYRQAPGKQRELVAIDSSGTSATVYTDVSKGRFTISRDNAEHTVYLMQDSLNPDDTAVYFCKPGTTSWGQGTQVTVSS
HIV-1_3p_ELISA#13 QVQLVESGGGLVQAGGSLRSLCLAS-SFFDSNVIAWYRQAPGKQRELVAIDSSGTSSTVYTDVSKGRFTISRDNAEHTVYLMQDSLNPDDTAVYFCKPGTTSWGQGTQVTVSS
HIV-1_3p_ELISA#36 QVQLVESGGGLVQAGGSLRSLCLAS-SFFDSNVIAWYRQAPGKQRELVAIDSSGTSSTVYTDVSKGRFTISRDNAEHTVYLMQDSLNPDDTAVYFCKPGTTSWGQGTQVTVSS
HIV-1_3p_ELISA#18 -VQLVESGGGLVQAGGSLRSLCLAS-SFFDSNVIAWYRQAPGKQRELVAIDSSGTSATVYTDVSKGRFTISRDTAKNTVYLMQDSLNPDDTAVYFCKSTGTSWGQGTQVTVSS
HIV-1_3p_ELISA#19 -VQLVESGGGLVQAGGSLRSLCLAS-SFFDSNVIAWYRQAPGKQRELVAIDSSGTSATVYTDVSKGRFTISRDTAKNTVYLMQDSLNPDDTAVYFCKSTGTSWGQGTQVTVSS
HIV-1_3p_ELISA#37 -VQLVESGGGLVQAGGSLRSLCLAS-SFFDSNVIAWYRQAPGKQRELVAIDSSGTSATVYTDVSKGRFTISRDTAKNTVYLMQDSLNPDDTAVYFCKSTGTSWGQGTQVTVSS
HIV-1_3p_ELISA#38 -VQLVESGGGLVQAGGSLRSLCLAS-SFFDSNVIAWYRQAPGKQRELVAIDSSGTSATVYTDVSKGRFTISRDTAKNTVYLMQDSLNPDDTAVYFCKSTGTSWGQGTQVTVSS

```

Figure 34: Sequence alignment of V_HH amino acid sequences of single positive clones from phage ELISA against HIV-1 capsid protein. Color code: CDR1: magenta, CDR2: blue, CDR3: green, hallmark residues: violet, identical sequences are marked with a red bar. Numbering after Kabat, 1991.

3 Results

```

yH2AX_3p_ELISA#4      QVQLVESGGGLVQAGGSLRLSCAASR-RTFRAYRMGWFRQAPGKERDFVASIRWSDGGTTYADSVKGRFTISRDKAKNTLYLQMNLSKPEDTAVYYCASSLTAAMT-----YEDWGQGTQVTVSS
yH2AX_3p_ELISA#13    DVQLVESGGGLVQAGGSLRLCAASG-RTFRPYRMGWFRQAPGKERDFVASIRWTDGGTTYADSVKGRFTISRDNAKNTLYLQMNLSKPEDTAVYYCASTLTAAMT-----YENWGQGTQVTVSS
yH2AX_3p_ELISA#3     DVQLVESGGGLVQPGGSLRLSCAASG-FSLDYAIGWFRQAPGKEREDVSCISSSGGSTNYADSVKGRFTISRDNAKNTVYLLQMNLSKPEDTAVYYCAADYGSSCPLRWK-VEVWGQGTQVTVFS
yH2AX_3p_ELISA#16    DVQLVESGGGLVQPGGSLRLSCAASG-FSLDYAIGWFRQAPGKEREDVSCISSSGGSTNYADSVKGRFTISRDNAKNTVYLLQMNLSKPEDTAVYYCAADYGSSCPLRWK-VEVWGQGTQVTVFS
yH2AX_3p_ELISA#2     DVQLVESGGGLVQPGGSLRLSCAASG-FSLDYAIGWFRQAPGKEREDVSCISSSGGSTNYADSVKGRFTISRDNAKNTVYLLQMNLSKPEDTAVYYCAADYGSSCPLRWK-VEVWGQGTQVTVFS
yH2AX_3p_ELISA#6     DVQLVESGGGLVQPGGSLRLSCAASG-FTLDYYAIGWFRQAPGKEREDVSCISSSGGSTNYADSVKGRFTISRDNAKNTVYLLQMNLSKPEDTAVYYCAADYGSSCPLRWK-VEVWGQGTQVTVSS
yH2AX_3p_ELISA#1     DVQLVESGGGFVQNGGSLRLSCAASG-FTLDYYAIGWFRQAPGKEREDVSCISSSGGSTNYADSVKGRFTISRDNAKNTVYLLQMNLSKPEDTAVYYCAADYGSSCPLRWK-VEVWGQGTQVTVSS
yH2AX_3p_ELISA#10    QVQLVESGGGLVQAGGSLRLSCAASG-SFFMSNVMAWYRQAPGKARELIAAIRGGDMSTVYDSDVKGRFTITRDDDKNILYLQMNLDKPEDTAMYYCKAS-GSS-----WGQGTQVTVSS
yH2AX_3p_ELISA#19    QVQLVESGGGLVQTGGSLRLTCTASVRRRFDYFRMGWFRQIPGQEREFLAAINGVGDERNIADSVKGRFTISRDNAKNTVYLLQMNILEPEDTAVYYCAAGGTAWILSRAANYPYWGQGTQVTVSS
  
```

Figure 35: Sequence alignment of V_HH amino acid sequences of single positive clones from phage ELISA against γ H2AX-BSA. Color code: CDR1: magenta, CDR2: blue, CDR3: green, hallmark residues: violet, identical sequences are marked with a red bar. Numbering after Kabat, 1991.

```

HIV-1_Nterm_2p_ELISA#1  QVQLVESGGGLVQAGGSLRLSCAASGYFSSYAMGWFRQAPGKEREFVAAISWIESTTDYADSVKGRFTISRDNAKKTLHLQMNLSKPEDTAVYYCAACDIPFGQAFCALYDYWGQGTQVTVSS
HIV-1_Nterm_2p_ELISA#2  QVQLVESGGGLVQAGGSLRLSCAASGYFSSYAMGWFRQAPGKEREFVAAISWIESTTDYADSVKGRFTISRDNARK--RCICKSLKPEDTAVYYCAACDIPFGQAFCALYDYWGQGTQVTVSS
HIV-1_Nterm_2p_ELISA#31 QVQLVESGGGLVQAGGSLRLSCAASGYFSSYAMGWFRQAPGKEREFVAAISWIESTTDYADSVKGRFTISRDNAKKTLHLQMNLSKPEDTAVYYCAACDIPFGQAFCALYDYWGQGTQVTVSS
HIV-1_Nterm_2p_ELISA#34 QVQLVESGGGLVQAGGSLRLSCAASGYFSSYAMGWFRQAPGKEREFVAAISWIESTTDYADSVKGRFTISRDNAKKTLHLQMNLSKPEDTAVYYCAACDIPFGQAFCALYDYWGQGTQVTVSS
HIV-1_Nterm_2p_ELISA#6  QVQLVESGGGLVQAGGSLRLSCAASGYFSSYAMGWFRQAPGKEREFVAAISWIESTTDYADSVKGRFTISRDNAKKTLHLQMNLSKPEDTAVYYCAACDIPFGQAFCALYDYWGQGTQVTVSS
HIV-1_Nterm_2p_ELISA#9  QVQLVESGGGLVQAGGSLRLSCAASGYFSSYAMGWFRQAPGKEREFVAAISWIESTTDYADSVKGRFTISRDNAKKTLHLQMNLSKPEDTAVYYCAACDIPFGQAFCALYDYWGQGTQVTVSS
HIV-1_Nterm_2p_ELISA#16 QVQLVESGGGLVQAGGSLRLSCAASGYFSSYAMGWFRQAPGKEREFVAAISWIESTTDYADSVKGRFTISRDNAKKTLHLQMNLSKPEDTAVYYCAACDIPFGQAFCALYDYWGQGTQVTVSS
HIV-1_Nterm_2p_ELISA#13 -----MGWYRQVPGRQRELVARLTSDDVSTNYADSVKGRFTISRDTAKRTLYLQMDSLKPEDTALYFCN-----AFISTFEIWGQGTQVTVSS
  
```

Figure 36: Sequence alignment of V_HH amino acid sequences of single positive clones from phage ELISA against N-terminus of HIV-1 capsid protein. Color code: CDR1: magenta, CDR2: blue, CDR3: green, hallmark residues: violet, identical sequences are marked with a red bar. Numbering after Kabat, 1991.

3 Results

```

GST_1p_ELISA#35  QVQLVESGGGLVQAGGSLRSLSCAAYSGRTFNNYAMSWFRQAPGKEREFVAAVSWIGASTYYSDSVKGRFTISRDSAANTLYLQMNSLKPEDTAVYYCAVG-----YGSKAYTYDYWGQGTQVTVSS
GST_1p_ELISA#48  QVQLVESGGGLVQAGGSLRSLSCAAYSGRTFNNYAMSWFRQAPGKEREFVAAVSWIGASTYYSDSVKGRFTISRDSAANTLYLQMNSLKPEDTAVYYCAVG-----YGSKAYTYDYWGQGTQVTVSS
GST_1p_ELISA#51  QVQLVESGGGLVQAGGSLRSLSCAAYSGRTFNNYAMSWFRQAPGKEREFVAAVSWIGASTYYSDSVKGRFTISRDSAANTLYLQMNSLKPEDTAVYYCAVG-----YGSKAYTYDYWGQGTQVTVSS
GST_1p_ELISA#49  QVQLVESGGGLVQAGGSLRSLSCAASGRTFNNYARAWFRQAPGKEREFVSAISWIGGSTYYADSVKGRFTISRDNAKNTLYLQMNSLKPEDTAVYYCAHG-----FGSRAETTYDYWGQGTQVTVSS
GST_1p_ELISA#10  DVQLVESGGGLVQPGGSLRSLSCAASGDTISDYSMGWFRQPGKEREFVTTISWIDGSTYYGDSVKGRFTISRDAKNTLYLQMNSLKPEDTAVYYCAAGR--QMAPASQHRLYAYWGQGTQVTVSS
GST_1p_ELISA#22  DVQLVESGGGLVQAGGSLRSLSCIASGRTFSSYAMAWFRQTPGKDRKSVSAISWIGG-TAYADSVKGRFTISRDNAKNTLYLQMNSLKPEDTAVYYCAAR-----EAHTEGYEYDYWGQGTQVTVSS
GST_1p_ELISA#25  QVQLVESGGGLVQAGGSLRSLSCIASGRTFSSYAMAWFRQTPGKDRKSVAAISWIGG-TAYADSVKGRFTISRDNAKNTLYLQMNSLKPEDTAVYYCAAR-----EAHTEGYEYDYWGQGTQVTVSS
GST_1p_ELISA#6    QVQLVESGGGLVQAGGSLRSLSCTASGRTFSSYAMCWFRQAPGKEREFVAAISWIDN-TSYADSVKGRFTISRDNAKNTLYLQMNSLKPEDTAVYYCAAR-----EAHSDYFGYDYWGQGTQVTVSS
GST_1p_ELISA#1   QVQLVESGGGLVQPGGSLRSLSCAASGFTLDYYAIGWFRQAPGKEREFVSCISSGGRTMYADSVKGRFTISRDNAKNTVYLQMNSLKPEDTAVYYCAADQYDPNHCSYGTWGYNYWGQGTQVTVSS
GST_1p_ELISA#39  DVQLVESGGGLVQPGGSLRSLSCAASGFTLDYYAIGWFRQAPGKEREFVSCISSVGGTMYADSVKGRFTISRDNAKNTVYLQMNSLKPEDTAVYYCAADQYDPRHCSYGTWGYHYWGQGTQVTVSS
GST_1p_ELISA#23  QVQLVESGGGLVQPGGSLRSLSCAASGFSLDHYAVAWFRQAPGKEREFVVSCYTRPGGSTSYTDSVKGRFSLRDNAKNTVYLQMNSLKPEDTAAYYCAADR--AACYTDSRYTYWGQGTQVTVSS
GST_1p_ELISA#50  QVQLVESGGGLVQPGGSLRSLSCAASGFSLDHYAVAWFRQAPGKEREFVVSCYTRPGGTINYADSVKGRFSLRDNAKNTVYLQMNSLKPEDTGAYYCAADR--AACYSYDSRYTYWGQGTQVTVSS
  
```

Figure 37: Sequence alignment of V_HH amino acid sequences of single positive clones from phage ELISA against GST. Color code: CDR1: magenta, CDR2: blue, CDR3: green, hallmark residues: violet, identical sequences are marked with a red bar. Numbering after Kabat, 1991.

```

Dnmt1_SP_1p_ELISA#26  QVQLVESGGGLVQPGGSLRSLSCAASGFTSDYYAIGWFRQAPGKEREFVSCISSGRSTDYADSVKGRFTISKDHAKNTVYLQMDSLKPEDTAVYYCAADKSRPFCSRDQSDRNDYWGQGTQVTVSS
Dnmt1_SP_2p_ELISA#33  QVQLVESGGGLVQPGGSLRSLSCAASGFTSDYYAIGWFRQAPGKEREFVSCISSGRSTDYADSVKGRFTISKDHAKNTVYLQMDSLKPEDTAVYYCAADKSRPFCSRDQSDRNDYWGQGTQVTVSS
Dnmt1_SP_2p_ELISA#1   QVQLVESGGGLVQPGGSLRSLSCAASGFTLDGYAIGWFRQAPGKEREFGVACISSGRSTTYADSVQGRFTISRDHAKNTVELQMNSLKPEDTAVYYCAAD-AREYCYSTYDLSNYVYVWSQGTQVTVSS
Dnmt1_SP_1p_ELISA#16  QVQLVESGGGLVQPGGSLRSLSCAASAFTLDYYAIGWFRQAPGKEREFGVSCISSSDGSTYYADSVKGRFTISRDNAKNTVYLQMNSLKPEDTAVYYCATDWGR-LCPPPLTTDYDYWGQGTQVTVSS
Dnmt1_SP_2p_ELISA#2   QVQLVESGGGLVHTGGSLRSLSCAASGRTSGTSTMGWFRQAPGKEREFEWVASISRRG-TTYVYDGVKGRFTISRDNAKNTVYLQMNSLKPEDTAVYYCAAR-----GPTDL-EFVYWGQGTQVTVSS
Dnmt1_SP_1p_ELISA#30  QVQLVESGGGLVQAGGSLRSLSCAASGRTFSSNYAMGWFRQAPGEERFVAAINGGGHTIDYADSVKGRFTISRDNAEATVYLQMNSLKPEDTAVYYCAASGSYYYSSRGRGHNGMDYWGRTLVTVSS
Dnmt1_SP_2p_ELISA#20  QVQLVESGGGLVQAGGSLRSLSCAASGRTFSSNYAMGWFRQAPGEERFVAAINGGGHTIDYADSVKGRFTISRDNAEATVYLQMNSLKPEDTAVYYCAASGSYYYSSRGRGHNGMDYWGRTLVTVSS
Dnmt1_SP_2p_ELISA#13  QVQLVESGGGLVQAGGSLRSLSCAASGRTFSSNYAMGWFRQAPGEERFVAAINGGGHTIDYADSVKGRFTISRDNAKATVYLQMNSLKPEDTAVYYCAASGSYYYSSRGRGHNGMDYWGRTQVTVSS
Dnmt1_SP_1p_ELISA#12  QVQLVESGGGLVQPGGSLRSLSCAASGRTFSSNYAMGWFRQAPGEERFVAAINGGGHTIDYADSVKGRFTISRDNAKATVYLQMNSLKPEDTAVYYCAASGSYYYSSRGRGHNGMDYWGRTQVTVSS
Dnmt1_SP_2p_ELISA#44  QVQLVESGGGLVQAGGSLRSLSCAASGRTFSSYMGWFRQTPGEERFVAAINGGGHTIDYADSVKGRFTISRDNAKATVYLQMNSLKPEDTAVYYCAASGSYYYSSRGRGHNGMDYWGRTQVTVSS
Dnmt1_SP_1p_ELISA#3   QVQLVESGGGLVQAGGSLRSLSCAASGRTFSSNYVMGWFRQAPGEERQFVAAISGGGDTIDYADSVVGRFTISRDNKATMYLQMNSLKPEDTAVYYCAGSSYYYSSRGRGHNGMPYWGRTQVTVSS
Dnmt1_SP_2p_ELISA#43  DVQLVESGGGLVQAGGSLRSLSCAASGRTFSSRYAMGWFRQAPGKEREFVAGIWWGGSTNYADSVKGRFTISRDNAKNTVYLQMNSLKPEDTAVYYCTAIN-----YGRQTPLYDDWGQGTQVTVSS
Dnmt1_SP_2p_ELISA#40  QVQLVESGGGLVQAGGSLRSLSCAASGRTFSNEHIAWFRRAPGKQRELVAGINIYH-TTYADSVKGRFTVSRDNAKNTVYLQMDTLKPEDTAVYYCNALT-----SWSRLESSNYWGQGTQVTVSS
  
```

Figure 38: Sequence alignment of V_HH amino acid sequences of single positive clones from phage ELISA against hDnmt1. Color code: CDR1: magenta, CDR2: blue, CDR3: green, hallmark residues: violet, identical sequences are marked with a red bar. Numbering after Kabat, 1991.

3.1.6 Selection of antigen specific V_HHs by the F2H-Assay

Even though the method phage ELISA on immobilized antigens is quick and convenient, especially because of the signal amplification which occurs due to the detection of multiple copies of pVIII on the phage surface using a specific antibody, the antigen presentation may not necessarily be beneficial or representative for the selection of antigen specific V_HHs regarding their downstream application as Chromobody in living cells. As described in 3.1.4.2 immobilized antigens may be denatured *in vitro* resulting in V_HHs recognizing the denatured antigen only but not the native folded antigen found inside living cells.

In order to select antigen specific V_HHs which recognize the native folded antigen the *native panning* described in 3.1.4.2 was combined with the fluorescent-two hybrid (F2H) assay developed by Zolghadr et al. in 2008. The F2H assay enables the visualization of protein-protein interactions in single living cells making it well suited to screen for antigen specific V_HHs. The method is based on a Baby-Hamster-Kidney (BHK) cell line stably expressing 200 - 1000 copies of a plasmid carrying 256 copies of a protein-protein interaction biosensor (*lac* operator sequence) at a single chromosomal site. By co-transfection of a so-called bait which is immobilized to the protein-protein interaction biosensor (PPIB) via the *lac* repressor (*lacI*) and visualized as a nuclear spot and a prey, a protein-protein interaction can be made visible in living cells by fluorescent read out (Figure 39) (Zolghadr et al., 2008).

The whole V_HH repertoire after the second *native panning* round against hDnmt1 described in 3.1.4.2 was cloned into a mammalian expression vector containing a red fluorescent protein via PCR. Throughout this thesis for all (monomeric) red fluorescent proteins, irrespective of which specific derivative was used (i.e. mRFP, mCherry, mPlum, mRFP Ruby or TagRFP) the acronym RFP will be used. The resulting library, representing the prey, contains the V_HH repertoire after the second panning round in fusion to RFP and is called Dnmt1-Chromobody F2H library (Figure 39 B)

3 Results

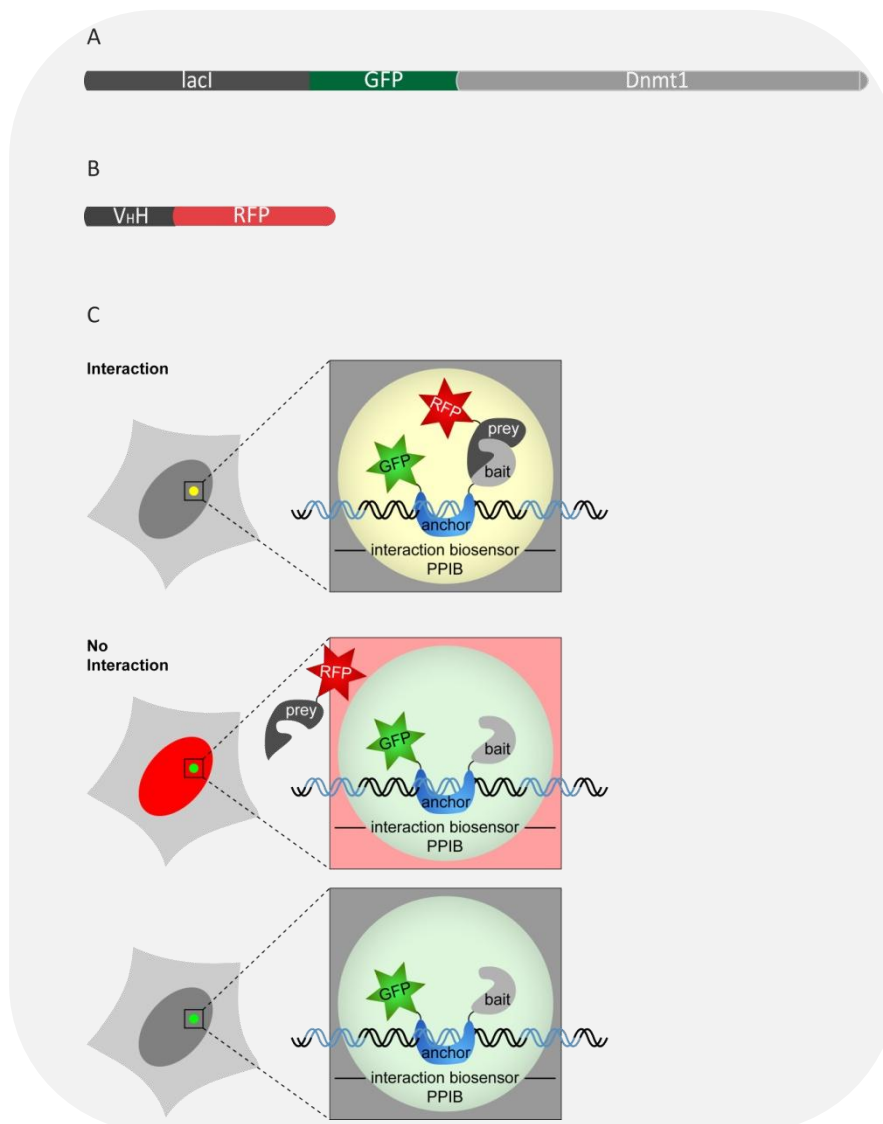


Figure 39: Schematic outline of the F2H assay. (A) Bait fusion protein comprising the *lacI* domain fused to GFP-hDnmt1. (B) Prey fusion protein comprising the hDnmt1-Chromobody library. (C) Principle of F2H assay: the *lacI* domain mediates the binding to the *lac* operator array resulting in a fluorescent spot in the nucleus. Upon interaction with the bait protein, it becomes enriched at the same spot resulting in co-localization of the fluorescent signals visible as yellow spot. If bait and prey do not interact, the *lac* operator array is visualized by the bait protein only resulting in a green spot. Modified after Zolghadr et al., 2008.

To select Chromobodies specifically recognizing hDnmt1, the BHK cell line described above was co-transfected with 96 individual clones of the hDnmt1-Chromobody F2H library each together with *lacI*-GFP-hDnmt1. The over expressed GFP-hDnmt1-fusion protein binds

3 Results

to the *lac* operator array, mediated by the *lacI*, which then becomes visible due to the focal enrichment of the GFP fluorescence. Chromobodies which specifically bind to hDnmt1 co-localize with GFP-hDnmt1 resulting in co-localization of the fluorescent signals of RFP and GFP. Figure 40 exemplarily shows 4 hDnmt1 specific Chromobodies (hDnmt1-cb-mCh): 2pA7, 2pC1, 2pC6 and 2pH11. In contrast to the hDnmt1 specific V_HHs selected in solid phase panning, with no Chromobody being functional inside living cells, V_HHs specific for hDnmt1 selected in native panning are functional in living cells. These results clearly demonstrate the importance of this newly designed and established screening method.

3 Results

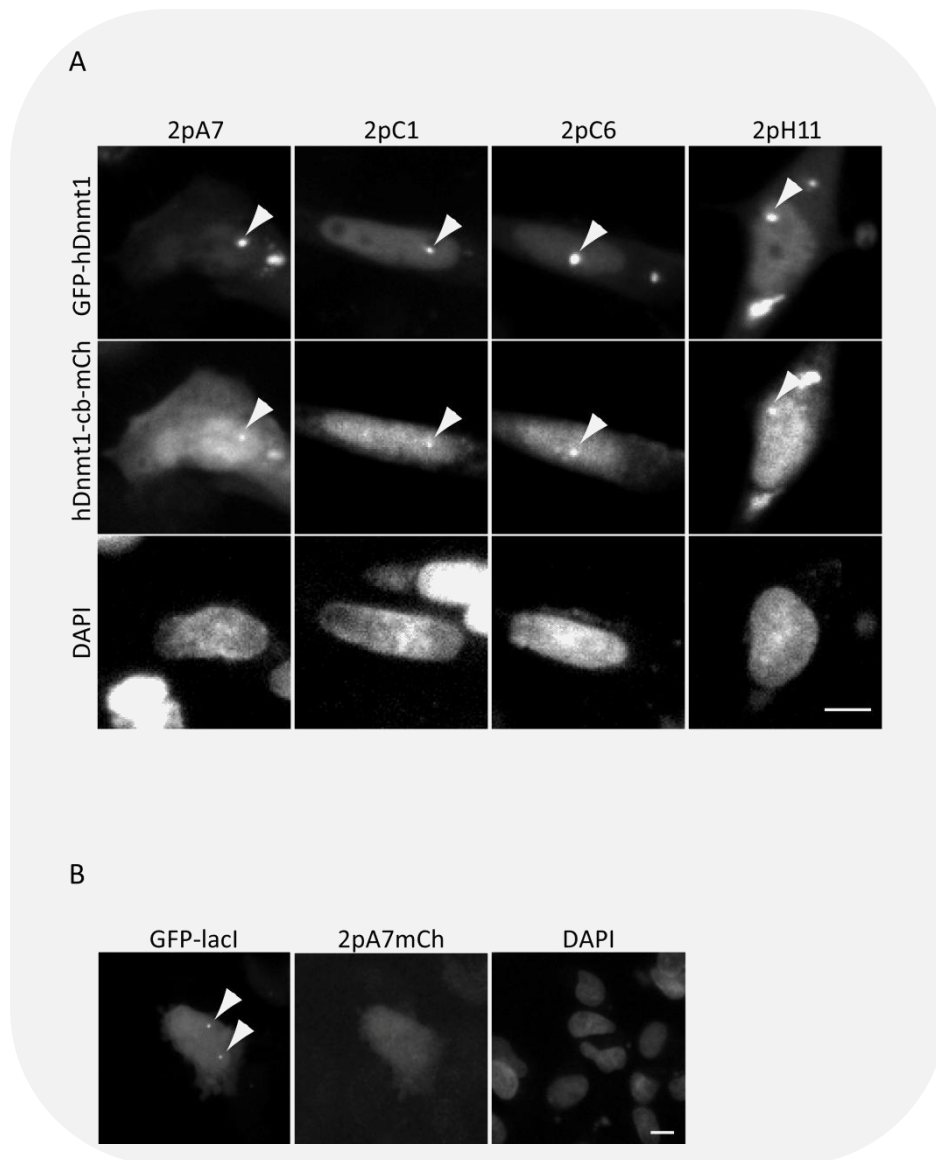


Figure 40: Exemplary results of F2H screen of hDnmt1 specific Chromobodies. (A) Transgenic BHK cells containing a chromosomal *lac* operator array were co-transfected with lacI-GFP-hDnmt1 (GFP-hDnmt1) and hDnmt1-Chromobody-RFP (hDnmt1-cb-mCh). The *lacI* part of the GFP-hDnmt1 construct mediates the binding to the *lac* operator array resulting in a spot (highlighted by arrowheads in upper row). The specific binding of the hDnmt1-Chromobodies to GFP-Dnmt1 can be detected by co-localization of the fluorescence signals of RFP and GFP (highlighted by arrowheads in middle row). (B) As negative control these transgenic BHK cells were co-transfected with GFP-lacI without being fused to hDnmt1 and with the hDnmt1-Chromobody-RFP (here exemplarily shown for hDnmt1-Chromobody-RFP 2pA7mCh). The GFP-lacI binds to the *lac* operator array resulting in a spot (highlighted by arrowheads). Since the hDnmt1-part is missing, the hDnmt1 Chromobody is dispersedly distributed throughout the nucleus indicating no interaction. Scale bars 5 μ m.

3.1.6.1 Sequence analysis after Fluorescence-2 Hybrid Assay

In contrast to phage ELISA, the F2H assay enables the identification of antigen specific V_HHs *in vivo*. To analyze the protein sequences of the antigen specific clones, the 4 positive clones obtained in the F2H screen were subjected to sequence analysis. Figure 41 shows the sequence alignments of the positive clones of the F2H screen against hDnmt1 with all sequences including the V_HH hallmark residues. In addition, the result shows that no sequence is enriched, however, two sequences, hDnmt1-mCh_2pA7 and hDnmt1-mCh_2pC1, are highly similar and differ in four amino acid residues, only. Those two sequences and the sequence of hDnmt1-mCh_2pH1 have neither an extended CDR3 nor an additional cysteine residue. In contrast, the sequence of hDnmt1-mCh_2pC6 has an extended CDR3 and two additional cysteine residues.

3 Results

```
hDnmt1-mCh_2pA7  QVQLVESGGGLVHPGGSLRLSCAASGSTFSLNSIGWYRQAPGKQRELVAGISLYG-DTNYSEAVKGRFTISRDNASTVYLMSSSLKPEDTAVYYCNIFS--TWSRFEPD--EWGQGTQVTVSS
hDnmt1-mCh_2pC1  -VQLQESGGGLVHPGGSLRLSCAASGTFSLNSIGWYRQAPGKQRELVAGISLYG-DTNYAEAVKGRFTISRDNASTVYLMNSLKPEDTAVYYCNIFS--TWSRFEPD--QWGQGTQVTVSS
hDnmt1-mCh_2pC6  QVQLVESGGGLVQPGGSLRLSCAASG--FTYRAIAWFRQAPGREREGISCSISTGRSTTYADSVQGRFTISRDHAKNTVDLEMNSLKAEDTAVYYCAADAREYCSGYDKSKYISWGQGTQVTVSS
hDnmt1-mCh_2pH1  QVQLVESGGGLVQAGGSLRLSCAAGSNILSTNAMGARQAPGKERELVAGLANGG-NTFYANSVKGRFTISKDTAKNTLYLEMNDLKLEDTGIIYCATLLPGGGGELKYGS--EGRGTQVTVSS
```

Figure 41: Sequence alignment of V_HH amino acid sequences of single positive clones against hDnmt1 from F2H screen. Color code: CDR1: magenta, CDR2: blue, CDR3: green, hallmark residues: violet. Numbering after Kabat, 1991.

3.2 Characterization of antigen specific V_HHs

The main focus in the first part of this thesis was to optimize the different steps involved in generating antigen specific V_HHs. The second part focuses on the characterization of antigen specific V_HHs. After the successful selection of antigen specific V_HHs using phage display and the identification via phage ELISA, they were further analyzed regarding their binding characteristics and their applicability in different biochemical and intracellular approaches in order to study their usability as Nanotraps and Chromobodies.

3.2.1 Biochemical characterization

The first characterization step was the biochemical characterization including epitope mapping, immunoprecipitation experiments and solubility tests.

3.2.1.1 Epitope mapping

V_HHs, like all antibodies or antibody fragments, recognize specific parts of an antigen which is referred to as epitope (Bonavida and Sercarz, 1971). The knowledge about the epitope of an antibody provides valuable information useful for disease prevention, diagnosis and treatment. It allows for predictions of potential biological interference upon binding, e.g. the influence on catalytic activity or the correct folding or the disturbance of an interaction with another protein. Hence, epitope mapping is an important step in characterizing antibodies or recombinant antibody fragments.

Primarily, the HIV-CA-specific V_HHs were analyzed with respect to their epitope specificity. There are several methods available to map an antibody's epitope, Here, phage ELISA and Dot Blot were employed. In a first test, HIV-1 capsid specific V_HHs were tested in a phage ELISA experiment as described in 3.1.5 using fulllength HIV-1 capsid protein in combination with truncated versions thereof (see Figure 42) (C-terminal domain (amino acid residues 146-231) and N-terminal domain (amino acid residues 1-146 or 1-151); proteins kindly provided by Vanda Lux, AG Hans-Georg Kräusslich, University hospital Heidelberg).

3 Results

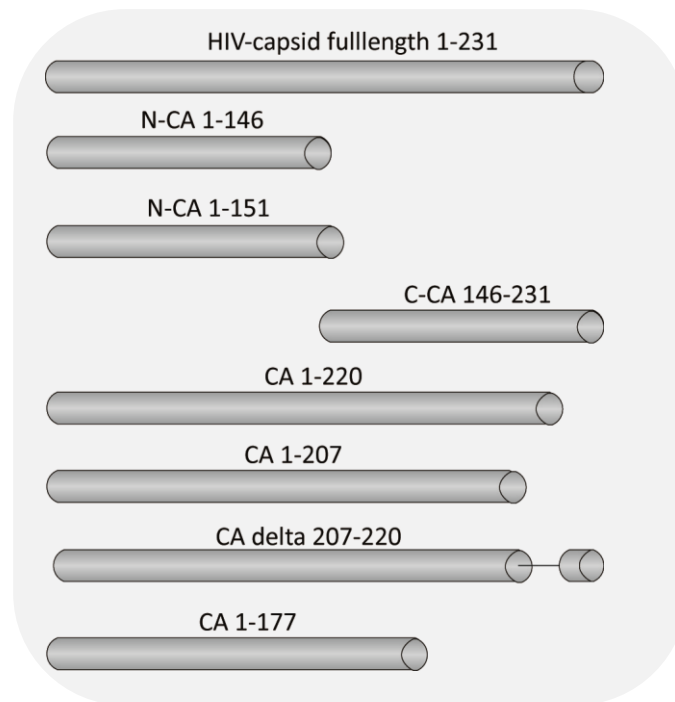


Figure 42: HIV-1 capsid protein domains and truncated versions tested in phage ELISA.

The result in Figure 43 shows that all phages displaying a HIV specific V_HH fragment at their surface recognize the fulllength version of the HIV-1 capsid protein. However, phages derived from the panning against the fulllength HIV-1 capsid protein (HIV#1, HIV#2, HIV#9, HIV#12 and HIV #19) recognize specifically the isolated C-terminal domain of the HIV-1 capsid protein but not the isolated N-terminal part of the protein. On the other side, phages derived from the panning against the N-terminal part of the HIV-1 capsid protein (HIV-Nterm#1) recognize beside the fulllength HIV-1 capsid protein he isolated N-terminal domain but do not recognize the isolated C-terminal part of the HIV-1 capsid protein.

3 Results

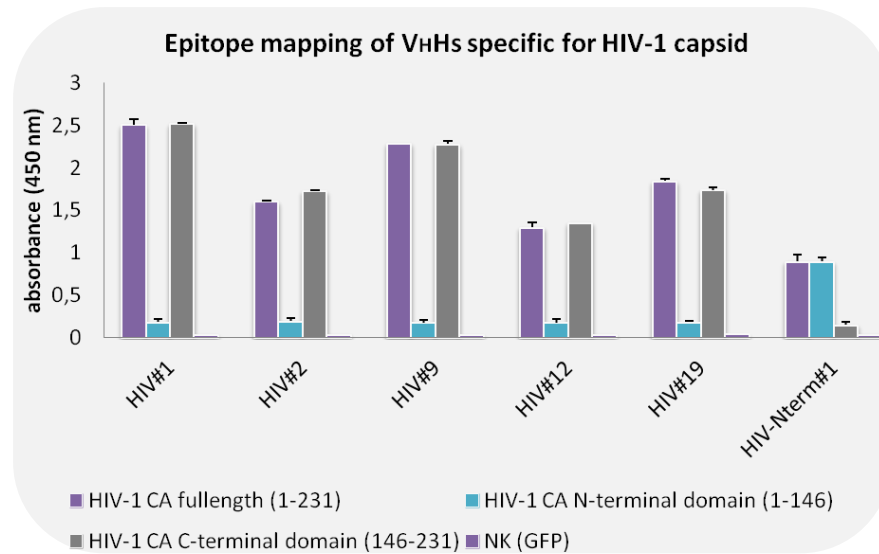


Figure 43: Epitope mapping of HIV-1 capsid protein specific V_HHs by phage ELISA. Phages comprising clones HIV#1, HIV#2, HIV#9, HIV#12, HIV#19 and HIV-Nterm#1 were tested on different versions of the HIV-1 capsid protein. All clones specifically bind to the fulllength HIV-1 capsid protein. The clones HIV#1, HIV#2, HIV#9, HIV#12 and HIV#19 specifically recognize the C-terminal part of the HIV-1 capsid protein and do not recognize the N-terminal part of the protein. In contrast, HIV-Nterm#1 does not recognize the C-terminal domain but does recognize the N-terminal domain of the HIV-1 capsid protein. The negative control GFP was not recognized by any of the V_HHs. The experiment was performed in duplicates; the error bars represent the standard deviation of the duplicate values. Numbers given in parentheses correspond to amino acid residues.

In order to further refine the epitope of the V_HHs specific for the C-terminal domain *in vitro* a phage ELISA was performed using overlapping peptides derived from the C-terminal domain: one 18-mer peptide, five overlapping 15-mer peptides and one 14-mer peptide (see Figure 44) (peptides kindly provided by Vanda Lux, AG Hans-Georg Kräusslich, University hospital Heidelberg). In addition, two truncated versions of the fulllength HIV-1 capsid protein were tested and the HIV-1 capsid protein N-terminal domain was used as negative control.

3 Results

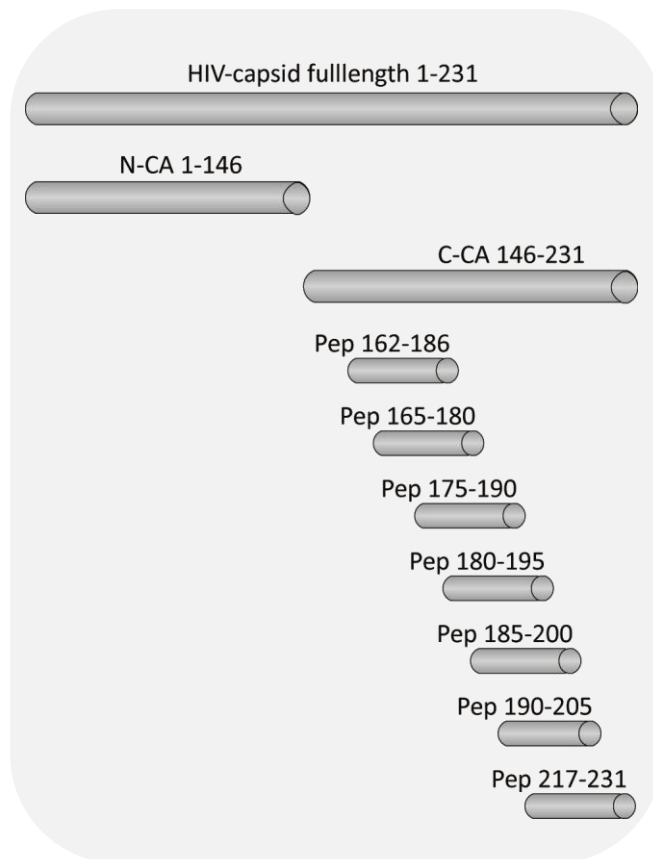


Figure 44: HIV-1 capsid protein domains and peptides tested in Dot Blot.

The results shown in Figure 45 show that all tested V_H Hs specifically recognize the truncated versions of the fulllength HIV-1 capsid protein amino acid residues 1-220 and residues 1-207. In contrast, none of the peptides are recognized. The slight differences in signal intensity in comparison to Figure 43, especially regarding HIV#19, may be due to fluctuations in phage production within the two experiments.

3 Results

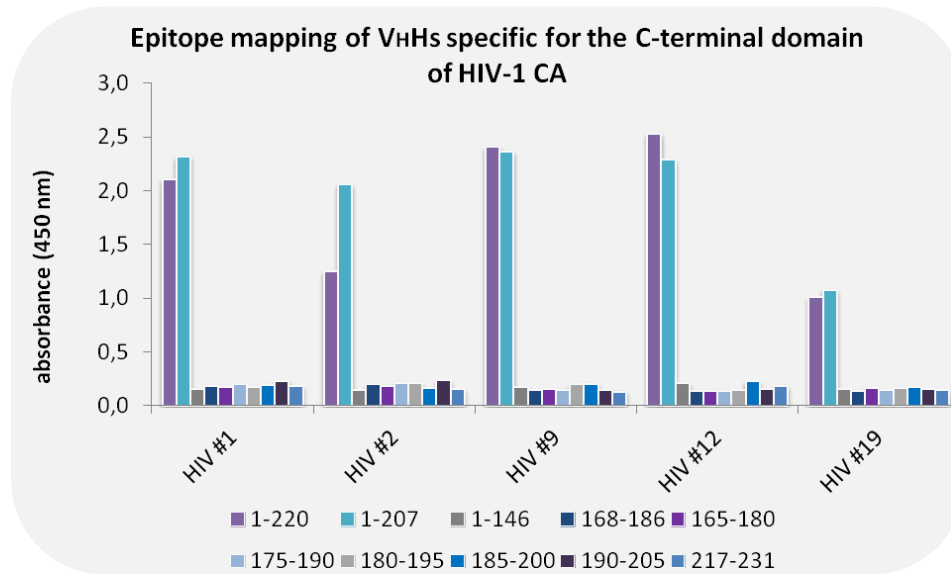


Figure 45: Epitope mapping of V_HHs specific for the C-terminal domain of the HIV-1 capsid protein by phage ELISA. Phages comprising clones specific for the C-terminal domain of HIV-1 capsid protein were tested for their binding specificity on different peptides of the HIV-1 capsid protein C-terminal domain. All clones specifically bind to the truncated versions 1-220 and 1-207 while none of the clones recognizes the N-terminal domain of the HIV-1 capsid protein (1-146). Additionally, none of the clones recognizes one of the peptides. Numbers given correspond to amino acid residues.

As shown above, phage ELISA is a quick and convenient method to analyze binding specificities of V_HHs *in vitro*. However, this method is depending on phage production which can vary dramatically in between different experiments. In addition, as described in 3.1.4.2 protein molecules when absorbed on polystyrene undergo conformational changes; hence, epitopes may become partially denatured. In order to avoid these drawbacks, another approach to refine the epitope was performed during this thesis: Dot Blot analysis. Dot Blot is a more native-like approach from both perspectives, nanobody and antigen, since the nanobody is recombinantly purified and the antigen is not immobilized on polystyrene. In brief, truncated versions of the C-terminal domain of the HIV-1 capsid protein were spotted on nitrocellulose and detected directly with recombinant produced and FITC labeled V_HHs.

3 Results

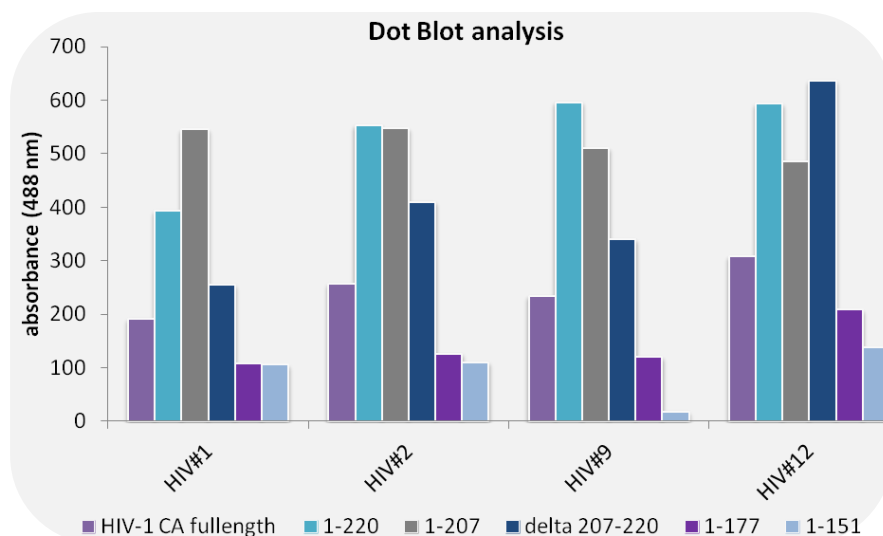


Figure 46: Epitope mapping of V_H Hs specific for the C-terminal domain of the HIV-1 capsid protein by Dot Blot analysis. Recombinant produced and FITC labeled V_H Hs specific for the C-terminal domain of HIV-1 capsid protein were tested for their binding specificity on different truncated versions of the HIV-1 capsid protein C-terminal domain. All clones specifically bind to the fulllength HIV-1 capsid protein and the truncated versions 1-220 and 1-207. In addition, all clones recognize the deletion mutant delta 207-220. The truncated version 1-177 is not recognized, except HIV#12 showing a weak signal. None of the clones recognizes the N-terminal domain of the HIV-1 capsid protein (1-151). Numbers correspond to amino acid residues.

The results in Figure 46 show a refining of the epitope of the C-terminal specific V_H Hs. With all tested clones a signal can be obtained with the fulllength HIV-1 capsid protein and the truncated versions 1-220 and 1-207 which confirms the result in Figure 45. In addition, the result shows that all V_H Hs recognize a mutant of the fulllength HIV-1 capsid protein with amino acid residues 207-220 deleted. The truncated version 1-177 is not recognized except for HIV#12 showing weak signals. The N-terminal domain was used as negative control and is not recognized by any of the V_H Hs. The results from the Dot Blot analysis indicate an epitope between amino acid residues 178-206. This experiment was also performed with peptides spotted on the nitrocellulose membrane; however, no signals were obtained (data not shown). The results indicate that the HIV-1 capsid protein V_H Hs rather bind to a conformational epitope than a linear epitope.

3.2.1.2 Immunoprecipitation

The two methods described above are highly suitable to map and refine the epitope of antibodies and antibody fragments such as V_HHs. However, methods employing phages also have drawbacks regarding the presentation of the V_HH on the tip of a phage which may lead to misfolding of the V_HH domain and, as a consequence, influence the antigen binding. In order to avoid these drawbacks and to confirm the specificity of V_HHs they were further characterized by immunoprecipitation (IP). For this purpose, V_HHs were expressed in *E. coli* and purified using IMAC and size exclusion chromatography. Then, they were covalently coupled to NHS-Sepharose beads and used for IP. In this format, specific V_HHs are referred to as Nanotraps. During this thesis the following Nanotraps were analyzed in IP experiments: HIV#1 (HIV-Trap#1), HIV#2 (HIV-Trap#2), HIV#9 (HIV-Trap#9), HIV#12 (HIV-Trap#12) and GST_1p_ELISA#35 (GST-Trap). HIV#19 was not further analyzed since the expression levels in *E. coli* were too low, which may be explained by the two additional cysteine residues.

Having been focused on the development and optimization of novel screening processes and the establishment of a working pipeline some of the identified antigen specific V_HHs during this work became autonomous projects subsequently conducted by coworkers and collaborators. Hence, in the following own results are shown for only two (HIV-1 capsid and GST) of the five initial targets.

In order to analyze the binding specificity of the HIV-Traps, lysates from HEK293T cells expressing HIV-1-GagGFP (85kDa) with the capsid protein as an internal domain of the Gag precursor protein were subjected to immunoprecipitation with the HIV-Traps. Input (I) and bound fractions (B) were analyzed by SDS PAGE and immunoblot analysis.

3 Results

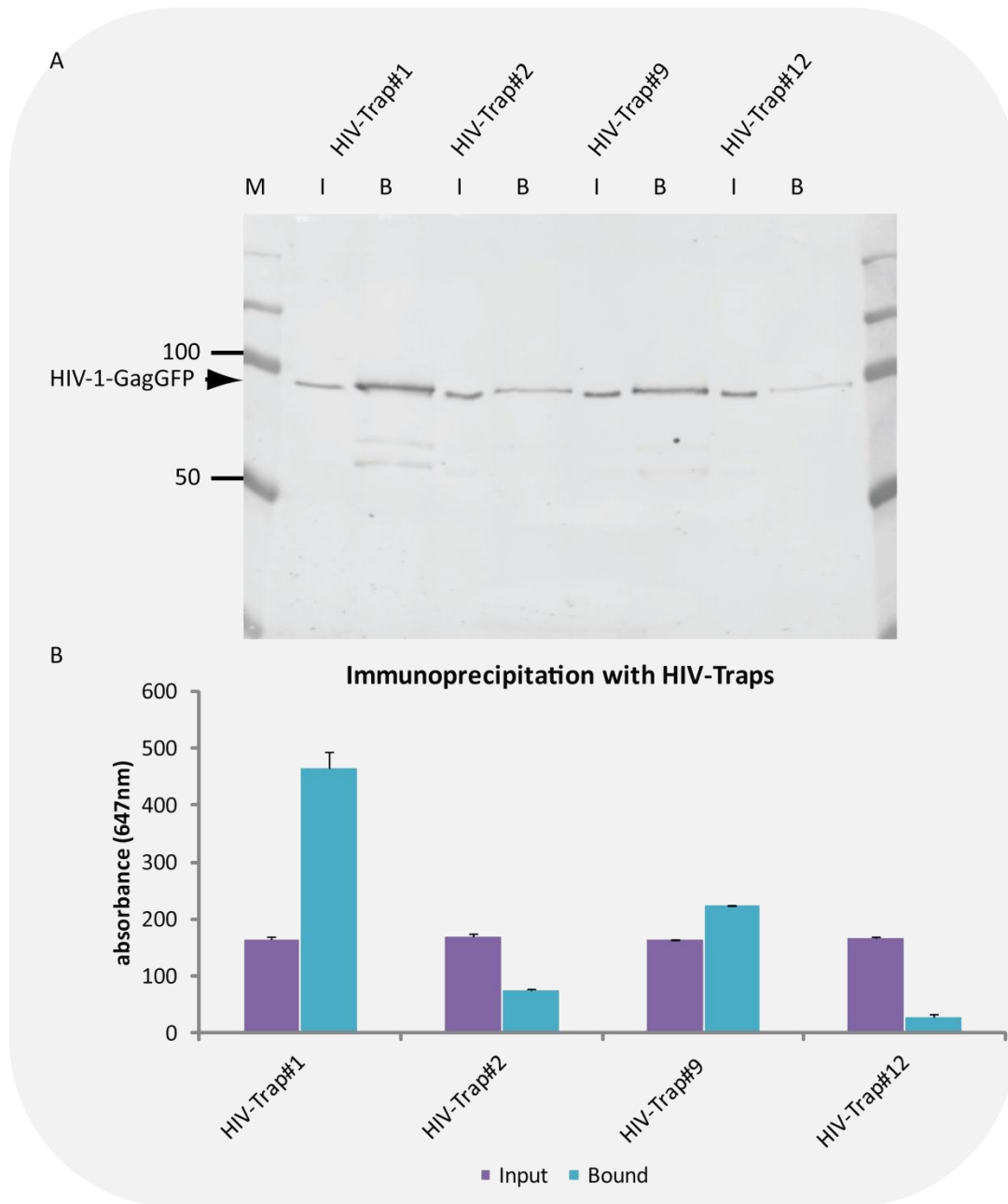


Figure 47: Immunoprecipitation with HIV-Traps. Cell extracts of HIV-1-GagGFP producing HEK293T cells were precipitated with each HIV-Trap. 2 % of input (I) and 20 % of bound fraction (B) were separated by SDS-PAGE followed by (A) immunoblot analysis. Predicted molecular weight of HIV-1-GagGFP (85 kDa) is marked by an arrow. (B) Quantitative analysis of immunoprecipitation experiment. The experiment was performed in duplicates; the error bars represent the standard deviation of the technical replicates.

3 Results

The results in Figure 47 A show, that all HIV-Traps precipitate the expressed HIV-1-GagGFP. The quantitative analyses (Figure 47 B) reveal that HIV-Trap#1 shows the best performance whereas HIV-Trap#12 only precipitates small amounts of antigen.

The specificity of the GST-Trap was tested in two different approaches. Initially, recombinant GST protein was used for immunoprecipitation with the GST-Trap. Input (I), non-bound (FT) and bound fractions (B) were analyzed by SDS PAGE with subsequent Coomassie staining.

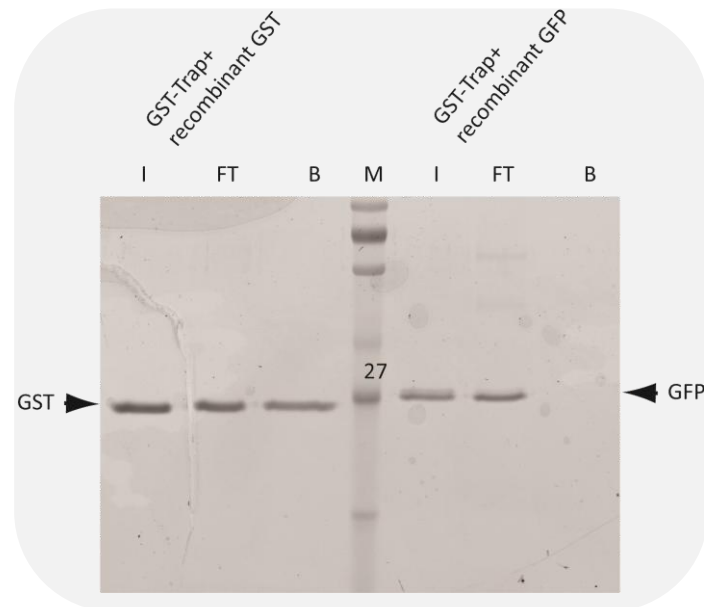


Figure 48: Immunoprecipitation with GST-Trap. Recombinant GST and GFP were precipitated with the GST-Trap. 2 μ g GST (I), 20 % non-bound fraction (FT) and 100 % bound fraction (B) were separated by SDS-PAGE followed by Coomassie staining. Predicted molecular weight of GST (26 kDa) and GFP (27 kDa) is marked by an arrow.

The result in Figure 48 shows that the GST-Trap specifically precipitates recombinant GST, but does not recognize GFP. However, to verify that the GST-Trap does not bind unspecifically to other proteins, lysates from GST expressing *E. coli* were subjected to immunoprecipitation with the GST-Trap in a second approach. Input (I) and bound fractions

3 Results

(B) were analyzed by SDS PAGE with subsequent Coomassie staining and immunoblot analysis.

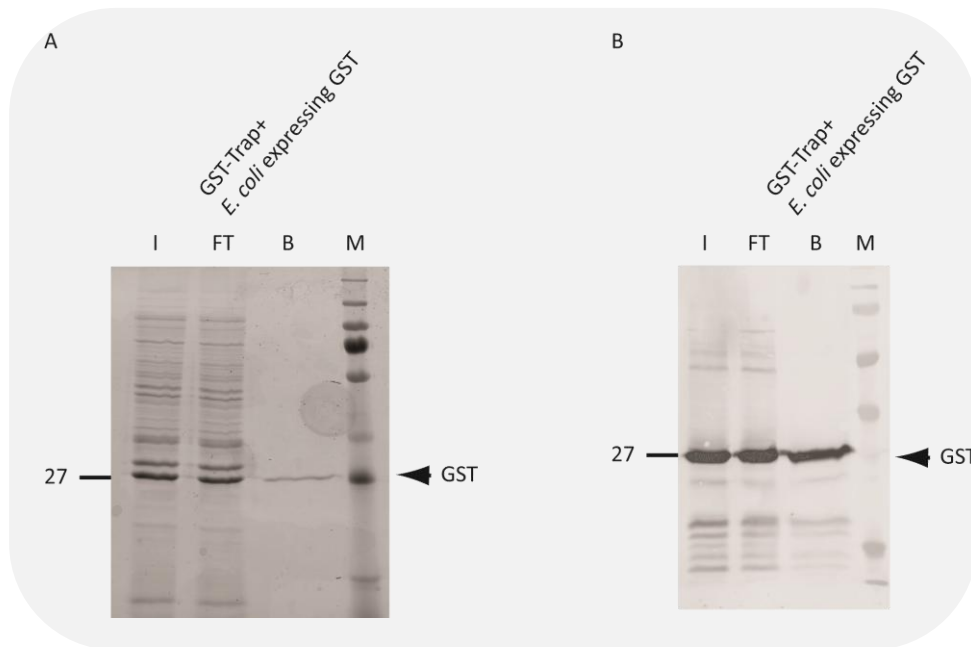


Figure 49: Immunoprecipitation with GST-Trap. *E. coli* cell extracts expressing GST were precipitated with the GST-Trap. 1 % of input (I), 1 % non-bound fraction (FT) and 30 % bound fraction (B) were separated by SDS-PAGE followed by (A) Coomassie staining and (B) immunoblot analysis. Predicted molecular weight of GST (26 kDa) is marked by an arrow.

The result in Figure 49 confirms that the GST-Trap specifically recognizes GST. The additional band detected in the bound lane may result from degradation products of GST.

3.2.1.3 Solubility-Test

Not only the recombinant production in *E. coli* requires solubility of $V_{\text{H}}\text{Hs}$ but it is also an important requirement in regard to their functionality as Chromobodies in mammalian cells. In general, $V_{\text{H}}\text{Hs}$ feature high stability and solubility (Muyldermans, 2001), however, during the work for this thesis aggregation and poor expression of $V_{\text{H}}\text{Hs}$ was observed in several cases. Different factors like additional cysteine residues and the length of the CDR3 may influence the solubility of Chromobodies inside living mammalian cells (Conrath et al., 2003).

3 Results

Therefore, three already described and functional Chromobodies, GFP-Chromobody, Lamin-Chromobody and Cytokeratin-Chromobody (Rothbauer et al., 2006), were analyzed regarding additional cysteine residues and their CDR3 length.

3 Results

```
Lamin-VHH      QVQLQESGGGLVQAGGSLTSLCTYSGLTFDDYINMGWERQGPGERERSAISFRG-ITYYVDSVKGRFTISRDNAKKTLYLQMNGLTPDDTATYYCAGSRFLSPFVRDGTKLINDWGQGTQVTVSS
GFP-VHH        QVQLVESGGALVQPGGSLRLSCAASGFVNRYSMRWYRQAPGKEREWVAGMSSAGDRSSYEDSVKGRFTISRDDARNTVYLQMNLSKPEDTAVYYCN-----VNVG----FEYWGQGTQVTVSS
Cytokeratin-VHH QVQLVESGGGLVQPGESLRLSCAASGFNFASYSMTWVRQAPGKELDWVATISFSGGSTYYDDSVKGRATISRDNASTVYLLQNSLKTEDTGMYYCTKGR-VSPPIPDG-----LSRGQGTQVTVSS
```

Figure 50: Alignment of three already described V_HH sequences. All three V_HHs have no additional cysteine and no extended CDR3.

3 Results

The alignment of the V_HH sequences shows, that none of the three V_HHs has an additional cysteine residue or an extended CDR3 (Figure 50) which is in accordance to the already published data (Rothbauer et al., 2006) showing their functionality in living cells. During this thesis, however, the functionality of V_HHs in mammalian cells was analyzed regarding the localization of the fluorescent protein. In brief, GFP-Chromobody, Lamin-Chromobody and Cytokeratin-Chromobody were cloned in a vector containing an N- or C-terminal fluorescent protein, respectively (see Figure 51). These constructs were expressed in HEK293T cells and analyzed. As transfection control a vector containing GFP only was used.

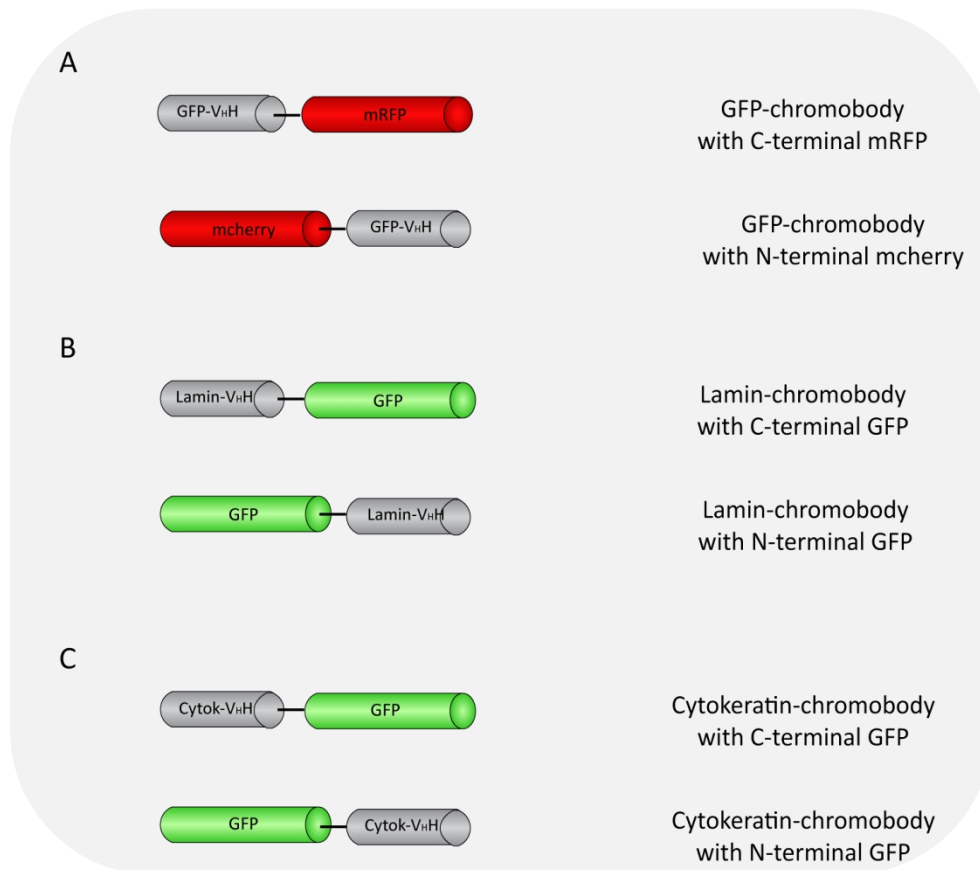


Figure 51: Chromobody constructs used in functionality tests.

First, the transfection rate was determined by counting transfected and untransfected cells (Table 29). The transfection rates show, that the Cytokeratin-Chromobody and the

3 Results

Lamin-Chromobody are both expressed in lower levels if the fluorescent protein is localized C-terminal. In contrast, the GFP-Chromobody is expressed well independent of the localization of the fluorescent protein.

Table 29: Comparison of transfection rate of Chromobodies. For each construct 50 cells were analyzed.

	TRANSFECTION RATE (%)
GFP-V _H H-mRFP	80
mcherry-GFP-V _H H	85
Lamin-V _H H-GFP	50
GFP-Lamin-V _H H	30
Cyto-V _H H-GFP	80
GFP-Cyto-V _H H	5
GFP (positive control)	80

After the determination of the transfection rate, the Chromobodies were analyzed regarding their solubility in immunoblot. In Figure 52 the results of the solubility tests are depicted. The results show, that the Cytokeratin-Chromobody (Figure 52 A) is expressed poorly if the fluorescent fusion protein is N-terminal fused, but well expressed with the fluorescent fusion protein being C-terminal fused. However, the level of the soluble fraction (SN) of the Cytokeratin-Chromobody is 50 %, independent of the localization of the fluorescent protein. The Lamin-Chromobody (Figure 52 B) with N-terminal fused GFP is not expressed at all, while the C-terminal fusion is expressed well. The level of the soluble fraction (SN) is 70 %. In contrast, the GFP-Chromobody (Figure 52 C) is 100 % soluble and is expressed well independent of the localization of the fluorescent protein. The detection of endogenous PCNA was performed as control for the complete lysis of the cells.

3 Results

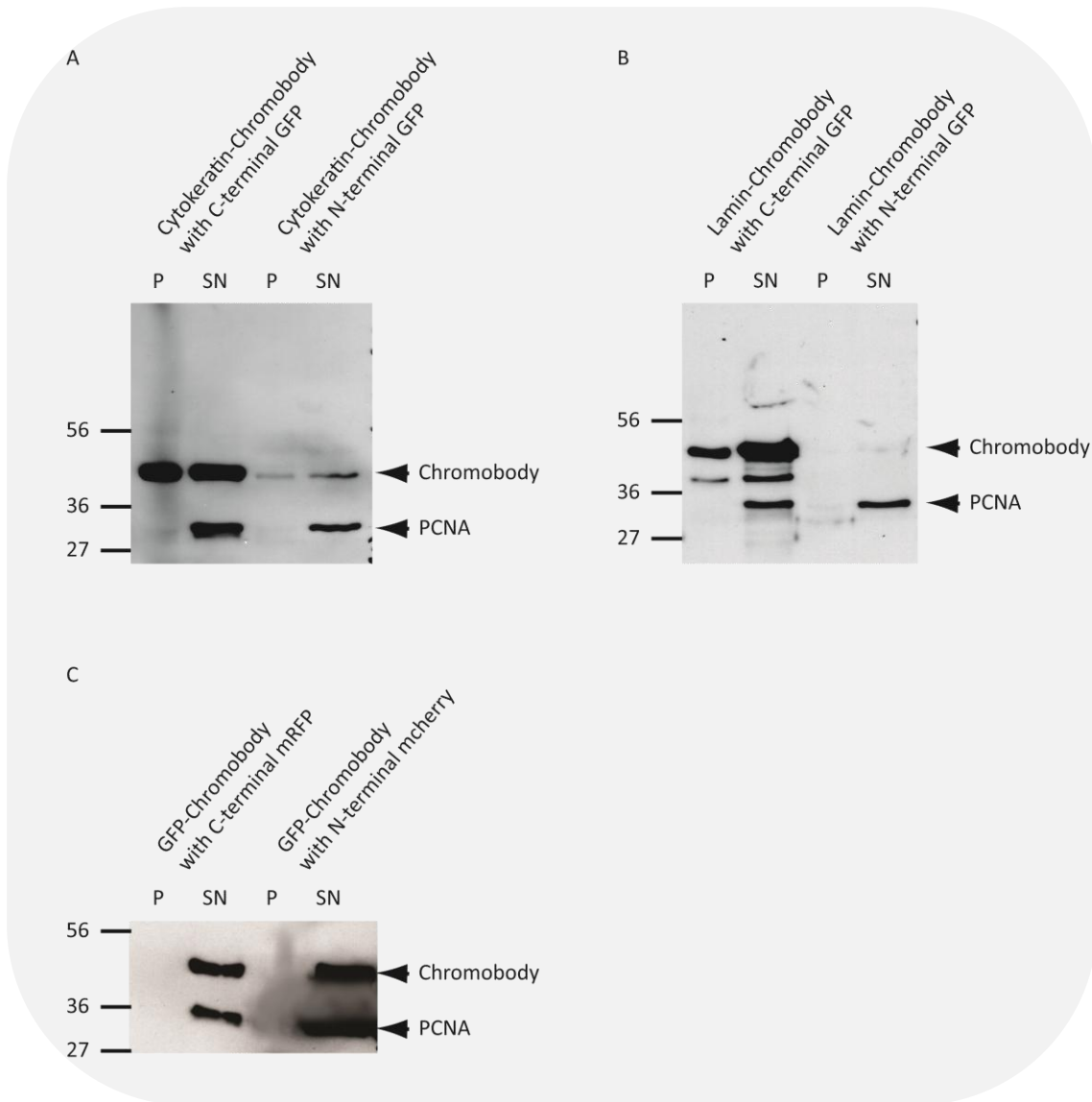


Figure 52: Solubility test with Chromobodies. (A) HEK293T cell extract expressing Cytokeratin-Chromobody with either C-terminal or N-terminal GFP were lysed and 1 % of pellet (P) and 1 % of supernatant (SN) separated by SDS-PAGE followed by immunoblot analysis. (B) HEK293T cell extract expressing Lamin-Chromobody with either C-terminal or N-terminal GFP were lysed and 1 % of pellet (P) and 1 % of supernatant (SN) separated by SDS-PAGE followed by immunoblot analysis. (C) HEK293T cell extract expressing GFP-Chromobody with either C-terminal mRFP or N-terminal mcherry were lysed and 1 % of pellet (P) and 1 % of supernatant (SN) separated by SDS-PAGE followed by immunoblot analysis. Predicted molecular weight of Chromobody (42 kDa) and PCNA (29 kDa) is marked by an arrow. Endogenous level of PCNA was detected by an anti-PCNA antibody as positive control.

3 Results

The results of the analyses of the Chromobodies show that solubility of V_HHs depends not only on the occurrence of additional cysteine residues and extended CDR3s but also on the position of the fluorescent protein (N- versus C-terminal).

3.2.2 Intracellular characterization

After the biochemical characterization of antigen specific V_HHs, their capacity to recognize and bind antigens in living cells was analyzed. To this end functionality tests and immunofluorescence were performed.

3.2.2.1 Functionality test

As described in 3.2.1.3, the solubility of Chromobodies is an inevitable requirement not only for the production in *E. coli* but also for their functionality in living mammalian cells. Therefore, in addition to the solubility test using cell extracts of HEK293T expressing Chromobodies (3.2.1.3), the Chromobodies were also tested for their functionality in HeLa Kyoto cells with regard to the C- or N-terminal localization of the fluorescent protein. To this end, HeLa Kyoto cells were transfected with the GFP-Chromobody, the Lamin-Chromobody and the Cytokeratin-Chromobody each fused N- or C-terminal to a fluorescent protein and fixed.

3 Results

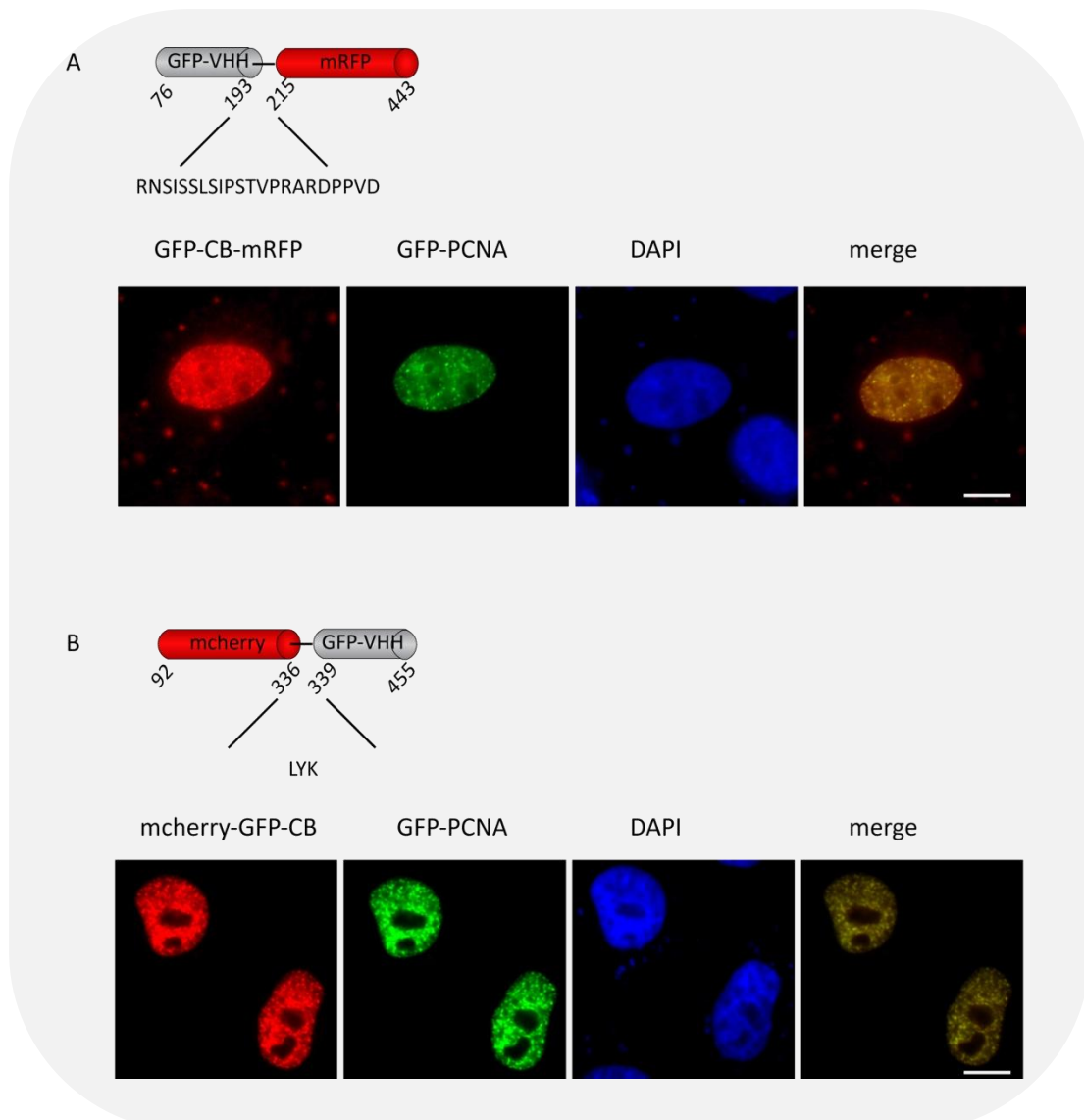


Figure 53: Functionality test of GFP-Chromobody. (A) GFP-CB-mRFP colocalizes with GFP-PCNA at replication foci. (B) mcherry-GFP-CB colocalizes with GFP-PCNA at replication foci. Scale bars 5 μ m.

The GFP-Chromobody colocalizes with GFP-PCNA independent of the localization of the fluorescent protein (Figure 53). This result is in accordance with the solubility test in 3.2.1.3 showing that both variants of the GFP-Chromobody are soluble and show comparable expression levels. However, this is contrary to previous observations which have indicated a functional dependency on the N- or C-terminal localization of the fluorescent protein (Leonhardt and Rothbauer, 2005). The main difference between these two opposite results is the length and the composition of the linker between the V_HH fragment and the

3 Results

fluorescent protein. Therefore, the results show that the position of the fluorescent protein within the Chromobody construct does not necessarily influence the functionality of the GFP-Chromobody.

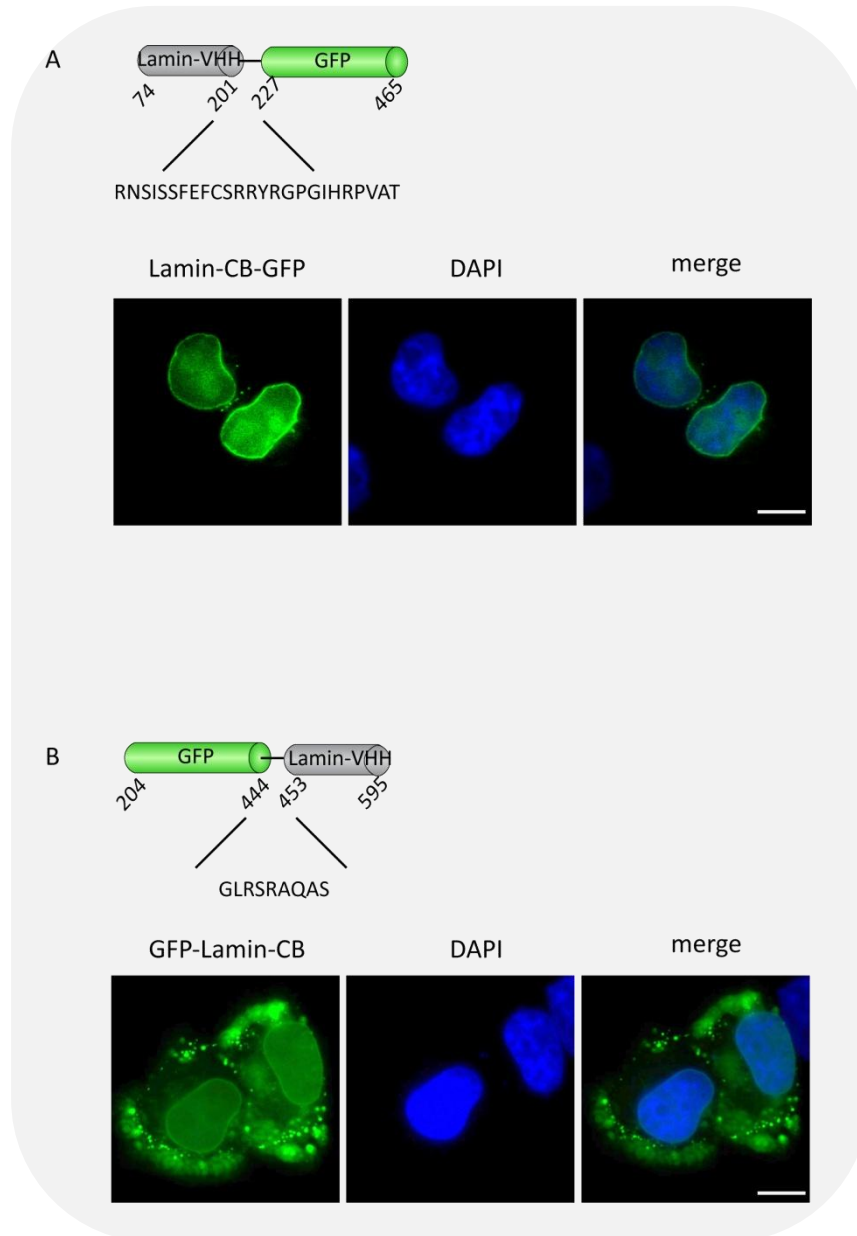


Figure 54: Functionality test of Lamin-Chromobody. (A) Lamin-CB-GFP highlights the nuclear rim structure that is characteristic for the nuclear lamina. (B) GFP-Lamin-CB highlights the nuclear rim structure that is characteristic for the nuclear lamina. In addition, aggregates of the Chromobody are visible. Scal bars 5 μ m.

3 Results

The Lamin-Chromobody colocalizes with nuclear lamina independent of the localization of the fluorescent protein (Figure 54). However, the GFP-Lamin-CB construct in Figure 54 B shows aggregates in the cytoplasm of the cells. Hence, the N-terminal fusion of the fluorescent protein negatively influences the functionality of the Lamin-Chromobody.

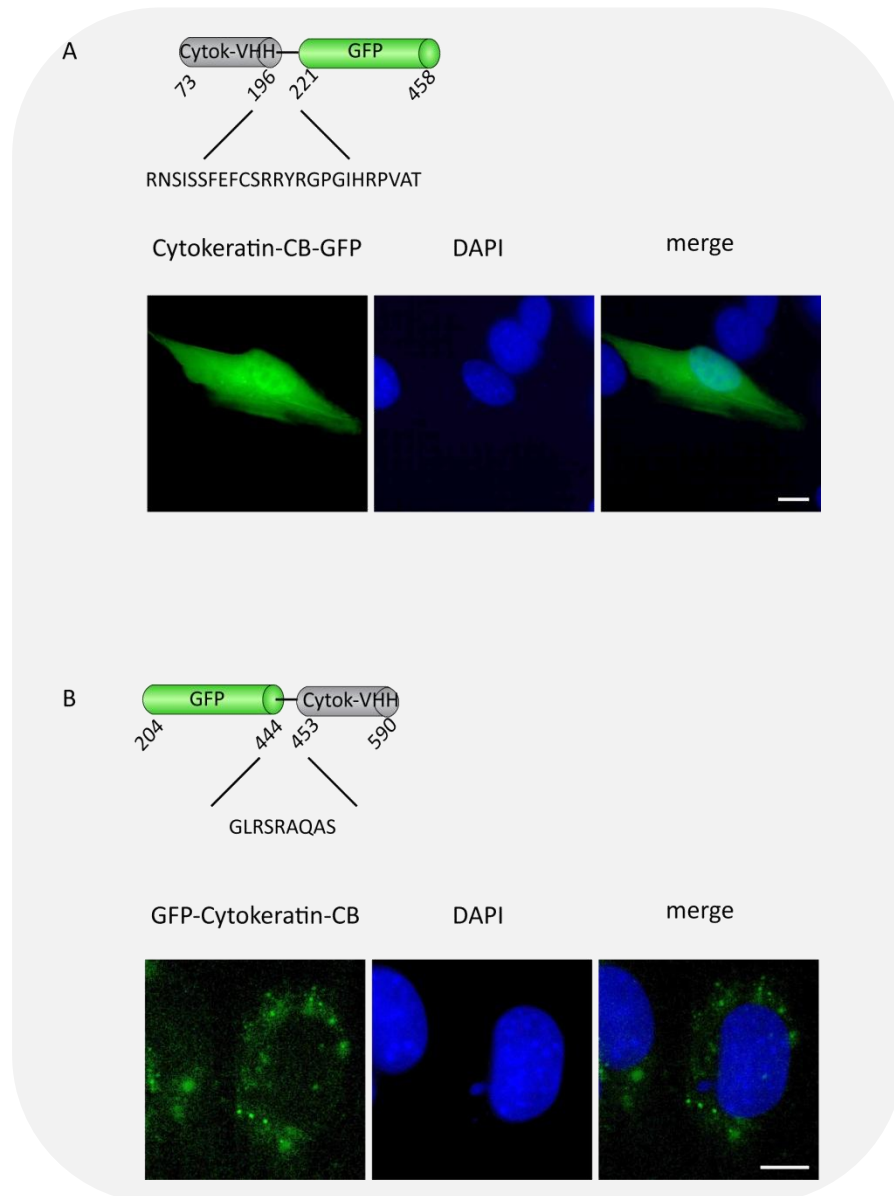


Figure 55: Functionality test of Cytokeratin-Chromobody. (A) Cytokeratin-CB-GFP highlights the nuclear cytoplasmic filaments. (B) GFP-Cytokeratin-CB aggregates. Scale bars 5 μm .

3 Results

The Cytokeratin-Chromobody colocalizes with cytoplasmic filaments if the fluorescent protein is localized at the C-terminus (Figure 55 A). However, the positioning of the GFP at the N-terminus of the Cytokeratin-Chromobody construct leads to a very low expression, formation of aggregates and no staining of the antigen structure. Therefore fusion with the fluorescent protein does influence the functionality of the Cytokeratin-Chromobody.

In general, V_HHs are characterized by their high stability and solubility (Muyldermans, 2001) which previously has also been showed in living mammalian cells (Rothbauer et al., 2006). However, the results depicted above illustrate that V_HH domains fused to a fluorescent protein may have a tendency to aggregate which may be due to the overexpression of the fusion protein, the position of the fluorescence protein or the presence/number of cysteine residues. Moreover, the length and the amino acid composition of the linker between V_HH fragment and the fluorescent protein are crucial.

4 Discussion

Antibodies are key components applied in basic research, diagnostics and therapy. They are powerful tools to study and to measure the distribution and localization of countless different antigens including proteins, posttranslational modifications or chemical entities. However, in order to study and understand continuous dynamic processes on a cellular level, data on dynamic localization, modification and interaction of cellular components are necessary. Here, the use of conventional antibodies is rather limited due to their complex structure which interferes with their application within living cells.

Naturally occurring heavy chain antibodies (hcAbs) derived from *Camelidae* are an attractive alternative to conventional and recombinant antibodies. In hcAbs, antigen binding is mediated through a single domain, referred to as V_HH (variable domain of heavy chain antibodies). V_HHs are characterized by a very small size (~ 15 kDa), extreme stability (van der Linden et al., 1999) (Arbabi Ghahroudi et al., 1997) and high solubility (Muyldermans, 2001). In addition, V_HHs have been shown to bind epitopes inaccessible for conventional antibodies (Lauwereys et al., 1998) (De Genst et al., 2006). Altogether, these features render V_HHs versatile tools for diverse applications in basic research, diagnostics and therapy.

The main objective of this thesis was to generate and characterize antigen specific V_HHs functional in biochemical and intracellular applications. The V_HHs were generated against a broad range of antigens from a peptide (γH2AX) to a component of a virus particle (HIV-1 capsid protein), a middle sized protein (PCNA), a fusion protein (β-Catenin-GST) and a large protein (hDnmt1).

4 Discussion

4.1 V_HH libraries

The first step for a successful selection of antigen specific V_HHs is the generation of a high quality primary V_HH library in terms of diversity and size, ideally comprising 10⁵ - 10⁹ clones (Arbabi Ghahroudi et al., 1997). Such libraries can be obtained by using either immunized animals to produce an immune library or non-immunized animals to produce a naïve library. The use of libraries derived from immunized animals is advantageous since library sizes of 10⁶ - 10⁷ clones is sufficient to select antigen specific V_HHs (Muyldermans, 2001). In addition, the selection of high affinity clones against the target antigen is facilitated (Smith et al., 2005) since the exposure to the antigen elicits the production of antigen-specific antibodies and somatic hypermutation takes place resulting in the creation of antibodies with improved affinity (Hoogenboom, 2005) (Ponsel et al., 2011). High affinity of a V_HH to its antigen is vital especially when used as Nanotrap in (co-) immunoprecipitations ((Co-) IPs). In this application the binding to the antigen needs to be strong and specific in order to enable the isolation of the protein of interest quantitatively and in a very short time. This proves particularly important when working with sensitive proteins (with regard to temperature or pH) with high tendency for degradation, like hDnmt1 for example.

4.1.1 Immunogenicity of Antigens

The generation of a comprehensive library from immunized alpacas requires an immune response against the immunized antigen, first. Naturally not all antigens are immunogenic: the immune system discriminates not only between the body's own and foreign molecules but also small, less complex antigens such as peptides are often non-immunogenic and do not elicit sufficient immune response (Stanley, 2002). Therefore, to stimulate an immune response, most antigens require to be injected in a mixture that enhances the immunogenicity of an antigen known as adjuvant (Janeway et al., 2001). The most commonly used adjuvant is Freund's adjuvant which contains heat-inactivated mycobacteria

4 Discussion

in a mineral oil-surfactant mixture (Freund, 1956). Even being widely used, Freund's adjuvant is associated with a severe and painful inflammatory response (Bennett et al., 1992). Hence, for the immunization of the alpacas an alternative adjuvant, Gerbu adjuvant, was used. Gerbu adjuvant is tolerated well, but is disadvantageous in terms of the production of antibodies in equal quality to those of other adjuvants (Stills, 2005). Since adjuvants enhance immune response but cannot themselves render antigens immunogenic, small antigens need to be conjugated to a large carrier protein in order to elicit an immune response. The most commonly used carriers are keyhole limpet hemocyanin (KLH), bovine serum albumin (BSA) and ovalbumin (OVA). Since KLH is evolutionary more remote from mammalian proteins and contains a high number of primary amines which enables the coupling of a high number of peptides (Grant, 2003) it was used as carrier to conjugate yH2AX.

The immune response of our alpacas was monitored in three exemplary serum tests: for the large protein hDnmt1, the fusionprotein β -Catenin-GST and the peptide yH2AX. The results show that both the large protein hDnmt1 and the fusionprotein β -Catenin-GST elicit an immune response in the alpaca. Hence, it can be concluded that the Gerbu adjuvant is sufficient to elicit an immune response in alpacas, in general. The peptide yH2AX, however, does not trigger an immune response - even immunized in the KLH-conjugated form. Although V_HHs were reported to bind haptens (Ladenson et al., 2006) they have a strong preference for conformational epitopes (Thys et al., 2011) which peptides are unlikely to produce (Brown et al., 2011). Conformational epitopes are mostly formed by native proteins (Horsfall et al., 1991) when the antigen is available in its native conformation. Therefore, the immunization of alpacas with peptides has two major drawbacks: the less efficient immune response and the preference for a native conformation of the antigen. The ability to recognize native proteins is vital especially for the application of V_HHs in living cells as Chromobody.

4 Discussion

During this thesis and in previous reports, Chromobodies functional in living cells were successfully generated against human DNA Methyltransferase 1 (hDnmt1), proliferating cell nuclear antigen (PCNA) (Burgess et al., 2012), HIV-1 capsid (Helma et al., 2012), green fluorescent protein (GFP) (Rothbauer et al., 2006), Lamin Dm0 (Rothbauer et al., 2006) and Cytokeratin 8 (Rothbauer et al., 2006) while V_HHs recognizing peptides could not be generated. These results suggest that the size of the antigen and the foreignness influences the immune response in alpacas.

4.1.2 V_HH Library Size and Diversity

As mentioned above, the size and diversity of a V_HH library is a quality feature and the starting basis for a successful generation of antigen specific V_HHs. To obtain a V_HH library, peripheral blood lymphocytes (PBL) were used as the source of cDNA synthesis for the V_HH libraries, even though PBLs are less enriched with antigen-specific V_HHs. When working with mice or rabbits as antibody source, tissue from the lymph node or spleen is usually used as basic raw material (Maass et al., 2007) since upon immunizations, lymphocytes are redistributed and remain in lymphoid organs or migrate to tissues rather than circulate in peripheral blood (Nduati et al., 2010). However, the use of PBLs is advantageous to lymphoid tissue such as spleen or lymph nodes, because PBLs are easily accessible and may be sampled repeatedly by taking a blood sample of an animal (Nduati et al., 2010).

Furthermore, the size of V_HH libraries is limited by the B cell and mRNA yield and the transformation efficiency of the bacterial host (Ponsel et al., 2011). The applied optimization of these procedures resulted in increased library sizes. The first library generated (yH2AX) has a size of 6×10^3 while the final library generated (hDnmt1) contains $1,5 \times 10^5$ clones.

With the generation of larger V_HH libraries, the task of assessing their diversity becomes more and more complex. Restriction analysis is a quick way to check diversity by the band patterns on an agarose gel. However, sequencing is a more preferable method since it also

4 Discussion

provides additional information which may not be obtained from restriction analysis such as frame shifts or stop codons (Carmen and Jeremius, 2002). But, evaluation of large libraries by sequencing is costly and time-consuming. Therefore, in order to evaluate the diversity of the V_HH libraries, ten to fourteen clones from each primary library were sequenced and aligned. This analysis showed that 80% of the libraries are highly diverse – only in the yH2AX primary V_HH library two sequences were found more than once which signifies a reduced diversity. However, during this thesis only a small number of sequences was analyzed. In order to assess the libraries' diversity more precisely, a higher number of sequences needs to be analyzed.

4.2 V_HH Selection

In order to select antigen specific V_HHs from the V_HH libraries, the phage display method was applied. The selection process called panning can be divided in five main steps: 1) coating with antigen, 2) blocking of free binding sites, 3) incubation of phages with the immobilized antigen, 4) washing and 5) elution (as described in 1.2.2.1). Besides blocking with a suitable blocking reagent and stringent washing, the way how the antigen is immobilized is of highest importance. In general, antigens are immobilized on a solid surface such as magnetic beads (Moghaddam et al., 2003), nitrocellulose (Hawlich et al., 2001) or plastic surfaces like polystyrol tubes (Hust et al., 2002) by passive adsorption which is advantageous since a wide range of molecules can be immobilized without prior treatment (Willats, 2002). However, passive absorption may result in the immobilized molecule being forced out of its functional conformation (Davies et al., 1994). Hence, antigens may become partially denatured, leading to the selection of V_HHs which recognize epitopes only present in denatured molecules (Chames et al., 2001). As described above, for the application of V_HHs as Chromobodies in living cells it is essential that the V_HH recognizes its antigen in living cells available as natively folded protein. The method of passive adsorption in polystyrol tubes was successfully used for the selection of HIV-1 capsid specific V_HHs (Helma et al., 2012) and PCNA specific V_HHs (Burgess et al., 2012) which both are functional in living cells but proved inadequate for the selection of hDnmt1 specific V_HHs functional in living cells.

4.2.1 A new method to select V_HHs for in vivo applications

In order to address the problem of antigen denaturing upon immobilization, many alternative methods are available such as the use of biotinylated antigens which are immobilized by streptavidin (Hoogenboom et al., 1998) or the use of a monoclonal antibody which is immobilized and binds the antigen for presentation (Verheesen et al., 2006). However, these methods are all hampered by the fact that phages tend to unspecifically

4 Discussion

bind to different kinds of structures such as support surfaces or proteins. In order to circumvent these drawbacks, a new selection method based on classical phage display was developed: *native panning*. Here, a GFP-fusion protein is precipitated from mammalian cell extract via a GFP-specific V_HH. This GFP-specific V_HH is coated in a 96 well plate (Pichler et al., 2012) resulting in the immobilization of the GFP-fusion protein which is then subjected to panning. Besides the native conformation of the presented antigen, also posttranslational modifications of the antigen are present in contrast to recombinantly purified proteins produced in *E. coli*.

The impact of this new method was demonstrated by using the hDnmt1 primary library for both panning methods in parallel. The results of the panning are similar with regard to the enrichment of antigen specific V_HHs during the panning rounds and the signal-to-noise ratio. However, the V_HH sequences derived from solid phase panning differed from those of the *native panning*. It can be concluded, that the different presentation of the antigen i.e. presentation of denatured versus native antigen, leads to the selection of different V_HHs. Furthermore, only the V_HHs derived from the *native panning* were functional in living cells, whereas the V_HHs derived from solid phase panning aggregated in living cells.

Interestingly, the hDnmt1 specific V_HHs selected in *native panning* do not recognize its antigen in immunofluorescence experiments although V_HHs have been shown to be functional in immunofluorescence analysis (Pichler et al., 2011). It seems that the denaturation caused by fixation methods changes the antigen structure in a way which hinders the V_HH to recognize its antigen. This result shows that the selection method needs to be chosen carefully with regard to the presentation of the antigen in the intended downstream application of the V_HH.

Different factors influence the functionality of V_HHs for cellular applications, such as selection method or accessibility of the antigen. In addition, the functionality *in vivo* is also determined by the localization of the fluorescent protein. The results of this thesis showed

4 Discussion

that the localization of the fluorescent protein may lead to aggregation of the V_HH *in vivo* preventing antigen detection.

4.3 Compensation of V_H - V_L combination

V_H HS lack the diversity introduced by V_H - V_L combination since the V_L is missing. In order to compensate this loss *Camelidae* make use of various mechanisms such as a higher somatic diversification rate (Conrath et al., 2003).

The diversification of antibody molecules results from processes like somatic hypermutation which preferably takes place at so called hypermutation hotspots such as AGY and TAY motif (Y = C or T) (Nguyen et al., 2000) improving the binding affinity of antibodies. The fact that V_H HS have a higher rate of somatic hypermutation than V_H S is due to the fact that *Camelidae* make use of a distinct set of V genes encoding the V domain of hcAbs (Nguyen et al., 2000). This tendency for a higher somatic hypermutation rate can be observed in the sequences of HIV-1 capsid protein specific V_H HS for example. The clones HIV-1_1p#1 and HIV-1_1p#4 have identical CDR3s, but they differ in their CDR1 by two out of nine amino acid residues (22%). The sequences of HIV-1_1p#3 and HIV-1_3p#4 have the same CDR3 and differ in the CDR1 by three out of nine (33%) and in the CDR2 even by 11 out of 16 amino acid residues (69%). In summary, the 41 analyzed V_H HS against HIV-1 capsid protein comprise eight different CDR1s, seven different CDR2s and seven different CDR3s which are combined.

Besides a higher somatic hypermutation rate due to the accumulation of new hypermutation hotspots (Nguyen et al., 2000), V_H HS are diversified by VDJ recombination like conventional antibodies. This can be observed in the yH2AX library for example with yH2AX_primary#3 and #4 having identical CDR1 and CDR2 but differ in the CDR3 which is due to the use of different D segments during VDJ recombination with the CDR3 loop providing important contacts with the antigen (Muyldermans et al., 1994) (De Genst et al., 2006).

4.4 CDR3, disulfide bonds and functionality

In addition to somatic diversification to compensate the loss of the V_H - V_L interaction and the resulting smaller antigen binding surface also the average length of CDR3s in V_H Hs is longer than in V_H S (Conrath et al., 2003). This extension not only results in a larger antigen-binding area but also increases the structural diversity of V_H Hs (Conrath et al., 2003) enabling V_H Hs to bind structures not recognized by conventional antibodies such as active clefts of enzymes with inhibitory or modulating effects (Transue et al., 1998). Since V_H S and V_H Hs use the same set of D and J segments, the emergence of the longer CDR3s may be explained by the use of longer D genes or the connection of two D genes (Muyldermans, 2001). The extended CDR3 of V_H Hs is often stabilized by an additional disulfide bond. This additional disulfide bond is formed with a cysteine in the CDR1 or CDR2 (Muyldermans, 2001).

In general, disulfide bonds are not formed within the reducing environment of the cytoplasm making conventional antibodies useless for an application in living cells. The sequence of hDnmt1-mCh_2pC6 has an extended CDR3 and one additional cysteine residue in the CDR2 and the CDR3, respectively. However, the intracellular recognition of hDnmt1 by the V_H H seems not to be impaired by the reducing environment of the cytoplasm resulting in the absence of disulfide bonds. This particular V_H H detects its antigen as good as the other three hDnmt1 specific V_H Hs containing no additional cysteines in living cells.

The extended CDR3 of V_H Hs is often associated with their ability to bind hidden epitopes like active sites of enzymes (Lauwereys et al., 1998; Conrath et al., 2001; Muyldermans, 2013). The often described inhibitory effect of V_H Hs cannot be observed with the selected V_H Hs for hDnmt1. One explanation may be the missing formation of the disulfide bonds resulting in a different loop structure which does not fit in the active site. Nevertheless, the formation of the disulfide bond in V_H Hs does not seem to play an important role for the visualization of the antigen.

4 Discussion

During this thesis V_HHs specific for different domains of the HIV-1 capsid protein were generated. The HIV-1 capsid protein consists of two domains, the N-terminal and the C-terminal domain. In the mature HIV-1 capsid a dimerization interface between the C-terminal domains of two capsid proteins is described (Mateu, 2009). The V_HH specific for HIV-1 N-terminal-domain (HIV-Nterm#1) comprises an extended CDR3 and two additional cysteines in the CDR3 and has been shown to specifically recognize the HIV-1 capsid protein in living cells allowing for the visualization of HIV-1 capsid protein without interference with its functionality (Helma et al., 2012). Contradictory to the extended CDR3 of HIV-Nterm#1, HIV-1 C-terminal domain specific V_HHs comprise an extreme short CDR3 (Figure 56 D). From the crystal structure (see Figure 56 A) it gets clear that HIV#9 crucially involves framework residues for antigen binding and the CDR3 plays only a minor role. HIV#9 binds to the HIV-1 capsid region which is important for the dimerization of the capsid protein C-terminal domains. The differential involvement of CDR3s in antigen binding was also shown with two V_HHs specific for GFP (Kirchhofer et al., 2010). The GFP-minimizer (Figure 56 B) comprises an extended CDR3 which is used to target GFP. In contrast, the GFP-enhancer (Figure 56 C) which has a short CDR3 uses both CDR2 and CDR3 to bind its antigen. However, both V_HHs influence the fluorescence properties of their antigen.

4 Discussion

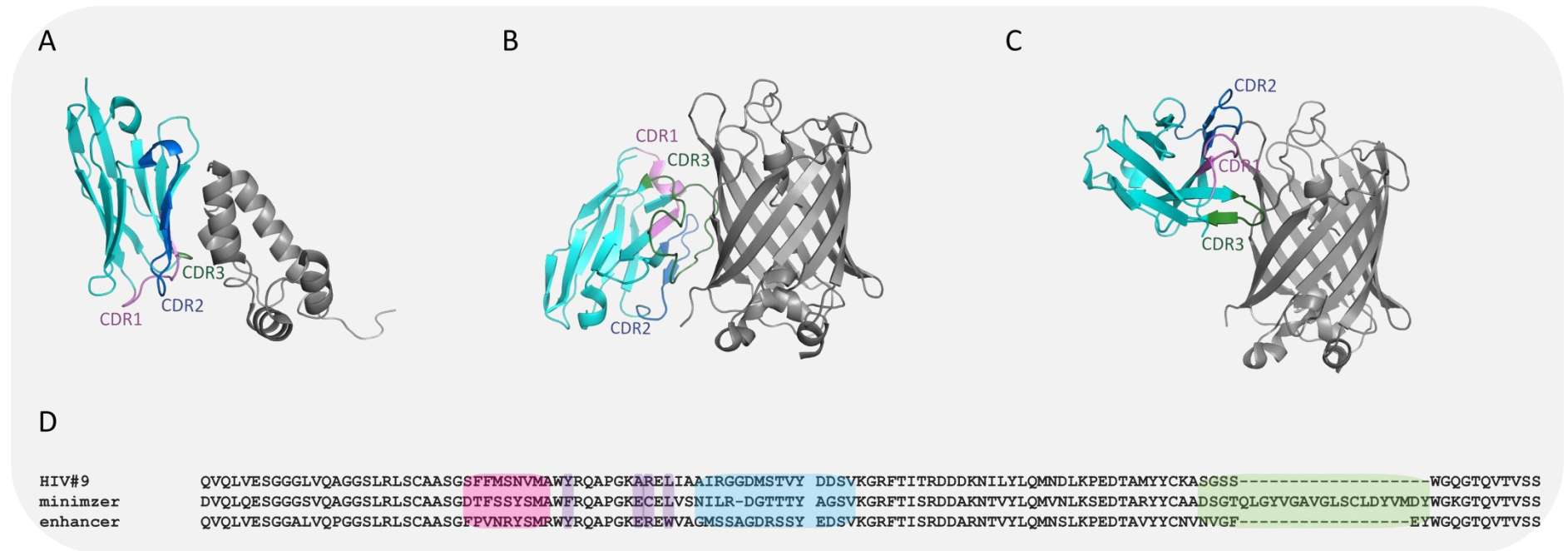


Figure 56: Examples of V_HH :antigen complexes. (A) HIV#9 with HIV-1 capsid C-terminal domain (PDB accession code: 2xt1). HIV#9 = cyan, HIV-1 capsid C-terminal domain = grey. (B) GFP-minimizer with GFP (PDB accession code 3g9a). GFP-minimizer = colored in cyan, GFP = grey. (C) GFP-enhancer with GFP (PDB accession code: 3k1k). GFP-enhancer = cyan, GFP = grey. (D) Amino acid sequence alignment of HIV#9, GFP-minimizer and GFP-enhancer. In all four figures, CDR1s are colored violet, CDR2s are colored blue and CDR3s are colored green.

4 Discussion

4.5 Outlook

V_HHs have a significant potential for various applications in basic research, diagnostics and therapy. Their small size and structure enables the recognition of epitopes not detectable by conventional antibodies or antibody fragments. In addition, V_HHs have the unique feature of functionality inside living cells. However, the generation of antigen specific V_HHs is challenging since many factors such as immunogenicity of the antigen, selection method and intended downstream application influence the generation process. The development of the *native panning* method presenting antigen which is properly folded in combination with the F2H assay enables to identify V_HHs recognizing native conformations.

The generation of V_HHs recognizing peptides, non-protein components or posttranslational modifications is especially demanding since V_HHs prefer to bind 3-dimensional epitopes. However, in particular the potential of recognizing posttranslational modifications is one of the most promising applications of V_HHs since today these structures can only be made visible by conventional antibodies in fixed cells. A live cell application for the detection of such structures would enable scientists to get a more detailed and authentic insight into these dynamic processes. In order to find V_HHs specific for such structures, the use of naïve libraries in combination with high-throughput panning and subsequent mutagenesis may be advantageous. V_HHs selected from naïve libraries are not as affine as V_HHs selected from an immune library. However, this attribute may be advantageous for live cell applications where strong binding of the V_HH to its antigen may unintentionally influence the behavior of the antigen.

5 Annex

5.1 References

- Ablynx. (2012). from <http://www.ablynx.com/en/research-development/pipeline/>.
- Alexander, A., M. Steinmetz, D. Barritault, B. Frangione, E. C. Franklin, L. Hood and J. N. Buxbaum (1982). "gamma Heavy chain disease in man: cDNA sequence supports partial gene deletion model." Proc Natl Acad Sci U S A **79**(10): 3260-3264.
- Arbabi Ghahroudi, M., A. Desmyter, L. Wyns, R. Hamers and S. Muyldermans (1997). "Selection and identification of single domain antibody fragments from camel heavy-chain antibodies." FEBS Lett **414**(3): 521-526.
- Behr, T., W. Becker, E. Hannappel, D. M. Goldenberg and F. Wolf (1995). "Targeting of liver metastases of colorectal cancer with IgG, F(ab')₂, and Fab' anti-carcinoembryonic antigen antibodies labeled with ^{99m}Tc: the role of metabolism and kinetics." Cancer Res **55**(23 Suppl): 5777s-5785s.
- Behring and Kitasato (1890). "Ueber das Zustandekommen der Diphtherie-Immunität und der Tetanus-Immunität bei Thieren." Dtsch Med Wochenschr **16**: 1113-1115.
- Bennett, B., I. J. Check, M. R. Olsen and R. L. Hunter (1992). "A comparison of commercially available adjuvants for use in research." J Immunol Methods **153**(1-2): 31-40.
- Beutler, B. (2004). "Innate immunity: an overview." Mol Immunol **40**(12): 845-859.
- Biocca, S., M. S. Neuberger and A. Cattaneo (1990). "Expression and targeting of intracellular antibodies in mammalian cells." EMBO J **9**(1): 101-108.
- Bonavida, B. and E. Sercarz (1971). "Structural basis for immune recognition of lysozymes. II. Reactive but non-immunogenic epitopes." Eur J Immunol **1**(3): 166-170.
- Borrebaeck, C. A. (2000). "Antibodies in diagnostics - from immunoassays to protein chips." Immunology Today **21**(8): 379-382.
- Boyiadzis, M. and K. A. Foon (2008). "Approved monoclonal antibodies for cancer therapy." Expert Opin Biol Ther **8**(8): 1151-1158.
- Bradbury, A. and J. D. Marks (2004). Phage Display. New York, Oxford University Press.

- Brown, M. C., T. R. Joaquim, R. Chambers, D. V. Onisk, F. Yin, J. M. Moriango, Y. Xu, D. A. Fancy, E. L. Crowgey, Y. He, J. W. Stave and K. Lindpaintner (2011). "Impact of immunization technology and assay application on antibody performance--a systematic comparative evaluation." *Plos One* **6**(12): e28718.
- Burgess, A., T. Lorca and A. Castro (2012). "Quantitative live imaging of endogenous DNA replication in mammalian cells." *Plos One* **7**(9): e45726.
- Carmen, S. and L. Jermutus (2002). "Concepts in antibody phage display." *Brief Funct Genomic Proteomic* **1**(2): 189-203.
- Carter, P. (2001). "Improving the efficacy of antibody-based cancer therapies." *Nat Rev Cancer* **1**(2): 118-129.
- Cattaneo, A. and S. Biocca (1999). "The selection of intracellular antibodies." *Trends Biotechnol* **17**(3): 115-121.
- Chalfie, M., Y. Tu, G. Euskirchen, W. W. Ward and D. C. Prasher (1994). "Green fluorescent protein as a marker for gene expression." *Science* **263**(5148): 802-805.
- Chames, P., H. R. Hoogenboom and P. Henderikx (2001). Selection of Antibodies Against Biotinylated Antigens. **178**: 147-157.
- Chothia, C., J. Novotny, R. Brucoleri and M. Karplus (1985). "Domain association in immunoglobulin molecules. The packing of variable domains." *J Mol Biol* **186**(3): 651-663.
- Cohen, S. and C. Milstein (1967). "Structure of antibody molecules." *Nature* **214**(5087): 449-452 passim.
- Collis, A. V., A. P. Brouwer and A. C. Martin (2003). "Analysis of the antigen combining site: correlations between length and sequence composition of the hypervariable loops and the nature of the antigen." *J Mol Biol* **325**(2): 337-354.
- Conrath, K. E., M. Lauwereys, M. Galleni, A. Matagne, J. M. Frere, J. Kinne, L. Wyns and S. Muyldermans (2001). "Beta-lactamase inhibitors derived from single-domain antibody fragments elicited in the camelidae." *Antimicrob Agents Chemother* **45**(10): 2807-2812.
- Conrath, K. E., U. Wernery, S. Muyldermans and V. K. Nguyen (2003). "Emergence and evolution of functional heavy-chain antibodies in Camelidae." *Dev Comp Immunol* **27**(2): 87-103.

- Coppieters, K., T. Dreier, K. Silence, H. de Haard, M. Lauwereys, P. Casteels, E. Beirnaert, H. Jonckheere, C. Van de Wiele, L. Staelens, J. Hostens, H. Revets, E. Remaut, D. Elewaut and P. Rottiers (2006). "Formatted anti-tumor necrosis factor alpha VHH proteins derived from camelids show superior potency and targeting to inflamed joints in a murine model of collagen-induced arthritis." Arthritis and Rheumatism **54**(6): 1856-1866.
- Cortez-Retamozo, V., N. Backmann, P. D. Senter, U. Wernery, P. De Baetselier, S. Muyldermans and H. Revets (2004). "Efficient cancer therapy with a nanobody-based conjugate." Cancer Res **64**(8): 2853-2857.
- David, M. P., J. J. Asprer, J. S. Ibane, G. P. Concepcion and E. A. Padlan (2007). "A study of the structural correlates of affinity maturation: antibody affinity as a function of chemical interactions, structural plasticity and stability." Mol Immunol **44**(6): 1342-1351.
- Davies, J., A. C. Dawkes, A. G. Haymes, C. J. Roberts, R. F. Sunderland, M. J. Wilkins, M. C. Davies, S. J. Tendler, D. E. Jackson and J. C. Edwards (1994). "A scanning tunnelling microscopy comparison of passive antibody adsorption and biotinylated antibody linkage to streptavidin on microtiter wells." J Immunol Methods **167**(1-2): 263-269.
- Davies, J. and L. Riechmann (1996). "Single antibody domains as small recognition units: design and in vitro antigen selection of camelized, human VH domains with improved protein stability." Protein Eng **9**(6): 531-537.
- De Genst, E., K. Silence, K. Decanniere, K. Conrath, R. Loris, J. Kinne, S. Muyldermans and L. Wyns (2006). "Molecular basis for the preferential cleft recognition by dromedary heavy-chain antibodies." Proc Natl Acad Sci U S A **103**(12): 4586-4591.
- de Haard, H. J., N. van Neer, A. Reurs, S. E. Hufton, R. C. Roovers, P. Henderikx, A. P. de Bruine, J. W. Arends and H. R. Hoogenboom (1999). "A large non-immunized human Fab fragment phage library that permits rapid isolation and kinetic analysis of high affinity antibodies." J Biol Chem **274**(26): 18218-18230.
- Delves, P. J. and I. M. Roitt (2000). "The immune system. First of two parts." N Engl J Med **343**(1): 37-49.
- Delves, P. J. and I. M. Roitt (2000). "The immune system. Second of two parts." N Engl J Med **343**(2): 108-117.
- Elsasser-Beile, U., G. Reischl, S. Wiehr, P. Buhler, P. Wolf, K. Alt, J. Shively, M. S. Judenhofer, H. J. Machulla and B. J. Pichler (2009). "PET imaging of prostate cancer xenografts with a highly specific antibody against the prostate-specific membrane antigen." J Nucl Med **50**(4): 606-611.

- Feldmann, M. (2002). "Development of anti-TNF therapy for rheumatoid arthritis." Nat Rev Immunol **2**(5): 364-371.
- Flajnik, M. F., N. Deschacht and S. Muyldermans (2011). "A case of convergence: why did a simple alternative to canonical antibodies arise in sharks and camels?" PLoS Biol **9**(8): e1001120.
- Freund, J. (1956). "The mode of action of immunologic adjuvants." Bibl Tuberc(10): 130-148.
- Goll, M. G. and T. H. Bestor (2005). "Eukaryotic cytosine methyltransferases." Annu Rev Biochem **74**: 481-514.
- Grant, G. A. (2003). Synthetic Peptides for production of Antibodies that Recognize Intact Proteins. Current Protocols in Immunology, John Wiley & Sons, Inc.
- Greenberg, A. S., D. Avila, M. Hughes, A. Hughes, E. C. McKinney and M. F. Flajnik (1995). "A new antigen receptor gene family that undergoes rearrangement and extensive somatic diversification in sharks." Nature **374**(6518): 168-173.
- Hamers-Casterman, C., T. Atarhouch, S. Muyldermans, G. Robinson, C. Hamers, E. B. Songa, N. Bendahman and R. Hamers (1993). "Naturally occurring antibodies devoid of light chains." Nature **363**(6428): 446-448.
- Hanes, J. and A. Plückthun (1997). "In vitro selection and evolution of functional proteins by using ribosome display." Proc Natl Acad Sci U S A **94**(10): 4937-4942.
- Harmsen, M. M. and H. J. De Haard (2007). "Properties, production, and applications of camelid single-domain antibody fragments." Appl Microbiol Biotechnol **77**(1): 13-22.
- Harmsen, M. M., C. B. van Solt, H. P. Fijten, L. van Keulen, R. A. Rosalia, K. Weerdmeester, A. H. Cornelissen, M. G. De Bruin, P. L. Eble and A. Dekker (2007). "Passive immunization of guinea pigs with llama single-domain antibody fragments against foot-and-mouth disease." Vet Microbiol **120**(3-4): 193-206.
- Harriman, W., H. Volk, N. Defranoux and M. Wabl (1993). "Immunoglobulin class switch recombination." Annu Rev Immunol **11**: 361-384.
- Harwood, N. E. and F. D. Batista (2010). "Early Events in B Cell Activation." Annual Review of Immunology, Vol 28 **28**: 185-210.
- Harwood, P. J., J. Boden, R. B. Pedley, G. Rawlins, G. T. Rogers and K. D. Bagshawe (1985). "Comparative tumour localization of antibody fragments and intact IgG in nude mice bearing a CEA-producing human colon tumour xenograft." Eur J Cancer Clin Oncol **21**(12): 1515-1522.

- Hawkins, R. E., S. J. Russell and G. Winter (1992). "Selection of phage antibodies by binding affinity. Mimicking affinity maturation." J Mol Biol **226**(3): 889-896.
- Hawlich, H., M. Muller, R. Frank, W. Bautsch, A. Klos and J. Kohl (2001). "Site-specific anti-C3a receptor single-chain antibodies selected by differential panning on cellulose sheets." Anal Biochem **293**(1): 142-145.
- He, M. and F. Khan (2005). "Ribosome display: next-generation display technologies for production of antibodies in vitro." Expert Rev Proteomics **2**(3): 421-430.
- He, M., M. Menges, M. A. Groves, E. Corps, H. Liu, M. Bruggemann and M. J. Taussig (1999). "Selection of a human anti-progesterone antibody fragment from a transgenic mouse library by ARM ribosome display." J Immunol Methods **231**(1-2): 105-117.
- Helma, J., K. Schmidhals, V. Lux, S. Nuske, A. M. Scholz, H. G. Krausslich, U. Rothbauer and H. Leonhardt (2012). "Direct and Dynamic Detection of HIV-1 in Living Cells." Plos One **7**(11): e50026.
- Hendershot, L., D. Bole, G. Kohler and J. F. Kearney (1987). "Assembly and secretion of heavy chains that do not associate posttranslationally with immunoglobulin heavy chain-binding protein." J Cell Biol **104**(3): 761-767.
- Hilshmann, N. and L. C. Craig (1965). "Amino acid sequence studies with Bence-Jones proteins." Proc Natl Acad Sci U S A **53**(6): 1403-1409.
- Holliger, P. and P. J. Hudson (2005). "Engineered antibody fragments and the rise of single domains." Nat Biotechnol **23**(9): 1126-1136.
- Honjo, T., K. Kinoshita and M. Muramatsu (2002). "Molecular mechanism of class switch recombination: linkage with somatic hypermutation." Annu Rev Immunol **20**: 165-196.
- Hoogenboom, H. R. (2005). "Selecting and screening recombinant antibody libraries." Nat Biotechnol **23**(9): 1105-1116.
- Hoogenboom, H. R., A. P. de Bruine, S. E. Hufton, R. M. Hoet, J. W. Arends and R. C. Roovers (1998). "Antibody phage display technology and its applications." Immunotechnology **4**(1): 1-20.
- Horsfall, A. C., F. C. Hay, A. J. Soltys and M. G. Jones (1991). "Epitope mapping." Immunology Today **12**(7): 211-213.

- Hozumi, N. and S. Tonegawa (1976). "Evidence for somatic rearrangement of immunoglobulin genes coding for variable and constant regions." Proc Natl Acad Sci U S A **73**(10): 3628-3632.
- Hudson, P. J. (1998). "Recombinant antibody fragments." Curr Opin Biotechnol **9**(4): 395-402.
- Hust, M., E. Maiss, H. J. Jacobsen and T. Reinard (2002). "The production of a genus-specific recombinant antibody (scFv) using a recombinant potyvirus protease." J Virol Methods **106**(2): 225-233.
- Huston, J. S., D. Levinson, M. Mudgett-Hunter, M. S. Tai, J. Novotny, M. N. Margolies, R. J. Ridge, R. E. Brucoleri, E. Haber, R. Crea and et al. (1988). "Protein engineering of antibody binding sites: recovery of specific activity in an anti-digoxin single-chain Fv analogue produced in Escherichia coli." Proc Natl Acad Sci U S A **85**(16): 5879-5883.
- Jakobovits, A. (1995). "Production of fully human antibodies by transgenic mice." Curr Opin Biotechnol **6**(5): 561-566.
- Janeway, C. A., Jr., P. Travers, M. Walport and E. al. (2001). Immunobiology: The Immune System in Health and Disease. New York, Garland Science.
- Jegg, A.-M. (2007). Isolierung und Charakterisierung von spezifischen Antikörperfragmenten gegen Dnmt1 und Histone. Department Biologie II. München, Ludwig-Maximilians-Universität München: 126.
- Johnson, G. and T. T. Wu (2000). "Kabat database and its applications: 30 years after the first variability plot." Nucleic Acids Res **28**(1): 214-218.
- Kabat, E. A., Wu, T. T., Gottesman, K. S., Foeller, C. (1991). Sequences of Proteins of Immunological Interest, DIANE Publishing.
- Kirchhofer, A., J. Helma, K. Schmidthals, C. Frauer, S. Cui, A. Karcher, M. Pellis, S. Muyldermans, C. S. Casas-Delucchi, M. C. Cardoso, H. Leonhardt, K. P. Hopfner and U. Rothbauer (2010). "Modulation of protein properties in living cells using nanobodies." Nat Struct Mol Biol **17**(1): 133-138.
- Knappik, A. and R. Brundiers Recombinant Antibody Expression and Purification: 1929-1943.
- Knappik, A., L. Ge, A. Honegger, P. Pack, M. Fischer, G. Wellnhofer, A. Hoess, J. Wolle, A. Pluckthun and B. Virnekas (2000). "Fully synthetic human combinatorial antibody libraries (HuCAL) based on modular consensus frameworks and CDRs randomized with trinucleotides." J Mol Biol **296**(1): 57-86.

- Kohler, G. and C. Milstein (1975). "Continuous cultures of fused cells secreting antibody of predefined specificity." Nature **256**(5517): 495-497.
- Ladenson, R. C., D. L. Crimmins, Y. Landt and J. H. Ladenson (2006). "Isolation and characterization of a thermally stable recombinant anti-caffeine heavy-chain antibody fragment." Anal Chem **78**(13): 4501-4508.
- Lange, I. G., A. Daxenberger and H. H. Meyer (2001). "Studies on the antibody response of Lama glama--evaluation of the binding capacity of different IgG subtypes in ELISAs for clenbuterol and BSA." Vet Immunol Immunopathol **83**(1-2): 1-9.
- Lauwereys, M., M. Arbabi Ghahroudi, A. Desmyter, J. Kinne, W. Holzer, E. De Genst, L. Wyns and S. Muyldermans (1998). "Potent enzyme inhibitors derived from dromedary heavy-chain antibodies." EMBO J **17**(13): 3512-3520.
- Leonhardt, H., H. P. Rahn and M. C. Cardoso (1998). "Intranuclear targeting of DNA replication factors." J Cell Biochem Suppl **30-31**: 243-249.
- Leonhardt, H. and U. Rothbauer (2005). Targeting and tracing of antigens in living cells. L.-M.-U. München.
- Li, Z., C. J. Woo, M. D. Iglesias-Ussel, D. Ronai and M. D. Scharff (2004). "The generation of antibody diversity through somatic hypermutation and class switch recombination." Genes Dev **18**(1): 1-11.
- Maass, D. R., J. Sepulveda, A. Pernthaler and C. B. Shoemaker (2007). "Alpaca (Lama pacos) as a convenient source of recombinant camelid heavy chain antibodies (VHHs)." J Immunol Methods **324**(1-2): 13-25.
- Maiolini, R. and R. Masseyeff (1975). "A sandwich method of enzymeimmunoassay. I. Application to rat and human alpha-fetoprotein." J Immunol Methods **8**(3): 223-234.
- Marks, J. D., H. R. Hoogenboom, T. P. Bonnert, J. McCafferty, A. D. Griffiths and G. Winter (1991). "By-passing immunization. Human antibodies from V-gene libraries displayed on phage." J Mol Biol **222**(3): 581-597.
- Mateu, M. G. (2009). "The capsid protein of human immunodeficiency virus: intersubunit interactions during virus assembly." FEBS J **276**(21): 6098-6109.
- Mattheakis, L. C., R. R. Bhatt and W. J. Dower (1994). "An in vitro polysome display system for identifying ligands from very large peptide libraries." Proc Natl Acad Sci U S A **91**(19): 9022-9026.

- McCafferty, J., A. D. Griffiths, G. Winter and D. J. Chiswell (1990). "Phage antibodies: filamentous phage displaying antibody variable domains." Nature **348**(6301): 552-554.
- Medzhitov, R. (2007). "Recognition of microorganisms and activation of the immune response." Nature **449**(7164): 819-826.
- Moghaddam, A., T. Borgen, J. Stacy, L. Kausmally, B. Simonsen, O. J. Marvik, O. H. Brekke and M. Braunagel (2003). "Identification of scFv antibody fragments that specifically recognise the heroin metabolite 6-monoacetylmorphine but not morphine." J Immunol Methods **280**(1-2): 139-155.
- Moldovan, G. L., B. Pfander and S. Jentsch (2007). "PCNA, the maestro of the replication fork." Cell **129**(4): 665-679.
- Morrison, S. L., L. A. Wims and V. T. Oi (1988). "Genetically engineered antibody molecules: new tools for cancer therapy." Cancer Invest **6**(2): 185-192.
- Murphy, K., P. Travers, M. Walport and C. Janeway (2012). Janeway's immunobiology. New York, Garland Science.
- Muyldermans, S. (2001). "Single domain camel antibodies: current status." J Biotechnol **74**(4): 277-302.
- Muyldermans, S. (2013). "Nanobodies: Natural Single-Domain Antibodies." Annu Rev Biochem.
- Muyldermans, S., T. Atarhouch, J. Saldanha, J. A. Barbosa and R. Hamers (1994). "Sequence and structure of VH domain from naturally occurring camel heavy chain immunoglobulins lacking light chains." Protein Eng **7**(9): 1129-1135.
- Muyldermans, S., T. N. Baral, V. C. Retamozzo, P. De Baetselier, E. De Genst, J. Kinne, H. Leonhardt, S. Magez, V. K. Nguyen, H. Revets, U. Rothbauer, B. Stijlemans, S. Tillib, U. Wernery, L. Wyns, G. Hassanzadeh-Ghassabeh and D. Saerens (2009). "Camelid immunoglobulins and nanobody technology." Vet Immunol Immunopathol **128**(1-3): 178-183.
- Muyldermans, S. and M. Lauwereys (1999). "Unique single-domain antigen binding fragments derived from naturally occurring camel heavy-chain antibodies." J Mol Recognit **12**(2): 131-140.
- Nduati, E. W., D. H. Ng, F. M. Ndungu, P. Gardner, B. C. Urban and J. Langhorne (2010). "Distinct kinetics of memory B-cell and plasma-cell responses in peripheral blood

- following a blood-stage *Plasmodium chabaudi* infection in mice." *Plos One* **5**(11): e15007.
- Nelson, A. L. and J. M. Reichert (2009). "Development trends for therapeutic antibody fragments." *Nat Biotechnol* **27**(4): 331-337.
- Nguyen, V. K., R. Hamers, L. Wyns and S. Muyldermans (1999). "Loss of splice consensus signal is responsible for the removal of the entire C(H)1 domain of the functional camel IGG2A heavy-chain antibodies." *Mol Immunol* **36**(8): 515-524.
- Nguyen, V. K., R. Hamers, L. Wyns and S. Muyldermans (2000). "Camel heavy-chain antibodies: diverse germline V(H)H and specific mechanisms enlarge the antigen-binding repertoire." *EMBO J* **19**(5): 921-930.
- Nguyen, V. K., C. Su, S. Muyldermans and W. van der Loo (2002). "Heavy-chain antibodies in Camelidae; a case of evolutionary innovation." *Immunogenetics* **54**(1): 39-47.
- Nizak, C., S. Martin-Lluesma, S. Moutel, A. Roux, T. E. Kreis, B. Goud and F. Perez (2003). "Recombinant antibodies against subcellular fractions used to track endogenous Golgi protein dynamics in vivo." *Traffic* **4**(11): 739-753.
- Noelle, R. and E. C. Snow (1992). "T helper cells." *Curr Opin Immunol* **4**(3): 333-337.
- Ochs, H. D. and R. J. Wedgwood (1987). "IgG subclass deficiencies." *Annu Rev Med* **38**: 325-340.
- Padlan, E. A. (1994). "Anatomy of the antibody molecule." *Mol Immunol* **31**(3): 169-217.
- Padlan, E. A., C. Abergel and J. P. Tipper (1995). "Identification of specificity-determining residues in antibodies." *FASEB J* **9**(1): 133-139.
- Parker, D. C. (1993). "T cell-dependent B cell activation." *Annu Rev Immunol* **11**: 331-360.
- Pichler, G., A. Jack, P. Wolf and S. B. Hake (2012). "Versatile toolbox for high throughput biochemical and functional studies with fluorescent fusion proteins." *Plos One* **7**(5): e36967.
- Pichler, G., P. Wolf, C. S. Schmidt, D. Meilinger, K. Schneider, C. Frauer, K. Fellingner, A. Rottach and H. Leonhardt (2011). "Cooperative DNA and histone binding by Uhrf2 links the two major repressive epigenetic pathways." *J Cell Biochem* **112**(9): 2585-2593.
- Pluckthun, A. (1992). "Mono- and bivalent antibody fragments produced in *Escherichia coli*: engineering, folding and antigen binding." *Immunol Rev* **130**: 151-188.

- Ponsel, D., J. Neugebauer, K. Ladetzki-Baehs and K. Tissot (2011). "High affinity, developability and functional size: the holy grail of combinatorial antibody library generation." Molecules **16**(5): 3675-3700.
- Porter, P., J. Coley and M. Gani (1988). "Immunochemical criteria for successful matching of monoclonal antibodies to immunoassays of peptide hormones for assessment of pregnancy and ovulation." Prog Clin Biol Res **285**: 181-200.
- Porter, R. R. (1963). "Chemical Structure of Gamma-Globulin and Antibodies." Br Med Bull **19**: 197-201.
- Rajewsky, K., I. Forster and A. Cumano (1987). "Evolutionary and somatic selection of the antibody repertoire in the mouse." Science **238**(4830): 1088-1094.
- Reth, M. (1992). "Antigen receptors on B lymphocytes." Annu Rev Immunol **10**: 97-121.
- Revs, H., P. De Baetselier and S. Muyldermans (2005). "Nanobodies as novel agents for cancer therapy." Expert Opin Biol Ther **5**(1): 111-124.
- Roberts, B. L., W. Markland, A. C. Ley, R. B. Kent, D. W. White, S. K. Guterman and R. C. Ladner (1992). "Directed evolution of a protein: selection of potent neutrophil elastase inhibitors displayed on M13 fusion phage." Proc Natl Acad Sci U S A **89**(6): 2429-2433.
- Rogakou, E. P., D. R. Pilch, A. H. Orr, V. S. Ivanova and W. M. Bonner (1998). "DNA double-stranded breaks induce histone H2AX phosphorylation on serine 139." J Biol Chem **273**(10): 5858-5868.
- Roovers, R. C., G. A. van Dongen and P. M. van Bergen en Henegouwen (2007). "Nanobodies in therapeutic applications." Curr Opin Mol Ther **9**(4): 327-335.
- Rothbauer, U., K. Zolghadr, S. Muyldermans, A. Schepers, M. C. Cardoso and H. Leonhardt (2008). "A versatile nanotrapp for biochemical and functional studies with fluorescent fusion proteins." Mol Cell Proteomics **7**(2): 282-289.
- Rothbauer, U., K. Zolghadr, S. Tillib, D. Nowak, L. Schermelleh, A. Gahl, N. Backmann, K. Conrath, S. Muyldermans, M. C. Cardoso and H. Leonhardt (2006). "Targeting and tracing antigens in live cells with fluorescent nanobodies." Nat Methods **3**(11): 887-889.
- Saerens, D., J. Kinne, E. Bosmans, U. Wernery, S. Muyldermans and K. Conrath (2004). "Single domain antibodies derived from dromedary lymph node and peripheral blood

- lymphocytes sensing conformational variants of prostate-specific antigen." J Biol Chem **279**(50): 51965-51972.
- Sanz, L., A. M. Cuesta, M. Compte and L. Alvarez-Vallina (2005). "Antibody engineering: facing new challenges in cancer therapy." Acta Pharmacol Sin **26**(6): 641-648.
- Schilling, J., B. Clevinger, J. M. Davie and L. Hood (1980). "Amino acid sequence of homogeneous antibodies to dextran and DNA rearrangements in heavy chain V-region gene segments." Nature **283**(5742): 35-40.
- Sidhu, S. S. (2001). "Engineering M13 for phage display." Biomol Eng **18**(2): 57-63.
- Skerra, A. and A. Pluckthun (1988). "Assembly of a functional immunoglobulin Fv fragment in Escherichia coli." Science **240**(4855): 1038-1041.
- Smith, G. P. (1985). "Filamentous fusion phage: novel expression vectors that display cloned antigens on the virion surface." Science **228**(4705): 1315-1317.
- Smith, J., R. E. Kontermann, J. Embleton and S. Kumar (2005). "Antibody phage display technologies with special reference to angiogenesis." FASEB J **19**(3): 331-341.
- Spinelli, S., L. G. Frenken, P. Hermans, T. Verrips, K. Brown, M. Tegoni and C. Cambillau (2000). "Camelid heavy-chain variable domains provide efficient combining sites to haptens." Biochemistry **39**(6): 1217-1222.
- Stanley, J. (2002). Essentials of Immunology & Serology, Delmar Thomson Learning.
- Steinmeyer, D. E. and E. L. McCormick (2008). "The art of antibody process development." Drug Discov Today **13**(13-14): 613-618.
- Stills, H. F., Jr. (2005). "Adjuvants and antibody production: dispelling the myths associated with Freund's complete and other adjuvants." ILAR J **46**(3): 280-293.
- Terpe, K. (2003). "Overview of tag protein fusions: from molecular and biochemical fundamentals to commercial systems." Appl Microbiol Biotechnol **60**(5): 523-533.
- Thys, B., D. Saerens, L. Schotte, G. De Bleeser, S. Muyldermans, G. Hassanzadeh-Ghassabeh and B. Rombaut (2011). "A simple quantitative affinity capturing assay of poliovirus antigens and subviral particles by single-domain antibodies using magnetic beads." J Virol Methods **173**(2): 300-305.
- Tonegawa, S. (1983). "Somatic generation of antibody diversity." Nature **302**(5909): 575-581.

- Transue, T. R., E. De Genst, M. A. Ghahroudi, L. Wyns and S. Muyldermans (1998). "Camel single-domain antibody inhibits enzyme by mimicking carbohydrate substrate." Proteins **32**(4): 515-522.
- Trinkle-Mulcahy, L., S. Boulon, Y. W. Lam, R. Urcia, F. M. Boisvert, F. Vandermoere, N. A. Morrice, S. Swift, U. Rothbauer, H. Leonhardt and A. Lamond (2008). "Identifying specific protein interaction partners using quantitative mass spectrometry and bead proteomes." J Cell Biol **183**(2): 223-239.
- Tsien, R. Y. (1998). "The green fluorescent protein." Annu Rev Biochem **67**: 509-544.
- Tsukamoto, T., N. Hashiguchi, S. M. Janicki, T. Tumber, A. S. Belmont and D. L. Spector (2000). "Visualization of gene activity in living cells." Nat Cell Biol **2**(12): 871-878.
- Valenta, T., G. Hausmann and K. Basler (2012). "The many faces and functions of beta-catenin." EMBO J **31**(12): 2714-2736.
- van der Linden, R. H., L. G. Frenken, B. de Geus, M. M. Harmsen, R. C. Ruuls, W. Stok, L. de Ron, S. Wilson, P. Davis and C. T. Verrips (1999). "Comparison of physical chemical properties of llama VHH antibody fragments and mouse monoclonal antibodies." Biochim Biophys Acta **1431**(1): 37-46.
- van Oss, C. J., R. J. Good and M. K. Chaudhury (1986). "Nature of the antigen-antibody interaction. Primary and secondary bonds: optimal conditions for association and dissociation." J Chromatogr **376**: 111-119.
- Verheesen, P., A. Roussis, H. J. de Haard, A. J. Groot, J. C. Stam, J. T. den Dunnen, R. R. Frants, A. J. Verkleij, C. Theo Verrips and S. M. van der Maarel (2006). "Reliable and controllable antibody fragment selections from Camelid non-immune libraries for target validation." Biochim Biophys Acta **1764**(8): 1307-1319.
- Ward, E. S., D. Gussow, A. D. Griffiths, P. T. Jones and G. Winter (1989). "Binding activities of a repertoire of single immunoglobulin variable domains secreted from Escherichia coli." Nature **341**(6242): 544-546.
- Ward, R. L., M. A. Clark, J. Lees and N. J. Hawkins (1996). "Retrieval of human antibodies from phage-display libraries using enzymatic cleavage." J Immunol Methods **189**(1): 73-82.
- Webby, C. J., A. Wolf, N. Gromak, M. Dreger, H. Kramer, B. Kessler, M. L. Nielsen, C. Schmitz, D. S. Butler, J. R. Yates, 3rd, C. M. Delahunty, P. Hahn, A. Lengeling, M. Mann, N. J. Proudfoot, C. J. Schofield and A. Bottger (2009). "Jmjd6 catalyses lysyl-hydroxylation of U2AF65, a protein associated with RNA splicing." Science **325**(5936): 90-93.

- Wesolowski, J., V. Alzogaray, J. Reyelt, M. Unger, K. Juarez, M. Urrutia, A. Cauerhff, W. Danquah, B. Rissiek, F. Scheuplein, N. Schwarz, S. Adriouch, O. Boyer, M. Seman, A. Licea, D. V. Serreze, F. A. Goldbaum, F. Haag and F. Koch-Nolte (2009). "Single domain antibodies: promising experimental and therapeutic tools in infection and immunity." Med Microbiol Immunol **198**(3): 157-174.
- Willats, W. G. (2002). "Phage display: practicalities and prospects." Plant Mol Biol **50**(6): 837-854.
- Winter, G. and C. Milstein (1991). "Man-made antibodies." Nature **349**(6307): 293-299.
- Woolven, B. P., L. G. Frenken, P. van der Logt and P. J. Nicholls (1999). "The structure of the llama heavy chain constant genes reveals a mechanism for heavy-chain antibody formation." Immunogenetics **50**(1-2): 98-101.
- Wu, T. T., E. A. Kabat and H. Bilofsky (1979). "Some sequence similarities among cloned mouse DNA segments that code for lambda and kappa light chains of immunoglobulins." Proc Natl Acad Sci U S A **76**(9): 4617-4621.
- Zolghadr, K. (2007). Development of new methods to study DNA methyltransferase function and protein interactions in living cells. Department Biology II. München, Ludwig-Maximilians-Universität München.
- Zolghadr, K., O. Mortusewicz, U. Rothbauer, R. Kleinhans, H. Goehler, E. E. Wanker, M. C. Cardoso and H. Leonhardt (2008). "A fluorescent two-hybrid assay for direct visualization of protein interactions in living cells." Mol Cell Proteomics **7**(11): 2279-2287.

5.2 Abbreviations

μM : micromolar

μm : micrometer

aa: amino acid

BSA: bovine serum albumin

CDR: complementarity determining region

DAPI: 4', 6-diamidino-2-phenylindole

DNA: desoxyribonucleic acid

Dnmt1: DNA methyltransferase 1

EDTA: ethylen-diamine-tetra-acetate

e.g.: for example

ELISA: enzyme-linked immunosorbent assay

EtBr: ethidiumbromide

F2H: fluorescent two-hybrid

Fab: fragment antigen binding

GFP: green fluorescent protein

GST: glutathione S-transferase

HEK: human embryonic kidney cell line

5 Annex

HRP: horseradish peroxidase

i.e.: id est (that is)

Ig: immunoglobulin

IgA: immunoglobulin A

IgE: immunoglobulin E

IgG: immunoglobulin G

IgM: immunoglobulin M

IL: interleukin

IP: immunoprecipitation

kDa: kilodalton

LacI: lac repressor

OD: optical density

PCNA: proliferating cell nuclear antigen

PCR: polymerase chain reaction

RFP: red fluorescent protein

RNA: ribonucleic acid

Rpm: rounds per minute

RT: room temperature

S: second

scFv: single chain variable fragment

SDS-PAGE: sodium dodecylsulfate polyacrylamid gel electrophoresis

TCR: Tcell receptor

V_H: heavy chain variable domain of a conventional antibody

V_{HH}: heavy chain variable domain of a heavy chain antibody

V_L: light chain variable domain of a conventional antibody

5.3 Eidesstattliche Erklärung

Ich versichere hiermit an Eides statt, dass die vorgelegte Dissertation von mir selbstständig und ohne unerlaubte Hilfe angefertigt ist.

München, den 18. April 2013

Katrin Schmidthals

5.4 Acknowledgement

First, I would like to thank Prof. Dr. Heinrich Leonhardt for giving me the opportunity to conduct my PhD thesis in his group. It was a great inspiration to work in his group with all his ideas for new experiments and projects giving me the unique chance to leave the DNA methylation field and spend my time with the alpacas and their amazing antibodies.

A very special thank you belongs to Prof. Dr. Ulrich Rothbauer with whom I had the pleasure to work with during the last years. Uli, I am very grateful for your scientific advice, suggestions and discussions – I have learnt a lot from you! Thank you very much for revising my thesis. I also thank you for giving me the opportunity to become a part of the great Chromobuddy-Team and allowing me to follow my interests besides basic research.

Next, I would like to acknowledge Prof. Dr. Angelika Böttger for accepting to be the second referee for my thesis. Thank you very much, Angelika!

A super special thank you goes to ALL the Chromobuddies! You guys are not only colleagues, but friends. Without you life in lab would have been sooo boring! Kourosh, thank you not only for your scientific support, but also for the fun and the most hysterical laughter in my whole life (wie lange dauert es nochmal ein Patent anzumelden??). Tina, thank you very much for supporting me with both scientific and not so scientific discussions. Andrea, thank you for everything – especially for cheering me up during the hard times and our emotional discussions at every inappropriate occasion. A special thank you to Jacqui for keeping our Chromobuddy-lab running and for the many funny party nights! Marion, it is such a pleasure to work with you – thank you so much for supporting me. Last but not least, I also want to thank Larisa, Benjamin and Jörg for being such great colleagues!

I also want to thank all members of the Leonhardt group. I've always enjoyed working with you all. Special thanks go to Anja for keeping the lab running but also for supporting me

during the (endless) time of writing this thesis by covering some of my ChromoTek duties. Thank you so much Anja!

A very special thank you goes to my friend Danny! Was it destiny we met in Munich?? I will never forget our student time with days and nights of both hard learning and hard partying together. Without you I would never have finished my studies (ich sag nur: da fehlen doch nur 6 halbe Punkte...). Thank you for everything!

Biggest thanks go to my family – my parents and my brothers! Mama und Papa, vielen Dank für Eure unglaubliche Unterstützung und dass ihr immer an mich geglaubt habt, auch während der zugegebenermassen langen, nicht enden wollenden Zeit meiner Doktorarbeit. Mama, es macht mich sehr traurig, dass Du nicht mehr in meinem Leben bist – Du fehlst mir jeden Tag! Meine lieben Brüder Alois, Oliver, Stefan, Jörg, Cord, ich danke Euch für Eure Unterstützung. Jörg, danke das Du mich manchmal auf den Boden der Tatsachen zurückgeholt hast (und für die Hinweise auf den akademischen Betrieb). Stefan, vielen Dank für Deine Unterstützung und Aufmunterungen (Achtung: die Russen kommen!), wenn es mal nicht so rund lief.

The most heartfelt thank you goes to my boyfriend Fini! Thank you so much for all your support – I would not have made it without you! I know you also had hard times during the time of writing. Thank you for your patience, for tolerating my frustration, for cheering me up, for your love and for simply letting me be who I am! I love you!

5.5 Publications/Patent applications

5.5.1 Publications

Helma, J., **K. Schmidthals**, V. Lux, S. Nuske, A. M. Scholz, H. G. Krausslich, U. Rothbauer and H. Leonhardt (2012). "Direct and Dynamic Detection of HIV-1 in Living Cells." *Plos One* **7**(11): e50026

Schmidthals, K., Helma, J., Zolghadr, K., Rothbauer, U. & Leonhardt, H. (2010) Novel antibody derivatives for proteome and high-content analysis. *Anal Bioanal Chem* **397**, 3203-3208, doi:10.1007/s00216-010-3657-0.

Kirchhofer, A., J. Helma, **K. Schmidthals**, C. Frauer, S. Cui, A. Karcher, M. Pellis, S. Muyldermans, C. S. Casas-Delucchi, M. C. Cardoso, H. Leonhardt, K. P. Hopfner and U. Rothbauer (2010). "Modulation of protein properties in living cells using nanobodies." *Nat Struct Mol Biol* **17**(1): 133-138

Zolghadr, K., **Schmidthals, K.**, Helma, J., Tomer, T., Leonhardt, H., Rothbauer, U. (2009). „Biomedizinische Forschung und Diagnostik mit fluoreszierenden Nanosonden.“ *Biospektrum* 03.09.

5.5.2 Patent applications

PCT/EP 2010/059622: Detection and Visualization of the Cell Cycle in Living Cells.